Mathematisches Forschungsinstitut Oberwolfach

Report No. 21/2008

# Atomistic Models of Materials: Mathematical Challenges

Organised by
Weinan E, Princeton
Gero Friesecke, München
David Pettifor, Oxford

April 27th – May 3rd, 2008

Abstract. The contributions in this report, written by leading mathematicians and materials scientists, summarize recent progress and main mathematical challenges in the exciting and fast growing interdisciplinary field of atomistic modelling of materials.

*Mathematics Subject Classification (2000):* 70xx, 81xx, 81V55, 74xx, 65xx, 39A12.

## Introduction by the Organisers

The past decades have witnessed an explosion of interest in the application of mathematical models to science and engineering down at the atomic scale. Atomistic models are large, complex, multiscale, and in particular discrete, and provide a rich source of fascinating challenges for mathematics. In particular, a basic goal is to understand (1) how and at which length- and timescales the behaviour of large atomistic systems becomes well approximated by traditional continuum descriptions (of dislocations, grains, fracture, elasticity or plasticity), and under which circumstances atomistic and continuum "modes" are nontrivially coupled (2) how atomistic models can be accurately and efficiently extracted from quantum mechanical models.

While mathematical research in this area is still in its early stages, interest by mathematicians in atomistic models is fast growing, and the goal of this workshop was to bring together leading mathematicians and materials scientists, in the unique Oberwolfach setting, in order to document recent results, discuss main open challenges, and stimulate an exchange between the two communities.

The workshop focused on the following topics, the basic goals described above being recurrent themes.

- Derivation of interatomic potentials for magnetic materials from quantum mechanics (Drautz, Pettifor)
- Atomistic modelling of grain boundaries, phase boundaries, and surfaces (Elsaesser, Kratzer)
- Efficient algorithms in electronic structure theory (Gang Lu, Garcia-Cervera, Haynes)
- Atomic-continuum coupling (Braides, Cicalese, Delle Site, Guddati, Luskin, Ming, Mugnai, Schlömerkemper, Schmidt)
- Electronic-continuum coupling (Jianfeng Lu)
- Dislocation models (Garroni, Nguyen-Manh, Yang)
- Molecular dynamics (Colombo, Engquist, Giannoulis, Hartmann, James, Leimkuhler, Li, Stoltz, Theil, Zimmer).

The organizers are particularly indebted to the participants from both mathematics and materials science for making such a committed effort to communicate their work to researchers from the other community, both in the actual talks and in this Oberwolfach report. Judging by the success of this effort, we are confident that this report can serve as a starting point and a stimulation for a great deal of future interaction between our communities.

Weinan E
Gero Friesecke
David Pettifor

## Workshop: Atomistic Models of Materials: Mathematical Challenges

## Table of Contents

# Abstracts

## Linear-scaling density-functional simulations with local orbitals and plane waves

Peter D. Haynes
(joint work with Chris-Kriton Skylaris, Arash A. Mostofi, Mike C. Payne)

Kohn-Sham density-functional theory (DFT) provides a solution to the problem of finding the ground state of many electrons moving in a static external potential via a fictitious system of non-interacting particles moving in a local effective potential. This fictitious system is traditionally represented in terms of extended single-particle wave functions $\{\psi_n(\mathbf{r})\}$ that are expanded in some basis set. The computational cost of solving the resulting equations scales as the cube of system size $N$ ($N$ may be the number of atoms or electrons) which is very favourable compared to many-body wave function based methods. However this scaling still places a limit on the system-sizes accessible to DFT, typically of a few hundred atoms. There has therefore been much interest in developing linear-scaling or order-$N$ methods where the computational cost increases only linearly [1].

The fictitious system may be represented entirely equivalently in terms of the single-particle density-matrix $\rho(\mathbf{r},\mathbf{r}')$ defined by

$$\rho(\mathbf{r},\mathbf{r}') = \langle \mathbf{r}|\hat{\rho}|\mathbf{r}'\rangle = \sum_n f_n \psi_n(\mathbf{r})\psi_n^*(\mathbf{r}') \tag{1}$$

where $f_n \in \{0,1\}$ is the occupation number for the state $\psi_n$ and $\hat{\rho}$ the projection operator onto the space spanned by the occupied states. The advantage of this representation is that it enables the exploitation of the nearsightedness of quantum mechanics [2] that is manifested in the exponential decay of the density-matrix of insulators and semiconductors i.e. $\rho(\mathbf{r},\mathbf{r}') \sim \exp(-\gamma|\mathbf{r}-\mathbf{r}'|)$ as $|\mathbf{r}-\mathbf{r}'| \to \infty$. A linear-scaling method may be derived by minimising the energy with respect to a truncated density-matrix that satisfies the conditions of normalisation and idempotency.

The linear scaling method implemented in the ONETEP code [3, 4, 5] involves writing the density-matrix in separable form [6, 7]:

$$\rho(\mathbf{r},\mathbf{r}') = \sum_{\alpha,\beta} \phi_\alpha(\mathbf{r}) K^{\alpha\beta} \phi_\beta^*(\mathbf{r}') \tag{2}$$

where the $\{\phi_\alpha(\mathbf{r})\}$ are linear combinations of the Kohn-Sham eigenstates $\psi_n(\mathbf{r}) = \sum_\alpha \phi_\alpha(\mathbf{r}) M_n^\alpha$ chosen to be localised and the density kernel

$$K^{\alpha\beta} = \sum_n M_n^\alpha f_n M_n^{\beta *} = \langle \phi^\alpha|\hat{\rho}|\phi^\beta\rangle$$

where the $\{\phi^\alpha(\mathbf{r})\}$ are the duals of the local orbitals $\{\phi_\alpha(\mathbf{r})\}$. This expression is essentially just a similarity transformation of the diagonal form in Eq. 1.

The local orbitals are chosen to vanish outside spheres centred on atoms and are optimised *in situ* [8] so that each adapts to the chemical environment of that

atom. Their relationship to the Kohn-Sham eigenstates has led to these local orbitals being called non-orthogonal generalised Wannier functions (NGWFs). The optimisation is carried out by expanding the NGWFs in terms of localised psinc [9] or Dirichlet functions that allow the use of fast Fourier transforms (FFTs) for applying the Laplacian and interpolation. These FFTs are performed in a fixed subcell of the simulation cell [10] so that the overall computational cost scales linearly with $N$. An added advantage of this basis is that it is equivalent to a set of plane waves, allowing direct comparison with traditional plane-wave pseudopotential DFT calculations [11]. The ONETEP code has been implemented for massively parallel computers [12] and applied to a wide variety of systems [13, 14] including molecules, proteins, solids and nanostructures.

## References


[1] S. Goedecker, *Linear scaling electronic structure methods*, Reviews of Modern Physics **71** (1999) 1085–1123.

[2] W. Kohn, *Density functional and density matrix method scaling linearly with the number of atoms*, Physical Review Letters **76** (1996) 3168–3171.

[3] `www.onetep.org`

[4] P. D. Haynes, C.-K. Skylaris, A. A. Mostofi and M. C. Payne, *ONETEP: linear-scaling density-functional theory with local orbitals and plane waves*, physica status solidi (b) **243** (2006) 2489–2499.

[5] C.-K. Skylaris, P. D. Haynes, A. A. Mostofi and M. C. Payne, *Introducing ONETEP: Linear-scaling density functional simulations on parallel computers*, Journal of Chemical Physics **122** (2005) 084119.

[6] G. Galli and M. Parrinello, *Large scale electronic structure calculations*, Physical Review Letters **69** (1992) 3547–3550.

[7] E. Hernández and M. J. Gillan, *Self-consistent first-principles technique with linear scaling*, Physical Review B **51** (1995) 10157–10160.

[8] C.-K. Skylaris, A. A. Mostofi, P. D. Haynes, O. Diéguez and M. C. Payne, *Nonorthogonal generalized Wannier function pseudopotential plane-wave method*, Physical Review B **66** (2002) 035119.

[9] A. A. Mostofi, P. D. Haynes, C.-K. Skylaris and M. C. Payne, *Preconditioned iterative minimisation for linear-scaling electronic structure calculations*, Journal of Chemical Physics **119** (2003) 8842–8848.

[10] A. A. Mostofi, C.-K. Skylaris, P. D. Haynes and M. C. Payne, *Total-energy calculations on a real space grid with localized functions and a plane-wave basis*, Computer Physics Communications **147** (2002) 788–802.

[11] C.-K. Skylaris and P. D. Haynes, *Achieving plane wave accuracy in linear-scaling density functional theory applied to periodic systems: A case study on crystalline silicon*, Journal of Chemical Physics **127** (2007) 164712.

[12] C.-K. Skylaris, P. D. Haynes, A. A. Mostofi and M. C. Payne, *Implementation of linear-scaling plane wave density functional theory on parallel computers*, physica status solidi (b) **243** (2006) 973–988.

[13] C.-K. Skylaris, P. D. Haynes, A. A. Mostofi and M. C. Payne, *Using ONETEP for accurate and efficient O(N) density functional calculations*, Journal of Physics: Condensed Matter **17** (2005) 5757–5769.

[14] C.-K. Skylaris, P. D. Haynes, A. A. Mostofi and M. C. Payne, *Recent progress in linear-scaling density functional calculations with plane waves and pseudopotentials: the ONETEP code*, Journal of Physics: Condensed Matter **20** (2008) 064209.

## Motion of discrete interfaces

Andrea Braides
(joint work with Maria Stella Gelli and Matteo Novaga)

We are interested in defining an energy-driven motion for discrete subsets in the plane, and more precisely subsets of the lattice $\mathbb{Z}^2$. The model energy we will look at is the ferromagnetic energy for Ising systems, that we may write as

$$F(E) = \#\{(i,j) : i \in E,\ j \notin E\} \qquad (E \subset \mathbb{Z}^2).$$

Upon identifying a set $E \subset \mathbb{Z}^2$ with the union of the cubes $i+Q$, where $i \in E$ and $Q = [-1/2, 1/2)^2$, we may interpret $F$ as a perimeter energy $\mathcal{H}^1(\partial E)$ defined on all such unions of coordinate cubes.

Since perimeter energies are linked to motions by curvature, we will explore the possibility of defining such a motion in the discrete setting following the time-discretization scheme by Almgren, Taylor and Wang [4] coupled with a passage discrete-to-continuous [1, 2]. To that end we scale the lattice to $\varepsilon\mathbb{Z}^2$ and the energies to

$$F_\varepsilon(E) = \varepsilon\#\{(i,j) : i \in E,\ j \notin E\} \qquad (E \subset \varepsilon\mathbb{Z}^2).$$

and fix a time scale $\tau = \Delta t$. A time-discrete motion at scale $\tau$ is defined recursively as follows:

- fix an initial datum $E_0 = E_0^\varepsilon \subset \varepsilon\mathbb{Z}^2$;
- define $E_{k+1}$ as a minimizer of the energy

$$E \mapsto F_\varepsilon(E) + \frac{1}{2\tau} D_\varepsilon(E, E_k),$$

where

$$\begin{aligned} D_\varepsilon(E,E') \quad = \quad & \sum_{i \in E \setminus E'} \varepsilon^2 \min\{\|i-j\|_\infty : j \in E'\} \\ & + \sum_{i \in E' \setminus E} \varepsilon^2 \min\{\|i-j\|_\infty : j \in \varepsilon\mathbb{Z}^2 \setminus E'\}; \end{aligned}$$

- define $E^{\tau,\varepsilon}(t) = E_{[t/\tau]}$.

For a class of initial data we can characterize the behaviour of $E^{\tau,\varepsilon}(t)$ as $\varepsilon \to 0$ and $\tau \to 0$. In particular, we have the following result.

**Theorem** (Braides, Gelli and Novaga [5]) *Let $E_0^\varepsilon$ converge to some bounded $E$, either a polyrectangle or a smooth convex set, in the Hausdorff metric. Then, up to subsequences, $E^{\tau,\varepsilon}(t)$ converges to a limit continuous motion $E(t)$ of $E$. Moreover, we have*

(i) *if $\varepsilon \ll \tau$ then $E(t)$ is the motion by crystalline curvature characterized by Almgren and Taylor in* [3]*;*

(ii) *if $\tau \ll \varepsilon$ then the motion is trivial: $E(t) = E$ for all $t$;*

(iii) *if $\varepsilon \approx \alpha\tau$ then the motion is more complex, and is characterized as the motion only of the sides orthogonal to the coordinate direction with a inward velocity*

*that is proportional to*

$$\alpha\Big[\frac{4}{\alpha L(t)}\Big],$$

*where* $L(t)$ *is the side length, at all times when the quantity* $4/\alpha L(t)$ *is not integer (if the side length is* 0 *then the velocity is infinite), and, in case of polyrectangles, also proportional to a 'curvature sign' which is* 1 *if* $E$ *is convex close to that side,* $-1$ *if it is concave, and* 0 *otherwise.*

In order to understand the type of phenomena entailed by this motion in the third regime we can analyze the case of $E$ a rectangle of side lengths $L_1$ and $L_2$:

(i) (*pinning threshold*) If $L_i > 4/\alpha$ then the motion is trivial: $E(t) = E$;

(ii) (*partial pinning*) If $L_1 > 4/\alpha$ and $L_2 < 4/\alpha$ then for an initial time interval only the two shorter sides move, thus shortening $L_1$, until $L_1(t) = 4/\alpha$;

(iii) (*quantized velocity*) when $4/\alpha L_i(t)$ is not integer the velocity is always an integer multiple of $\alpha$;

(iv) (*non-uniqueness*) in the cases when $4/\alpha L_i(t)$ is integer the velocity of the corresponding side is not uniquely determined. If such set of $t$ is not negligible we may have non-uniqueness effects (*e.g.*, when the initial datum is a square of side length $4/\alpha$).

For non-rectangular initial sets we may have other phenomena that are not present in the usual geometric motions:

(v) (*non-convex pinned sets*) if the initial set $E$ is a polyrectangle such that all the sides either have curvature sign 0 or are longer than $4/\alpha$ then $E(t) = E$ for all $t$;

(vi) (*pinning after initial motion*) if the initial set $E$ contains a square of side-length larger than $4/\alpha$ then $E(t)$ contains that square for all times, also if the motion is not trivial. This happens for example for $E$ a (large) ball. In that case the four points in which the coordinate have extremals have 'infinite curvature', so that four segments are generated at $0^+$, which move inward until their length is the critical size $4/\alpha$.

Finally, note that in the case $\varepsilon << \tau$ we have a separation of scales effect: the motion is the same as that obtained by first letting $\varepsilon \to 0$ (in which case the energies $F_\varepsilon$ are approximated by a crystalline perimeter [1, 2]), and then applying the discrete-in-time scheme (as in [3]).

## References


[1] R. Alicandro, A.Braides, and M.Cicalese. Phase and anti-phase boundaries in binary discrete systems: a variational viewpoint. *Netw. Heterog. Media* **1** (2006), 85–107.

[2] R. Alicandro, A.Braides, and M.Cicalese. *From Lattice Systems to Continuous Variational Problems*, in preparation.

[3] F. Almgren and J.E. Taylor. Flat flow is motion by crystalline curvature for curves with crystalline energies. *J. Differential Geom.* **42** (1995), 1-22.

[4] F. Almgren, J.E. Taylor, and L. Wang. Curvature driven flows: a variational approach. *SIAM J. Control Optim.* **50** (1983), 387-438.

[5] A. Braides, M.S. Gelli, and M. Novaga. Motion and pinning of discrete interfaces. Preprint SNS, Pisa, 2008.

## Computation of free energy differences

Gabriel Stoltz
(joint work with Tony Lelièvre, Felix Otto and Mathias Rousset)

After briefly recalling some basis of statistical physics, in particular the computation of averages with respect to the canonical measure

$$\langle A \rangle = \int_E A(q,p)\, d\mu(q,p),$$

with

$$d\mu(q,p) = Z^{-1} \mathrm{e}^{-\beta H(q,p)}, \qquad Z = \int_E \mathrm{e}^{-\beta H(q,p)}\, dq\, dp,$$

$Z$ being the so-called partition function, I turn to the metastability problem, namely that averages along a trajectory of an ergodic process such as

$$dq_t = -\nabla V(q_t)\, dt + \sqrt{\frac{2}{\beta}}\, dW_t$$

are theoretically converging to the state space averages

$$\lim_{T \to +\infty} \frac{1}{T} \int_0^T A(q_t)\, dt = \langle A \rangle = \int_E A(q)\, d\pi(q), \qquad d\pi(q) = Z^{-1} \mathrm{e}^{-\beta V(q)},$$

but the convergence may be rather slow from a numerical viewpoint. Notice that there is no restriction in sampling only the configurational part of the canonical measure $d\pi$ since it is trivial to sample the kinetic part (which is a tensor product of gaussians). A remedy to this metastability problem is to bias the dynamics in the direction of the slowly evolving variable, called $\xi \equiv \xi(q)$. This can be done by sampling the modified canonical measure associated with the potential $V(q) - F(\xi(q))$, where

$$F(q) = -\beta^{-1} \ln \int_E \mathrm{e}^{-\beta V(q)}\, \delta_{\xi(q)-z}\, dq\, dp$$

is defined up to a constant (since only free energy differences matter). Differences of free energies are also valuable from a physical viewpoint since they allow to discuss the relative stabilities of different species.

In order to simplify the presentation of the most popular methods to compute free energy differences, it is convenient to restrict to the case of the so-called alchemical transitions, indexed by some external parameter in the Hamiltonian:

$$\Delta F(\lambda) = -\beta^{-1} \ln \left( \frac{\displaystyle\int_E \mathrm{e}^{-\beta H_\lambda(q,p)}\, dq\, dp}{\displaystyle\int_E \mathrm{e}^{-\beta H_0(q,p)}\, dq\, dp} \right).$$

The main methods are classified from a mathematical viewpoint in the Table below.

| | | |
|---|---|---|
| Free energy perturbation | → | Homogeneous MCs and SDEs |
| Thermodynamic integration | → | Projected MCs and SDEs |
| Nonequilibrium dynamics | → | Nonhomogenous MCs and SDEs |
| Adaptive dynamics | → | Nonlinear SDEs and MCs |
| Selection procedures | → | Particle systems and jump processes |

Adaptive dynamics (such as the adaptive biasing force [2], nonequilibrium metadynamics [1], etc) are very interesting methods. We have recently proposed

- a general framework [3] to study them in a unified fashion and understand their consistencies;
- an improved numerical implementation;
- and proved a convergence result in some limiting case using entropy estimates [4, 5].

## References


[1] G. Bussi, A. Laio, and M. Parrinello, *Equilibrium free energies from nonequilibrium metadynamics*, Phys. Rev. Lett. **96**(9) (2006), 090601.

[2] E. Darve and A. Pohorille, *Calculating free energies using average force*, J. Chem. Phys. **115**(20) (2001), 9169–9183.

[3] T. Lelièvre, M. Rousset and G. Stoltz, *Computation of free energy profiles with parallel adaptive dynamics*, J. Chem. Phys. **126** (2007), 134111.

[4] T. Lelièvre, F. Otto, M. Rousset and G. Stoltz, *Long-time convergence of an Adaptive Biasing Force method*, arXiv preprint **0706.1695** (2007)

[5] T. Lelièvre, M. Rousset and G. Stoltz, *Long-time convergence of an Adaptive Biasing Force method*, Nonlinearity **21** (2008) 1155–1181.


## Atomistic and Continuum Models (not only) of Thin Films

Bernd Schmidt

The relation of atomistic and continuum models of matter is an important and very active area of current research, both from a computational and from the analytical point of view. Thin elastic structures are of particular interest not only in technical applications. One also encounters completely new phenomena (as, e.g., large deformations at low energies). The main aim of this note is to report on recent results on rigorous derivations and investigations of effective theories for thin elastic films starting from atomistic models. In particular, we examine new effects that may arise for 'atomistically thin' objects, where a continuum approach is not expected to be justified anymore.

In the membrane energy regime a rigorous version of a scheme proposed by G. Friesecke and R. D. James in [3] is proven. Let $\mathcal{L}_k := \mathbb{Z}^3 \cap ([0,k]^2 \times [0,h])$ be the reference configuration of a thin film of $\nu$ atomic layers, $\nu$ fixed, $k \gg \nu$. Rescale and interpolate the deformations $y^{(k)} : \mathcal{L}_k \to \mathbb{R}^3$ to obtain

$$\tilde{y}^{(k)}(x) := \frac{1}{k} y^{(k)}(kx_1, kx_2, x_3), \quad \tilde{y}^{(k)} : [0,1]^2 \times [0,h] \to \mathbb{R}^3.$$

and $\nu - 1$ director fields

$$k\Delta^i \tilde{y}(x_1, x_2) := k\left(\tilde{y}^{(k)}(x_1, x_2, i) - \tilde{y}^{(k)}(x_1, x_2, 0)\right)$$

measuring the relative shift of the layers of the film.

Choose a constant $c_0 > 0$ and define admissible limit deformations: $u \in W^{1,\infty}([0,1]^2; \mathbb{R}^3)$, $\mathbf{b} = (b^1, \ldots, b^{\nu-1}) \in L^\infty([0,1]^2; (\mathbb{R}^3)^{\nu-1})$ such that $u$ satisfies a minimal strain hypothesis: there exists $c_1$ such that

$$|u(x) - u(z)| \geq c_1|x - z|.$$

We say that $y^{(k)} \to (u, \mathbf{b})$ as $k \to \infty$ if $\|\tilde{y}^{(k)} - u\| := \sup_{x \in \tilde{\mathcal{L}}_k} |\tilde{y}^{(k)}(x) - u(x)| \leq c_0/k$ and $k\Delta^i \tilde{y}^{(k)} \overset{*}{\rightharpoonup} b^i$ in $L^\infty$. (So $c_0$ prescribes a rate of convergence and the atoms are allowed to explore a region comparable to atomic dimensions in the limiting process.)

The energy is assumed to be a (frame indifferent) function of the full set of atomic positions

$$E^{(k)}(y) = E(y(x) \mid x \in \mathcal{L}_k)$$

satisfying the following

**Assumption.** Suppose $u$ is admissible. For all $C > 0$ there are constants $M > 0$ and $q > 3$ such that, whenever $\|\tilde{y} - u\| \leq C/k$, then

(i) $|E(\mathcal{M} \cup \mathcal{N}) - E(\mathcal{M}) - E(\mathcal{N})| \leq \sum_{w \in \mathcal{M}, v \in \mathcal{N}} M(1 \wedge |w - v|^{-q})$ for disjoint sets $\mathcal{M}, \mathcal{N} \subset y(\mathcal{L}_k)$ of atoms and

(ii) $\left|\frac{\partial}{\partial y_i} E^{(k)}(\{y_1, \ldots, y_{\nu(k+1)^2}\})\right| \leq M$, where $\{y_1, \ldots, y_{\nu(k+1)^2}\} = y(\mathcal{L}_k)$.

**Theorem 1.** Under the above assumptions there is a macroscopic energy density $\varphi$ such that the $\frac{1}{\nu k^2} E^{(k)}$ $\Gamma$-converge to

$$E(u, \mathbf{b}) := \int_{[0,1]^2} \varphi(\nabla u(x), b^1(x), \ldots, b^{\nu-1}(x)) dx.$$

Moreover, $\varphi$ is continuous and given by

$$\varphi(A, \mathbf{b}) = \lim_{k \to \infty} \frac{1}{\nu k^2} \inf_{y \in \mathcal{N}_k(A, \mathbf{b})} E(y),$$

as the solution to the associated cell problem, where

$$\mathcal{N}_k = \left\{ y : \mathcal{L}_k \to \mathbb{R}^3 : \|y - A\| \leq c_0 \text{ and } \frac{1}{(k+1)^2} \sum_{x' \in \mathbb{Z}^2 \cap [0,k]^2} \Delta^i y(x') = b^i \right\}.$$

Note that the dependence on $u$ through $\nabla u$ is as expected from membrane theory, while the occurrence of the directors $b^i$ is an 'ultra-thin film phenomenon'. For the proof of this result and examples of atomistic interaction potentials that satisfy our basic assumption, we refer to [11].

Qualitative properties of the effective macroscopic energy density are examined in [10]. It is proven that in fact the scale on which relaxations are taken into account is not only physically the most reasonable, but also the only one which

yields a non-trivial energy expression in the limit mathematically. Furthermore, symmetry properties and the energy response to extremal deformations and to small strains are studied. Specializing to certain mass-spring models, interesting phenomena are observed concerning the energy response to small tensile and small compressive deformations.

In the derivation of non-linear plate theory for bending dominated deformations we choose a more specific model for which the continuum limit can be computed explicitly. The reference configuration is the same as before, except that we now assume that the film consists of $\nu+1$ atomic layers.

Let $\vec{z} = (z^1, \dots, z^8) = \frac{1}{2}\begin{pmatrix} -1 & 1 & 1 & -1 & -1 & 1 & 1 & -1 \\ -1 & -1 & 1 & 1 & -1 & -1 & 1 & 1 \\ -1 & -1 & -1 & -1 & 1 & 1 & 1 & 1 \end{pmatrix}$ label the corners of $[-\frac{1}{2}, \frac{1}{2}]^3$, by $\bar{x}$ denote centers of unit cells and define the discrete gradient of a deformation $y$ by

$$\bar{\nabla} y(x) = (y(\bar{x}+z^1) - y(\bar{x}), \dots, y(\bar{x}+z^8) - y(\bar{x})) \in \mathbb{R}^{3\times 8},$$

where $x \in \bar{x} + [-\frac{1}{2}, \frac{1}{2})^3$, $\bar{y} = \frac{1}{8}(y(\bar{x}+z^1) + \ldots + y(\bar{x}+z^8))$.

Our basic assumption is now that the energy decomposes as

$$E^{(k)}(y) = \sum_{\bar{x}} W(\bar{x}, \vec{y}(\bar{x})), \quad W(\bar{x}, \cdot) = W_{\text{cell}}(\cdot) + W_{\text{surface}}(\bar{x}, \cdot)$$

with $W_{\text{surface}}$ 'compatible with $W_{\text{cell}}$' (as in suitable mass spring models). Note that, in order to investigate bending dominated deformations, we do not rescale the energy $\frac{1}{k^2}$.

**Theorem 2.** Under suitable assumptions on the cell energy and for the appropriate definition of discrete-to-continuum convergence, $E^{(k)} \xrightarrow{\Gamma} E$. If $u : [0,1]^2 \to \mathbb{R}^3$ is a $W^{2,2}$-isometric immersion, then–up to surface terms–

$$E(u) = \int_{[0,1]^2} \left[ \frac{\nu}{8} Q_3^{\text{rel}}\left(-\operatorname{II}_{12} M + N \cdot \vec{z}_-\right) + \frac{\nu^3 - \nu}{24} Q_3^{\text{rel}}\left(N \cdot \vec{z}\right) \right],$$

where for the second fundamental form $\operatorname{II} \in \mathbb{R}^{2\times 2}$ of $u$

$$N = \begin{pmatrix} \operatorname{II}_{11} & \operatorname{II}_{12} & 0 \\ \operatorname{II}_{21} & \operatorname{II}_{22} & 0 \\ 0 & 0 & 0 \end{pmatrix}, \quad \text{and} \quad M = \begin{pmatrix} 0 & 0 & 0 & 0 & 0 & 0 & 0 & 0 \\ 0 & 0 & 0 & 0 & 0 & 0 & 0 & 0 \\ 1 & 0 & 1 & 0 & 1 & 0 & 1 & 0 \end{pmatrix},$$

$\vec{z}_- = (-z^1, -z^2, -z^3, -z^4, z^5, z^6, z^7, z^8)$, $Q_3^{\text{rel}}(\vec{y}) := \min_{v\in\mathbb{R}^3} Q_3(y_1, \dots, y_4, y_5 + v, \dots, y_8 + v)$, $Q_3 = D^2 W_{\text{cell}}$.

**Theorem 3.** For 'thick films', i.e., $k \to \infty$, $\nu \to \infty$ such that $\nu/k \to 0$ we get

$$\Gamma - \lim \frac{1}{\nu^3} E^{(k)}(u) = \int_{[0,1]^2} \frac{1}{24} Q_3^{\text{rel}}\left(N \cdot \vec{z}\right).$$

For the precise statements of these results and proofs we refer to [9]. Crucial ingredients to the proofs are [2] and [4].

**Remark.** The result for thick films agrees with first applying the Cauchy–Born rule for the 3d-passage from discrete to continuum and then performing the continuum 3d to 2d Γ-limit for bending dominated deformations. In contrast, for ultra-thin films we need to consider cell deformations which are not affine.

Motivated by the observation that a continuum description captures the true energy to leading order, we also briefly mention the results in [8, 6] on 'roll-up' phenomena of thin internally stressed multi-layers. Here Kirchhoff's plate theory is derived in the multilayer case and applied to study the geometry of energy minimizers (with free boundaries). Restricting to Euler-Bernoulli theory, also the effect of a non-interpenetration condition is examined. It turns out that for the most interesting energy regime the optimal shape is given by a double spiral.

We close this report noting that the techniques developed for thin films prove useful also in other contexts. It was possible to extend a recent result of Braides, Solci and Vitali on the derivation of linear elasticity from atomistic models (see [1]) to full nearest and next-to-nearest neighbor interactions, more general boundary conditions and systems whose individual atomic bonds are not equilibrated in the energy minimizing configuration (see [5]).

**Acknowledgment** The largest part of these results are part of my PhD thesis [7]. I am grateful to my PhD supervisor Prof. S. Müller for his guidance, support and helpful advice. This work was supported by the German science foundation (DFG) under project FOR522.

## References

[1] A. Braides, M. Solci and E. Vitali, *A derivation of linear elastic energies from pair-interaction atomistic systems*, Netw. Heterog. Media **2** (2007), 551–567.

[2] S. Conti, G. Dolzmann, B. Kirchheim and S. Müller, *Sufficient conditions for the validity of the Cauchy-Born rule close to $SO(n)$*, J. Eur. Math. Soc. (JEMS) **8** (2006), 515–539.

[3] G. Friesecke and R. D. James, *A scheme for the passage from atomic to continuum theory for thin films, nanotubes and nanorods*, J. Mech. Phys. Solids **48** (2000), 1519–1540.

[4] G. Friesecke, R. D. James and S. Müller, *A theorem on geometric rigidity and the derivation of nonlinear plate theory from three-dimensional elasticity*, Comm. Pure Appl. Math. **55** (2002), 1461–1506.

[5] B. Schmidt, *On the derivation of linear elasticity from atomistic models*, submitted (2008).

[6] B. Schmidt, *Plate theory for stressed heterogeneous multilayers of finite bending energy*, J. Math. Pures Appl. **88** (2007), 107–122.

[7] B. Schmidt, *Effective theories for thin elastic films*, Dissertation, Universität Leipzig (2006).

[8] B. Schmidt, *Minimal energy configurations of strained multi-layers*, Calc. Var. Partial Diff. Eq. **30** (2007), 447–497.

[9] B. Schmidt, *A derivation of continuum nonlinear plate theory from atomistic models*, SIAM Mult. Model. Simul. **5** (2006), 664–694.

[10] B. Schmidt, *Qualitative properties of a continuum theory for thin films*, Annales de l'I.H.P. – Analyse non linéaire **25** (2008), 43–75.

[11] B. Schmidt, *On the passage from atomic to continuum theory for thin films*, Arch. Ration. Mech. Anal. (2008), in press.

## Travelling waves in atomistic chains and kinetic relations

Johannes Zimmer
(joint work with Hartmut Schwetlick)

Martensitic materials pose good test problems for the analysis of the passage from atomistic to continuum. The reason is that on the microscopic level, they can be well approximated by a chain of atoms governed by Newton's equations; thus, the system is *microscopically Hamiltonian*. However, martensitic materials can undergo phase transitions, and moving phase boundaries can generate dissipation, so that the system is *macroscopically dissipative*. The simplest possible situation for which this phenomenon can be understood is that of a single phase boundary propagating in a one-dimensional chain of atoms $\{q_j\}_{j\in\mathbb{Z}}$ on the real line. Neighbouring atoms are linked by a spring with elastic potential $V$, and it is convenient to assume that only nearest neighbours interact. The longitudinal elongation of atom $k$ is given by $u_k\colon \mathbb{R}\to\mathbb{R}$. The argument of the elastic potential $V$ is the discrete strain, that is, the difference of the deformations, $u_{k+1}(t)-u_k(t)$. The springs are bistable, with the two stable states representing two stable phases. The equations of motion are assumed to be governed by Newton's law, so that in suitable units

$$\ddot{u}_k(t) = V'(u_{k+1}(t)-u_k(t)) - V'(u_k(t)-u_{k-1}(t)) \tag{1}$$

for every $k\in\mathbb{Z}$. A travelling wave *ansatz* is $u_k(t)=u(k-ct)$ for $k\in\mathbb{Z}$; with this formulation, Equation (1) becomes

$$c^2\ddot{u}(x) = V'(u(x+1)-u(x)) - V'(u(x)-u(x-1)). \tag{2}$$

We remark that the Hamiltonian is

$$\int_{\mathbb{R}} \left[\tfrac{1}{2}c^2\dot{u}(t)^2 + V(u(t+1)-u(t))\right]\,\mathrm{d}t.$$

Equation (2) is an instance of a so-called *lattice differential equation*. Models of crystal lattices, photonic structures, and Josephson junctions, furnish other examples of lattice differential equations. A number of interesting papers [2, 4, 5] demonstrates the variety of problems and methods encountered in this field.

It is convenient to reformulate the travelling-wave formulation (2) in terms of the discrete strain $\epsilon(x)=u(x)-u(x-1)$; it then simply reads

$$c^2\epsilon''(x) = \Delta_1 V'(\epsilon(x)), \tag{3}$$

where $\Delta_1 g(x) := g(x+1)-2g(x)+g(x-1)$ is the discrete Laplacian. Though one would like to treat smooth nonconvex potentials, rigorous results are presently only available for the special interaction potential

$$V(\epsilon) = \frac{1}{2}\min\{(\epsilon+1)^2,(\epsilon-1)^2\}. \tag{4}$$

This potential also appears in other works [9, 10]. For this choice of $V$, (3) becomes

$$c^2\epsilon''(x) = \Delta_1\epsilon(x) - 2\Delta_1 H(\epsilon(x)), \tag{5}$$

with $H$ denoting the Heaviside function. The wave travels with speed $c$.

To formulate the result, we introduce the *dispersion relation* $D_c(\kappa) = 4\sin^2\left(\frac{\kappa}{2}\right) - c^2\kappa^2$. We choose a velocity regime so that the the dispersion relation vanishes for exactly one positive value, which we denote $\kappa_0$. This assumption restricts the analysis to fast subsonic, almost sonic wave speeds. We remark that for martensitic phase transitions, there is a distinction between fast (*umklapp*) and slow (*schiebung*) martensitic transformations. The former move with a velocity close to that of an elastic wave, the latter are observable under an optical microscope [3, 8].

It is then possible to show that there exists, for fixed wave speed $c$ close to the sound speed $c_0 := 1$, a *family* of solutions of (5). Every family is heteroclinic in the sense that the strain is negative (positive) for negative (positive) arguments. This corresponds to solutions with the strain in one well for negative arguments and in the second well for positive arguments. The precise formulation is as follows.

**Theorem 1.** *Suppose the dispersion relation has one positive zero $\kappa_0$ with $\kappa_0^2 < \frac{1}{2}$. Then there exists a family of heteroclinic wave solutions, parametrised by a real number $\xi$ with $|\xi| \leq 1$. The solutions are such that $\epsilon(x) > 0$ for $x > 0$ and $\epsilon(x) < 0$ for $x < 0$ for all admissible values of the parameter $\xi$.*

We briefly discuss the Rankine-Hugoniot condition, and introduce the notation $[\![f]\!]$ for $f(s(t)+,t) - f(s(t)-,t)$, where $s(t)$ is the position of the interface. We write $f(s-)$ respectively $f(s+)$ for the one-sided limit of $f$ in $s$ from the left respectively from the right.

The *Rankine-Hugoniot conditions* for strain $u_x$ and velocity $\dot{u}$ read

$$[\![\sigma(u_x)]\!] = -\rho c\,[\![\dot{u}]\!]\,,$$
$$c\,[\![u_x]\!] = -\,[\![\dot{u}]\!]\,.$$

We combine these conditions and write for $\epsilon = u_x$

$$\rho c^2\,[\![\epsilon]\!] = [\![\sigma(\epsilon)]\!]\,. \tag{6}$$

Here, the solution can be shown to oscillate on both sides of the interface. It is, however, meaningful to consider the *averaged strains*, e.g.,

$$\bar{\epsilon}_+ := \lim_{x\to\infty}\lim_{s\to\infty}\frac{1}{s}\int_x^{x+s}\epsilon(\xi)\mathrm{d}\xi.$$

A direct calculation shows that the Rankine-Hugoniot condition holds,

$$\bar{\epsilon}_+ - \bar{\epsilon}_- = 2\frac{1}{1-c^2}. \tag{7}$$

To motivate kinetic relations, let us consider a heat-conducting thermoelastic body. We denote the heat flux by $q$, the specific entropy by $s$, the absolute temperature by $T$, and the material velocity (mass flux) by $c$. For a moving surface of discontinuity with normal $n$, the surface entropy production is $R := c\,[\![s]\!] + \left[\!\left[\frac{q\cdot n}{T}\right]\!\right]$. The second law of thermodynamics imposes the inequality $R \geq 0$. One can see that this restricts possible jumps for supersonic waves (shocks) as well as the constitutive structure of entropy production $R$ for subsonic waves (kinks) [7]. For subsonic waves, this yields an additional condition $R = R(c)$.

A moving interface is exposed to the so-called *configurational force* $f$. Since the entropy production $R$ is related to the configurational force, it is reasonable to define a *kinetic relation* as a functional relationship between $f$ and wave speed $c$. We refer the reader to [6, 1] for more information on kinetic relations. The configurational force is given by

$$f := \int_{\bar{\epsilon}_-}^{\bar{\epsilon}_+} \sigma(\epsilon)\mathrm{d}\epsilon - \{\sigma\}\,[\![\epsilon]\!]\,. \tag{8}$$

Here, $\bar{\epsilon}_\pm$ is taken to be the limit of the averaged strain, $[\![\epsilon]\!] := \epsilon(s(t)+,t) - \epsilon(s(t)-,t)$ and $\{\sigma\} := \frac{1}{2}(\sigma(s(t)+,t) + \sigma(s(t)-,t))$. For the problem under consideration, one computes directly

$$f = -\frac{2c^2}{c^2 - \frac{\sin(\kappa_0)}{\kappa_0}} \cdot \xi. \tag{9}$$

We remark that contrary to the common assumption, $f$ is not a function of $c$ alone, but depends on a two-parameter family, with the wave speed being one parameter, and the other parameter $\xi$ as in Theorem 1. This form of the kinetic relation is only valid for subsonic wave speeds with $\kappa_0^2 \leq \frac{1}{2}$ as in Theorem 1. Evidently, the kinetic relation is trivial, $f = 0$, for the symmetric wave, $\xi = 0$.

We close by pointing out that one would want to impose the validity of the entropy inequality $fc \geq 0$ for the solutions of Theorem 1. For $c > 0$, this inequality is violated for any solution with $\xi > 0$, while it holds for $\xi \leq 0$. Conversely, solutions with $\xi \geq 0$ satisfy the entropy inequality for $c < 0$; the symmetric solution, with trivial kinetic relation, satisfies the entropy inequality for positive and negative wave speeds.

## References


[1] R. Abeyaratne, J. L. Knowles, *Kinetic relations and the propagation of phase boundaries in solids*, Arch. Rational Mech. Anal. **114** (1991), 119–154.

[2] S.-N. Chow, J. Mallet-Paret, W. Shen, *Traveling waves in lattice dynamical systems*, J. Differential Equations **149** (1998), 248–291.

[3] Föster, Scheil *Untersuchung des zeitlichen Ablaufes von Umklappvorgängen in Metallen*, Z. Metallkd. **32** (1940), 165–201.

[4] G. Friesecke, R. L. Pego, *Solitary waves on FPU lattices. I. Qualitative properties, renormalization and continuum limit*, Nonlinearity **12** (1999), 1601–1627.

[5] G. Iooss, K. Kirchgässner, *Traveling waves in in a chain of coupled nonlinear oscillators*, J. Comm. Math. Phys. **211** (2000), 439–464.

[6] L. Truskinovskiĭ, *Dynamics of nonequilibrium phase boundaries in a heat conducting nonlinearly lastic medium*, Prikl. Mat. Mekh. **51** (1987), 1009–1019.

[7] L. Truskinovsky, *Inertial effects in the dynamics of martensitic phase boundaries*, in Shape-Memory Materials and Phenomena — Fundamental Aspects and Applications (Liu, C. T. and Wuttig, M. and Otsuka, K. and Kunsmann, H., eds.) **48** (1992), 103–108.

[8] L. Truskinovsky, *Transition to detonation in dynamic phase changes*, Arch. Rat. Mech. Anal. **125** (1994), 375–397.

[9] L. Truskinovsky, A. Vainchtein, *Kinetics of martensitic phase transitions: Lattice model*, SIAM J. Appl. Math. **66** (2005), 1205–1221.

[10] L. Truskinovsky, A. Vainchtein, *Quasicontinuum models of dynamic phase transitions*, Contin. Mech. Thermodyn. **18** (2006), 1–21.

## First-principles theory and atomistic modelling of grain and phase boundaries in materials

Christian Elsässer

Technologically relevant structural and functional materials usually have polycrystalline microstructures which consist of crystalline, micrometer- to nanometer-sized grains. These grains are mutually misoriented, they are connected through grain boundaries, and they contain lattice dislocations. Furthermore, the grains, the dislocation cores and the boundaries may contain point defects, i.e., impurity or dopant atoms, in variable concentrations. Many macro- and microscopic properties of the materials, like mechanical hardness, plasticity and fracture toughness, chemical oxidation or corrosion resistance, atomic diffusion or electrical conduction, electronic or magnetic properties, etc., are affected or controlled by the structures and energetics of the interfaces, dislocations, or point defects.

A very active and rapidly growing discipline of materials science is the theoretical modelling and computational simulation of relationships between atomic-scale features of the structural or compositional imperfections in the materials and their resulting functional properties (see, e.g., Ref. [1]). The most fundamental modelling level is based on the quantum mechanics of crystals that are composed of atomic nuclei and electrons. In order to obtain computational methods which enable calculations of properties of crystals with sufficient accuracy, reliability, and predictive power as well as with affordable computational effort, the following few physical approximations are commonly made (see, e.g., Ref. [2]).

First, in the Born-Oppenheimer approximation (BOA) the dynamics of the light and fast electrons that constitute a quantum-mechanical fermion gas, is decoupled from the dynamics of the heavy and slow nuclei that mostly behave like classical point particles with mass and charge. In the BOA, the electron gas instantaneously follows all movements of the nuclei and remains in its ground state.

Second, to calculate the properties of this ground state of the electron gas for an arrangement of nuclei, most importantly to calculate its total energy, the density functional theory (DFT) has become a well established and very successful approach (see, e.g., Ref. [3]). In the DFT, the fundamental physical quantity is the density of the electron gas. Hohenberg and Kohn showed that the total energy is a functional of the density, E[n] [4]. This functional fulfills a variational principle with respect to all densities, and it is minimised by the ground-state density $n_0$ and equal to the ground-state energy $E_0$. Using this variational principle, Kohn and Sham showed a way of mapping the real many-particle gas of interacting electrons on a ficticious system of non-interacting fermions having the same density, and consequently the same ground-state properties, as the real gas [5]. The formally exact mapping leads to a set of coupled self-consistent-field equations, the Kohn-Sham equations, to calculate this density. To define the Kohn-Sham equations completely, only one further physical approximation for a typically small part of the total energy E[n], the so-called exchange-correlation energy, is needed. Several

such approximate functionals, e.g., local-density or generalised-gradient approximations (LDA, GGA), are available for numerical computations of ground-state electron densities $n_0$ (**r**) and total energies $E[n_0]$ (cf. Refs. [2, 1]).

Third, the calculated total energies for various relevant arrangements of the nuclei compose an energy hyperface in the parameter space of all coordinates of the nuclei, the *adiabatic potential*, whose local minima determine stable or at least metastable structures of materials (thermodynamic phases), whose local saddle points indicate transition states (for kinetic or reactive processes), and whose general landscape determines the trajectories of moving atoms (molecular dynamics).

This DFT approach contains no adjustable material-specific model parameters. Therefore it is commonly called *from first principles* or *ab initio*, and consequently the results have a strong predictive power. However, first-principles DFT calculations are computationally very demanding, and atomic-scale model systems are typically limited in size to only few hundred particles. Therefore, strong efforts are made to allow further physical approximations to the DFT in order to make much larger atomistic model systems tractable, for instance by approximating physically the self-consistent-field Hamiltonian in the Kohn-Sham equations by a semi-empirical tight-binding (TB) Hamiltonian for the electronic structure, or further by reformulating mathematically the solution of the tight-binding electronic-structure problem in terms of interatomic many-body bond-order potentials (BOP) in real space. (The physical theory and mathematical development of BOP derived from DFT via TB models was presented by D. G. Pettifor and R. Drautz on this workshop.)

Four applications of ab-initio DFT calculations and atomistic BOP simulations to study structural properties of defects in metallic materials were presented. First, for pure grain boundaries in the body-centered cubic transition metals Nb, Mo, Ta, and W, relationships between the atomistic interface structure, the local electronic structure and bonding, and the interfacial stability were discussed [6]. Second, the effect of segregated impurity atoms on a Mo grain boundary was studied [7], and third, a structural transformation in a MoC precipitate at a Mo grain boundary under a mechanical shear load was analysed [8]. Fourth, the interaction of a gliding screw dislocation with a twin boundary in W was discussed [9].

With these four case studies it was intended to give an imagination of the wealth of structural and chemical features which exist at the atomic length scale in ordinary polycrystalline materials, and which determine many of their structural and functional properties up to macroscopic dimensions. Computational multi-scale modeling and simulation of materials is a long-term and multi-disciplinary challenge for materials scientists from mechanical engineering, from solid-state physics and chemistry, as well as from applied mathematics. The atomic-scale modeling of materials by ab-initio DFT calculations and atomistic simulations using semi-empirical TB and BOP models can provide accurate, reliable, and predictive materials data, based on fundamental principles of physics, which can be useful for parametrisations of computational techniques for larger length scales.

## References

[1] J. Hafner, *Atomic-scale computational materials science*, Acta mater. **48** (2000), 71–92.

[2] R. O. Jones and O. Gunnarsson, *The density functional formalism, its applications and prospects*, Rev. Mod. Phys. **61** (1989), 689–746.

[3] W. Kohn, *Nobel Lecture: Electronic structure of matter – wave functions and density functionals*, Rev. Mod. Phys. **71** (1999), 1253–1266.

[4] P. Hohenberg and W. Kohn, *Inhomogeneous electron gas*, Phys. Rev. **136** (1964), B864–B871.

[5] W. Kohn and L. J. Sham, *Self-consistent equations including exchange and correlation effects*, Phys. Rev. **140** (1965), A1133–A1138.

[6] T. Ochs, O. Beck, C. Elsässer, and B. Meyer, *Symmetrical tilt grain boundaries in bcc transition metals – an ab-initio local-density-functional study*, Phil. Mag. A **80** (2000), 351–372.

[7] R. Janisch and C. Elsässer, *Segregated light elements at grain boundaries in Niobium and Molybdenum*, Phys. Rev. B **67** (2003), 224101.

[8] R. Janisch and C. Elsässer, *Growth and mechanical properties of a MoC precipitate at a Mo grain boundary: an ab-initio study*, Phys. Rev. B **77** (2008), 094118.

[9] M. Mrovec, Y. Cheng, C. Elsässer, and P. Gumbsch *Atomistic simulations of dislocation – grain-boundary interactions in tungsten*, in P. Gumbsch (ed.), Proc. Int. Conf. MMM2006, Fraunhofer IRB Verlag (2006), pp. 213–216.


## Ergodic Hoover-Langevin thermostats


Florian Theil

(joint work with Ben Leimkuhler, Emad Noorizadeh)


Molecular dynamics (MD) is an integral part of molecular simulations. One particular advantage of MD is its ability to extract macroscopic information from the detailed dynamical trajectories of the system. Therefore, it is essential to ensure that the algorithm used in MD does not change the qualitative dynamical behavior of the physical system.

In order to relate MD simulation with results of statistical physics we onsider a physical system which can be modelled with a Hamiltonian $H(q,p)$, $q,p \in \mathbb{R}^n$. In particular we are interested in computing long-time averages of observables $O$ along solutions $(q(t),p(t))$ of Hamilton's equations $\dot{q} = \frac{\partial H}{\partial p}, \dot{p} = -\frac{\partial H}{\partial q}$. It is helpful to distinguish between two different kinds of observables: static observables and dynamic observables. Static observables are functions on the phase space, $O = O(q,p)$. Long-time averages of static observables can be computed without solving Hamilton's equations by phase space averaging:

$$\langle O \rangle = \int_{\mathbb{R}^{2n}} O(q,p)\,\mathrm{d}\rho_\beta(q,p), \tag{1}$$

where $\rho_\beta = \frac{1}{Z}\exp(-\beta H(q,p))$ is the Boltzmann-Gibbs distribution and $\beta$ is the inverse temperature. The time average is defined as

$$\overline{O} = \lim_{\tau\to\infty} \frac{1}{\tau}\int_0^\tau O(q(t),p(t))\,\mathrm{d}t. \tag{2}$$

If the observable $O$ depends only on few degrees of freedom, then the second principle of thermodynamics implies that $\overline{O} - \langle O \rangle$ is very close to 0 if $n$ is large and $H$ is "reasonable". Thus the computation of long-time averages can be reduced to a sampling problem.

On the other hand, long-time averages of dynamic observables $O(q(t), p(t), q(t+\delta), p(t+\delta))$ (e.g. autocorrelation functions) cannot be computed without solving Hamilton's equation.

## 1. Thermostats

These considerations motivate the search for sampling methods from the canonical distribution that alter the original Hamiltonian evolution in a minimal way. Various methods have been developed to sample the canonical measure, they can be categorized into stochastic and deterministic methods.

The best known representative of the stochastic methods is the Langevin-thermostat. It replaces Newtonian dynamics with the following stochastic dynamics:

$$\frac{\mathrm{d}q}{\mathrm{d}t} = M^{-1}p, \tag{3}$$

$$\mathrm{d}p = -\nabla V \,\mathrm{d}t - \gamma\, p\,\mathrm{d}t + \sqrt{2\gamma\beta^{-1}}\, M^{\frac{1}{2}}\,\mathrm{d}W, \tag{4}$$

where we have assumed that $H(q,p) = \frac{1}{2}p^T M p + V(q)$, $M$ is a mass matrix and $W$ is a vector of $n$ independent Brownian motions. It can be easily checked that the Boltzmann-Gibbs distribution $\rho_\beta^{\mathrm{aug}}$ is invariant along solution of (3)-(4). It is provably a sampling method, but has the tendency to decrease time correlations, hence it is less useful to compute the expectation of dynamic observables.

A popular deterministic method is known as Nosé-Hoover dynamics (NHD) [1, 2]. This method augments the physical system with one additional variable $\xi$ called thermostat variable. The thermostat variable represents an artificial heat bath and is coupled to all the degrees of freedom of the physical system.

NHD replaces Newtonian dynamics with the following extended dynamical system:

$$\dot{q} = M^{-1}p, \tag{5}$$

$$\dot{p} = -\nabla_q V - \xi p, \tag{6}$$

$$\mu\dot{\xi} = p^T M^{-1} p - \tfrac{n}{\beta}, \tag{7}$$

where the parameter $\mu$ is an (artificial) thermostat coefficient that influences the coupling of the heat bath to the system. It can be easily checked that the augmented Boltzmann-Gibbs distribution

$$\rho_\beta^{\mathrm{aug}} \propto \exp\left(-\beta\left(H + \tfrac{\mu}{2}\xi^2\right)\right) \tag{8}$$

is constant along solution of (5)-(7).

The Nosé-Hoover evolution is very close to the Hamiltonian evolution, hence the computation of dynamic observables is not affected. On the other hand, there

are examples that show that the Nosé-Hoover thermostat is not always a sampling method for the canonical distribution.

## 2. The Langevin-Hoover thermostat

We propose the following family of stochastic dynamics which combines that advantages of the Nosé-Hoover method with the advantages of the Langevin thermostat and avoids the respective shortcomings.

$$\frac{\mathrm{d}q}{\mathrm{d}t} = M^{-1}p, \tag{9}$$

$$\frac{\mathrm{d}p}{\mathrm{d}t} = -\nabla V(q) - A(\xi)p, \tag{10}$$

$$\mathrm{d}\xi = \tfrac{1}{\mu}(p^T M^{-1}p - \tfrac{n}{\beta})\,\mathrm{d}t - \tfrac{1}{2}\mu\beta\sigma^2\xi\,\mathrm{d}t + \sigma\,\mathrm{d}W, \tag{11}$$

where $M$ is a positive definite diagonal matrix, $q, p \in \mathbb{R}^n$, $A(\xi) = \xi\mathrm{Id} + MS(t,\xi)$, $S \in \mathbb{R}^{n\times n}$ is skew-symmetric (i.e., $S^T = -S$), $\xi \in \mathbb{R}$, $W$ is the standard Brownian motion and $\sigma \in \mathbb{R}$ is an additional parameter of the thermostat. For $\sigma = 0$ one obtains the classic Nosé-Hoover thermostat.

**Proposition 2.** *The augmented Boltzmann-Gibbs distribution $\rho_\beta^{\mathrm{aug}}$ is invariant under the flow generated by equations (9-11).*

The proof of Proposition 2 consists in checking that $\rho_\beta^{\mathrm{aug}}$ is a stationary solution of the Fokker-Planck equation.

The focus of our analysis is to provide sufficient conditions which entail that the flow is ergodic for the augmented Boltzmann-Gibbs distribution. In Theorem 3 we show that quadratic Hamiltonians which satisfy a certain non-resonance condition generate ergodic flows. The significance of this result is due to the fact that the harmonic oscillator is one of the most notorious examples where the Nosé-Hoover thermostat is not ergodic.

**Theorem 3.** *Let $M, B \in \mathbb{R}^{n\times n}$ be two symmetric and positive definite matrices such that*

$$\omega_k \neq \omega_l \text{ for all } k \neq l, \tag{12}$$

*where $\omega_k = \varphi_k \cdot M^{-1}B\varphi_k$ are the eigenvalues and $\varphi_1, \ldots, \varphi_n \in \mathbb{R}^n$ are the normalized eigenvectors of $M^{-1}B$. If $H(q,p) = \frac{1}{2}p \cdot M^{-1}p + \frac{1}{2}q \cdot Bq$ and*

$$U = \left\{ (q,p) \;\middle|\; \prod_{k=1}^{n} \left((q\cdot\varphi_k)^2 + (p\cdot\varphi_k)^2\right) \neq 0 \right\} \times \mathbb{R}, \tag{13}$$

*then the flow generated by equations (9-11) is ergodic on $U$.*

The proof of Theorem 3 is based on a standard application of Hörmander's theorem.

References

[1] Nosé S 1984 A unified formulation of the constant temperature molecular dynamics method *J. Chem. Phys.* **81** 511-519

[2] Hoover W 1985 Canonical dynamics: equilibrium phase space distributions *Phys. Rev. A.* **31** 1695-1697

## Fracture mechanics at the nanoscale: continuum or discrete? A materials science perspective

Luciano Colombo

(joint work with Mariella Ippolito, Alessandro Mattoni)

Continuum mechanics has been traditionally used to describe the macroscopic mechanical behavior of solid bodies (like, e.g., elastic or plastic deformations, failure strength, fracture mechanics), while atomistic theories have been used at the nanoscale (where chemical bonding features dominate). Recently it has been widely recognized that, in order to reach a predictive multiscale description of materials mechanical behavior, different methodologies must be concurrently integrated in order to properly modeling the interplay between phenomena occurring at separate length scales. This is, in particular, the case of fracture: a phenomenon which is truly initiated at the very atomic scale by a bond snap event, but it shows up as a material macroscopic opening .

The atomic scale represents in any case the smallest length scale at which the above multiscale paradigm must operate. Therefore, a robust and reliable model of atomic interactions - properly accounting for nanostructure evolution - is mostly needed. Such a model can be developed at different levels of erudition, ranging from the most fundamental quantum mechanical one to the more computationally efficient approach based on empirical force fields. Nowadays we benefit of a full set of interatomic potentials for (almost) any material kind, as well as of numerical algorithms and methods allowing simulations on a number of atoms that properly represent an interesting mechanical system. Accordingly, atomistic simulations are extensively used within the multiscale paradigm.

In this work we review a series of our recent theoretical investigations on brittle fracture in nanostructured silicon carbide, a system of great technological impact for advanced structural applications. We made use of large-scale atomistic simulations (molecular dynamics) to investigate several features related to the presence of a nano-sized crack into a bulk sample which, in turn, could host elastic inclusions and/or nanovoids. In particular, we investigate: crack resistance [1], fracture toughness [2], and failure strenght [3].

Overall we show that atomistic simulations are able to mach the continuum results (worked out within standard linear elastic fracture mechanics, LEFM) provided that the relevant physical parameters for the above fracture-related phenomena are computed far away from the crack tip. On the other hand, present atomistic data offer a quantitative and trustworthy picture about mechanical properties at the nanoscale (i.e. nearby the crack tip), where continuum fails. We also

derive a generic picture about brittleness, based on universal properties of chemical bonding [4].

Finally, we use atomistic data –which naturally take into account the discrete distribution of mass in the crystal lattice– to improve continuum models. By means of a discretized version of LEFM, we effectively insert the notion of "lattice discreteness" into continuum and we reconcile LEFM to atomistics [3, 5]. While this result proves that continuum could be effectively projected down to the atomic scale, we understand that our proposed approach is material-specific and only heuristically proved. We therefore claim that there is room –and real need of– for a more systematic, generic and mathematically robust treatment of the "discreteness" notion into continuum mechanics.

### References

[1] A. Mattoni, L. Colombo, F. Cleri, *Atomic scale origin of crack resistance in brittle fracture*, Phys. Rev. Lett. **95**, 115501(2005)

[2] M. Ippolito, A. Mattoni, L. Colombo, *Fracture toughness of nanostructured silicon carbide*, Appl. Phys. Lett. **87**, 141912 (2005)

[3] M. Ippolito, A. Mattoni, N. Pugno, L. Colombo, *Failure strenght of brittle materials containing nanovoids*, Phys. Rev. B **75**, 224110 (2007)

[4] A. Mattoni, M. Ippolito, L. Colombo, *Atomistic modeling of brittleness in covalent materials*, Phys. Rev. B **76**, 224103 (2007)

[5] M. Ippolito, A. Mattoni, L. Colombo, N. Pugno, *Role of lattice discreteness on brittle fracture: atomistic simulations versus analytical models*, Phys. Rev. B **73**, 104111 (2006)

## On a discrete-to-continuum limit involving multiple scales and its application to magnetic forces

Anja Schlömerkemper

(joint work with Bernd Schmidt)

The starting point for the discrete-to-continuum limit considered here is a lattice of magnetic dipole moments. The superposition of all dipole-dipole forces between two parts of the lattice gives the magnetic force in the discrete setting. In the limit as the lattice parameter shrinks to zero the continuum force formula is derived, cf. [3, 6] and [7, 8].

The limiting force contains a novel contribution that depends on the underlying lattice structure and is due to the hyper-singularity of the dipole-dipole interaction, which in fact causes most of the mathematical difficulties. The novel formula allowed to resolve a long standing open problem posed by Brown [1] about some puzzling non-linearity that appears in a magnetic force formula extensively discussed by him in [1].

In joint work with Popović and Praetorius [3, 4] we compare the novel magnetic force formula with formulae that are derived purely within a continuum setting. In particular we compare the limiting formula with the above mentioned force formula extensively discussed by Brown [1]. In analytical as well as numerical studies we show that the novel force formula is significantly different to the one

discussed by Brown. Moreover we analyze how the difference between these two force formula depends on the geometry and size of the domains.

To understand the significant difference between these force formulae better and to relate the previous analysis and numerics to experiments, Schmidt and myself [9] computed a discrete-to-continuum limit of magnetic forces by introducing a further parameter. The further parameter describes the distance of the two parts of the material on a microscopic scale and introduces a new scale, which is intermediate to the atomistic and continuum scales. This allows a better understanding of magnetic forces between two 'very close' rigid bodies. I will outline this in more mathematical terms in the following and refer to [9] for details as well as to another summary of this issue in [10].

We consider a Bravais lattice denoted by $\mathcal{L} \subset \mathbb{R}^d$, $d \geq 2$, whose unit cell has volume one. The rescaled Bravais lattice is $\frac{1}{\ell}\mathcal{L}$ for $\ell \in \mathbb{N}$. The continuum limit corresponds to taking $\ell \to \infty$. Next we fix the assumptions on the two bodies between which we calculate the magnetic force. As outlined in [9], the assumptions on the geometry of the bodies can be relaxed. Furthermore we give the assumptions on the magnetic dipole moments which are attached to each lattice point.

**Assumption $\mathcal{A}$.** Let $d \in \mathbb{N}$ be fixed.

(1) $A$ and $B$ are open polytopes in $\mathbb{R}^d$ such that $A \cap B = \emptyset$. Moreover, $A$ and $B$ are in contact, i.e., the surface measure of $\partial A \cap \partial B \subset \partial A$ is positive. The set $B_\varepsilon = B + \varepsilon\nu$, where $\nu \in \mathcal{L}$ is fixed and $\varepsilon = \frac{a}{\ell}$ with $a \in \mathbb{N}$, satisfies $\overline{A} \cap \overline{B_\varepsilon} = \emptyset$ for all $\varepsilon > 0$.

(2) The corresponding magnetizations $\mathbf{m}_A : A \to \mathbb{R}^d$ and $\mathbf{m}_B : B \to \mathbb{R}^d$ are Lipschitz continuous and are supported on $\overline{A}$ and $\overline{B}$, respectively, i.e., there holds $\mathbf{m}_A \in W^{1,\infty}(A)$ and $\mathbf{m}_B \in W^{1,\infty}(B)$. Moreover, the magnetization $\mathbf{m}_{B_\varepsilon} : B_\varepsilon \to \mathbb{R}^d$ satisfies $\mathbf{m}_{B_\varepsilon}(x) = \mathbf{m}_B(x - \varepsilon\nu)$ for all $x \in B_\varepsilon$. All magnetization fields are extended by zero to the entire space $\mathbb{R}^d$.

We suppose the following, physically natural scaling of the magnetic dipole moments:

$$\mathbf{m}_A^{(\ell)}(x) := \frac{1}{\ell^d}\mathbf{m}_A(x) \quad \text{if } x \in A \cap \frac{1}{\ell}\mathcal{L},$$
$$\mathbf{m}_{B_\varepsilon}^{(\ell)}(x) := \frac{1}{\ell^d}\mathbf{m}_{B_\varepsilon}(x) \quad \text{if } x \in B_\varepsilon \cap \frac{1}{\ell}\mathcal{L}.$$

The superposition of the magnetic forces exerted by dipole moments in $B_\varepsilon$ on all dipole moments in $\overline{A}$ is, see e.g. [6],

$$\mathbf{F}_k^{(\ell)}(A,B) := \gamma \sum_{x \in \overline{A} \cap \frac{1}{\ell}\mathcal{L}} \sum_{y \in B_\varepsilon \cap \frac{1}{\ell}\mathcal{L}} \partial_i\partial_j\partial_k N(x-y)\big(\mathbf{m}_A^{(\ell)}\big)_i(x)\big(\mathbf{m}_{B_\varepsilon}^{(\ell)}\big)_j(y), \tag{1}$$

where $\gamma$ is a physical constant and $N$ denotes the fundamental solution of the Laplacian. Note that we apply Einstein's summation convention. In the continuum limit we obtain the following result:

**Theorem 4** ([9]). *Suppose Assumption $\mathcal{A}$ is satisfied. Then*

$$\mathbf{F}^{\lim}(A,B,a) = \lim_{\ell \to \infty} \mathbf{F}_k^{(\ell)}(A,B,a)$$

*exists and satisfies*

$$\begin{aligned}\mathbf{F}^{\lim}(A,B,a) &= \int_A (\mathbf{m}_A(x)\cdot\nabla)\mathbf{H}_{A\cup B}(x)\,dx\\ &\quad+\frac{\gamma}{2}\int_{\partial A}(\mathbf{m}_A(x)\cdot\mathbf{n}_A(x))\big((\mathbf{m}_A(x)-\mathbf{m}_B(x))\cdot\mathbf{n}_A(x)\big)\mathbf{n}_A(x)\,ds_x\\ &\quad+\frac{1}{2}\sum_{i,j,p=1}^{d} S_{ijkp}\int_{\partial A\cap\partial B}(\mathbf{m}_A)_i(x)(\mathbf{m}_B)_j(x)(\mathbf{n}_A)_p(x)\,ds_x\\ &\quad-\gamma\int_{\partial A\cap\partial B}(\mathbf{m}_A)_i(x)(\mathbf{m}_B)_j(x)\times\\ &\qquad\times\sum_{z\in\mathcal{L}\setminus\{0\}}\partial_i\partial_j\partial_k N(z)\big(\big(\mathbf{n}_A(x)\cdot(z-a\nu)\big)_+-(\mathbf{n}_A(x)\cdot z)_+\big)\,ds_x\\ &=:\mathbf{F}^{\lim}(A,B)+\mathbf{G}(a),\end{aligned}$$

*where* $\mathbf{n}_A$ *denotes the outer normal to* $\partial A$ *and* $\mathbf{H}_{A\cup B}$ *is a solution of the magnetostatic Maxwell equations, cf. e.g.* [2]. *The fourth order tensor* $(S_{ijkp})$ *is defined as the value of a certain singular lattice sum of a cut-off of* $N$, *see* [6, 7].

If $a=0$, the term $\mathbf{G}(a)$ is zero and we thus, consistently, obtain the previous discrete-to-continuum limit $\mathbf{F}^{\lim}(A,B)$ as in [3, 6]. This corresponds to the case that the (minimal) distance between the lattice points in $A$ and those in $B$ is one lattice spacing, i.e. the bodies are quasi in contact on the scale of the lattice.

The other extreme case is that the bodies are infinitely far apart on the scale of the lattice but are still in contact on the continuum scale. This corresponds to considering the limit as $a\to\infty$. We obtain Brown's force formula [1, p. 57], see also [3, Section 3.1], [5, Theorem 2.1].

**Theorem 5** ([9]). *Let Assumption* $\mathcal{A}$ *hold. Then*

$$\lim_{a\to\infty}\mathbf{F}^{\lim}(A,B,a)=\mathbf{F}^{\mathrm{Br}}(A,B),$$

*where*

$$\mathbf{F}^{\mathrm{Br}}(A,B):=\int_A(\mathbf{m}_A(x)\cdot\nabla)\mathbf{H}_{A\cup B}(x)\,dx+\frac{\gamma}{2}\int_{\partial A}(\mathbf{m}_A(x)\cdot\mathbf{n}_A(x))^2\mathbf{n}_A(x)\,ds_x.$$

We obtain Brown's formula also in the scaling regime $\varepsilon=a/\ell$, where $a=a(\ell)\to\infty$ such that $a/\ell\to 0$ as $\ell\to\infty$. This corresponds to two bodies which are in contact on the continuum scale and whose microscopic distance tends to infinity as $\ell\to\infty$.

**Theorem 6** ([9]). *Suppose Assumption* $\mathcal{A}$ *holds and let* $\varepsilon(\ell):=a(\ell)/\ell$, $a(\ell)\in\mathbb{N}$, *such that* $\varepsilon(\ell)\to 0$ *and* $a(\ell)\to\infty$ *as* $\ell\to\infty$. *Then*

$$\lim_{\ell\to\infty}\mathbf{F}_k^{(\ell)}(A,B)=\mathbf{F}^{\mathrm{Br}}(A,B),$$

*where* $\mathbf{F}_k^{(\ell)}(A,B)$ *is as in* (1) *with* $\varepsilon=\varepsilon(\ell)$.

Finally we consider the case of two macroscopically separated bodies, which corresponds to $a$ scaling with $\ell$. In this case we obtain a well-known formula $\mathbf{F}^{\mathrm{sep}}$ for the magnetic force between two bodies being a macroscopic distance apart, see e.g. [1], [5, Section 5.1].

**Proposition 7** ([9]). *Suppose $A$ and $B$ are not in contact, i.e., $\overline{A}\cap\overline{B}=\emptyset$, but still satisfy the remaining conditions of Assumption $\mathcal{A}$. Then the discrete-to-continuum limit $\mathbf{F}^{\mathrm{lim}}_{\mathrm{sep}}(A,B)$ exists and satisfies*

$$\mathbf{F}^{\mathrm{lim}}_{\mathrm{sep}}(A,B)=\int_A(\mathbf{m}_A(x)\cdot\nabla)\mathbf{H}_B(x)dx=\mathbf{F}^{\mathrm{sep}}(A,B).$$

In conclusion, the discrete-to-continuum limit which involves multiple scales allows to derive the previously known formulae $\mathbf{F}^{\mathrm{lim}}$, $\mathbf{F}^{\mathrm{Br}}$ and $\mathbf{F}^{\mathrm{sep}}$ by looking at different scaling regimes for the parameter $a$. This provides in particular a link between the limiting force formula $\mathbf{F}^{\mathrm{lim}}$ and Brown's formula $\mathbf{F}^{\mathrm{Br}}$.

Conceptually the limiting formula is more appropriate in general. However, if the microscopic distance between two bodies is relatively large, Brown's formula turns out to be an approximation. See [9] for an example which shows an exponential decay of $\mathbf{G}(a)$ with $a$. Already for $a=1$, this example yields $\mathbf{F}^{\mathrm{lim}}(A,B,1)=6.451$. From [4] it is known that $\mathbf{F}^{\mathrm{lim}}(A,B,0)=17.414$ and $\mathbf{F}^{\mathrm{lim}}(A,B,\infty)=\mathbf{F}^{\mathrm{Br}}(A,B)=6.431$ in the same units. Thus for $a=0$, $\mathbf{F}^{\mathrm{lim}}$ and $\mathbf{F}^{\mathrm{Br}}$ are significantly different, whereas Brown's formula gives a good approximation of the limiting force if $a=1$.

Our analysis involving the further scale supports that $\mathbf{F}^{\mathrm{lim}}$ is the appropriate force formula if $a=0$, i.e., if the bodies are in contact on macroscopic as well as on the microscopic scale. This is for instance the case if the force on a subregion of a continuum body is considered, i.e. if $A$ is treated as a subregion of a larger body $A\cup B$. In fact, this was the starting point of the study of magnetic forces by Brown and also in [5, 6].

## References


[1] W. F. Brown, *Magnetoelastic Interactions,* Springer, Berlin (1966)

[2] Y. V. Egorov and M. A. Shubin, *Foundations of Classical Theory of Partial Differential Equations*, Springer-Verlag, Berlin, 1998

[3] N. Popović, D. Praetorius and A. Schlömerkemper, Analysis and numerical simulation of magnetic forces between rigid polygonal bodies. Part I: Analysis, *Cont. Mech. Thermodyn.* **19**, 67–80 (2007)

[4] N. Popović, D. Praetorius and A. Schlömerkemper, Analysis and numerical simulation of magnetic forces between rigid polygonal bodies. Part II: Numerical Simulation, *Cont. Mech. Thermodyn.* **19**, 81–109 (2007)

[5] A. Schlömerkemper, Magnetic forces in discrete and continuous systems, Dissertation, University of Leipzig, 2007

[6] A. Schlömerkemper, Mathematical derivation of the continuum limit of the magnetic force between two parts of a rigid crystalline material, *Arch. Rational Mech. Anal.* **176**, 227–269 (2005)

[7] A. Schlömerkemper, Lattice approximation of a surface integral and convergence of a singular lattice sum, *Asymptot. Anal.* **52**, 95–115 (2007)

[8] A. Schlömerkemper, About solutions of Poisson's equation with transition condition in non-smooth domains, MPI MIS, Leipzig, Preprint 53/2006 (2006), to appear in *Z. Anal. Anwend.*
[9] A. Schlömerkemper and B. Schmidt, Discrete-to-continuum limit of magnetic forces: dependence on the distance between bodies, MPI MIS, Leipzig, Preprint 29/2007 (2007), to appear in *Arch. Rational Mech. Anal.*
[10] A. Schlömerkemper and B. Schmidt, Scaling limits of magnetic forces between two bodies, submitted to *PAMM Proc. Appl. Math. Mech.*

## The Adaptive Resolution Simulation method (AdResS): Basic principles and mathematical challenges

Luigi Delle Site

Many problems in condensed matter are inherently multiscale and it is exactly the interplay between the different scales that often constitutes the essence of the physical or chemical properties. This means that from a theoretical or computational point of view an exhaustive description of the system requires the simultaneous treatment of all the relevant scales implied, however, the computational costs should be affordable. In this sense the ideal aim is to treat in a simulation only as many degrees of freedom (DOF) as strictly required by the description of the property of interest and it is often the case that some regions require a treatment on a higher level of detail than the remainder of the system. The AdResS method fulfills such requirements; it allows to vary the DOF of a molecule on-the-fly, from atomistic to coarse-grained and vice versa, according to the resolution required in the spatial region where the molecule transits. It is based on the introduction of a transition region $\Delta$ and a weighting function $w(x)$ which allows for a smooth transition from one resolution to another and is such that $w(x_1) = 0; w(x_2) = 1$ (as sketched in Fig.1). The two scales are then coupled by interpolating the intermolecular forces according to the values of the molecular weighting functions:

$$\mathbf{F}_{\alpha\beta} = w(X_\alpha)w(X_\beta)\mathbf{F}^{\text{atom}}_{\alpha\beta} + [1 - w(X_\alpha)w(X_\beta)]\mathbf{F}^{cm}_{\alpha\beta},$$

where $\alpha$ and $\beta$ labels two distinct molecules and $X_{\alpha,\beta}$ is the $x$ coordinate of the molecular center of mass. $\mathbf{F}^{\text{atom}}_{\alpha\beta}$ is derived from the atomistic potential where each atom of one molecule interacts with each atom of the other, and $\mathbf{F}^{cm}_{\alpha\beta}$ is obtained from a coarse-grained potential between the centers of masses of the coarse-grained molecules; the latter is derived on the basis of the reference all-atom system. Despite this force is not conservative, a complementary theoretical analysis provides the means by which relevant thermodynamical quantities can be controlled to preserve equilibrium [4, 5, 6]. Such an analysis is based on the statistical interpretation of the process of varying resolution whose essential points are: **(a)** The change of resolution represents a kind of *geometrical induced phase transition* where the similarity with a real physical phase transition regards the latent heat $\phi$, associated, in this case, with acquiring or releasing DOFs. This means:$\mu_B = \mu_A + \phi$, with $\mu$ being the chemical potential. Since the approach is based on the forces, within this framework one cannot write explicitly the energy

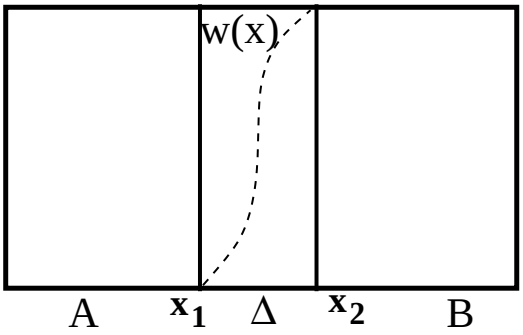


Figure 1: Schematic representation of the multiple resolution system: The high resolution (e.g. atomistic) region **B**, low resolution (e.g. coarse grained) region **A** and the transition region $\Delta$. $w(x)$ is a switching function which allows a smooth transition from a coarse grained to an atomistic resolution and vice versa. The various regions must be in thermodynamical equilibrium, that is same pressure, same temperature and balance of chemical potentials as reported later in the text. This representation is taken from [1, 2]

or the free energy of the system and thus derive from them the explicit form of $\phi$. However in a simulation this can be done *numerically* by coupling the system to a position dependent thermostat which takes care of providing or removing $\phi$ to ensure equilibrium between the different regions [1, 3, 4]. **(b)** The switching procedure implies that the dimensionality of the phase space associated with a DOF is continuously changing from 1, i.e. the contributions of the DOF to any physical quantity is fully counted, to 0, i.e. the DOF contribution is no more counted. This implies that in $\Delta$ one deals with non integer dimensions. The process of counting means, in a statistical sense, how much in determining a quantity (at a given resolution) the DOF contributes. This can be translated in mathematical terms by introducing the infinitesimal volume element of the fractional space of the DOF, (let us call it $q$):

$$dV_\alpha = d^\alpha q\, \Gamma(\alpha/2)/2\pi^{\alpha/2}\Gamma(\alpha) = |q|^{\alpha-1}dq/\Gamma(\alpha) = dq^\alpha/\alpha\Gamma(\alpha)$$

where $\alpha = w(\hat{x})$, that is the degree of fractionality in the region $x = \hat{x}$ (i.e. the resolution of the molecule which transits in the region $x = \hat{x}$). The statistical average of any physical quantity is then made by integrating (i.e. counting) over such fractional infinitesimal volume in the phase space:

$$\langle A \rangle_\alpha = \frac{\int_0^\infty e^{-\beta H(q)} q^{\alpha-1} A(q) dq}{\int_0^\infty e^{-\beta H(q)} q^{\alpha-1} dq};$$

with $A$ being a generic physical quantity and $H(q)$ the Hamiltonian of the system. Using this formalism one finds: $\langle K_\alpha \rangle = \alpha \langle K \rangle$, where $\langle K_\alpha \rangle$ is the average kinetic energy of the DOF $q$, when the degree of resolution is $w(\hat{x}) = \alpha$, and $\langle K \rangle$ is the

same quantity when the DOF is fully switched on (high resolution region). The equivalence above leads to the **extension of the equipartition theorem to non integer dimensions**: $\langle K_\alpha \rangle = \alpha \frac{k_B T}{2}$, and thus to the operative definition of temperature $T$ in $\Delta$. This means that the condition $T_B = T_\Delta = T_A$ can be fulfilled and the thermal equilibrium assured [5, 6, 8, 9]. The combination of the theoretical principles, as outlined above, and the numerical simplicity of the interpolation formula makes the method rather robust and very efficient as shown in several applications [7, 8, 9]. From the theoretical point of view two more question must be addressed:

(1) Why the interpolation formula is not applied using a more natural choice, that is using potentials;
(2) Since the numerical results show that the method properly describes the change of resolution, the natural question is if it is possible a formal derivation of the interpolation formula from some *first principles* of statistical physics.

Regarding **(1)**, an analysis using generic switching functions $f$ and $g$ was carried on [2]. They are defined as follows: $g : g = 0, \forall x \in B; g = 1, \forall x \in A$ and $f : f = 0, \forall x \in A; f = 1, \forall x \in B$. The consequence of using: $U^{\text{coupling}} = f(X_\alpha, X_\beta) U_{cg} + g(X_\alpha, X_\beta) U_{\text{atom}}$ is that an unphysical drift forces $\mathbf{F}_{\text{drift}} = U_{\text{atom}} \frac{\partial f}{\partial x} + U_{cg} \frac{\partial g}{\partial x}$, is generated. It is unphysical because there are no physical principles by which it should come, since $f$ and $g$ are not physical quantities, however if considered physical, it leads to the violation of the third Newton's law [6]. Thus it should be set to zero. This leads to a system of partial differential equations of the first order in $f$ and $g$ , but with two boundary conditions for each function. Obviously the system is overdetermined and thus has got no solutions. The situation does not change if one generalizes the potential: $U^{\text{coupling}} = f(X_\alpha, X_\beta) U_{cg} + g(X_\alpha, X_\beta) U_+ \Theta$, in fact in this case the overdetermination is simply shifted from $f$ and $g$ to $\Theta$. If $\mathbf{F}_{\text{drift}}$ is set to zero by hand, and the coupling is done using the forces as in AdResS, then the $U^{\text{coupling}}$ cannot represent the energy of the system, as instead erroneously claimed in the work of Ensing *et al.* [10]. A further possibility is that of fixing only one boundary condition, e.g. that of the high resolution region in $x_2$, and to adjust $f$ and $g$ in $\Delta$ and $A$ so that $\mathbf{F}_{\text{drift}} = 0$, (i.e. open boundary option). The problem would still remain because the condition of statistical equilibrium, on the free energy density, at the boundary: $\partial_x F|_{x=x_2} = 0$, implies $\partial_x f|_{x=x_2} = 0$ (same on $g$) [5]. This is an additional boundary condition and thus the system is again overdetermined. The option of $U^{\text{coupling}}$ is not theoretically well founded and since one would like to retain the numerical simplicity and the robustness of the current approach the answer to point **(2)** becomes very important. The challenge proposed by this method is that of deriving the interpolation formula on the forces from first principles of statistical mechanics. In particular the formal determination of the latent heat $\phi$ would allow to remove the use of the thermostat and make the method internally consistent, possibly allowing for an explicit formula of some generalized thermodynamical potential.

## References

[1] M. Praprotnik, L. Delle Site and K. Kremer, *Adaptive resolution molecular dynamics simulation: Changing the degrees of freedom on the fly*, J.Chem.Phys. 123 (2005), 224106.

[2] L. Delle Site, *Some fundamental problems for an energy-conserving adaptive-resolution molecular dynamics scheme.*, Phys.Rev.E **76** (2007), 04770.

[3] M. Praprotnik, L. Delle Site and K. Kremer, *Adaptive Resolution Scheme (AdResS) for Efficient Hybrid Atomistic/Mesoscale Molecular Dynamics Simulations of Dense Liquids*, Phys.Rev.E **73** (2006), 066701.

[4] M. Praprotnik, L. Delle Site and K. Kremer, *Multiscale Simulation of Soft Matter: From Scale Bridging to Adaptive Resolution*, Annu.Rev.Phys.Chem. **59** (2008), 545–571.

[5] M. Praprotnik, K. Kremer and L. Delle Site, *Adaptive molecular resolution via a continuous change of the phase space dimensionality*, Phys.Rev.E **75** (2007), 017701.

[6] M. Praprotnik, K. Kremer and L. Delle Site, *Fractional dimensions of phase space variables: A tool for varying the degrees of freedom of a system in a multiscale treatment.* , J.Phys.A:Math.Gen. **40** (2007), F281-F288.

[7] M. Praprotnik, L. Delle Site and K. Kremer, *A macromolecule in a solvent: Adaptive resolution molecular dynamics simulation*, J.Chem.Phys. 126 (2007), 134902.

[8] M. Praprotnik, S. Matysiak, L. Delle Site, K. Kremer and C. Clementi, *Adaptive resolution simulation of liquid water* , J.Phys.Cond.Matt. 19 (2007), 292201.

[9] S. Matysiak, C. Clementi, M. Praprotnik, K. Kremer, and L. Delle Site, *Modeling Diffusive Dynamics in Adaptive Resolution Simulation of Liquid Water*, J.Chem.Phys. 128 (2008), 024503.

[10] B. Ensing, S.O. Nielsen, P.B. Moore, M.L. Klein, and M. Parrinello,*Energy Conservation in Adaptive Hybrid Atomistic/Coarse-Grained Molecular Dynamics*, J.Chem.Th.Comp.**3** (2007) 1100-1105.


## Atomistic Modeling of Surface Diffusion and Epitaxial Growth

Peter Kratzer

This contribution aims at identifying possible challenges for mathematicians in describing epitaxial growth on the atomic scale. The focus will be on specific materials, whose surface properties and whose epitaxial growth kinetics can be explored by performing density-functional theory calculations. An overview of how first-principles simulations can be applied to thin film growth of both metals [1] and semiconductors [2] can be found in the cited review articles.

The first part of this contribution is devoted to the modeling of surface diffusion. The basic concept in this field is the adiabatic potential energy surface (PES). It describes the potential energy of an adatom for all possible positions $(x, y)$ on a given substrate surface, taking into account the optimum adsorption height as well as relaxations of the substrate atoms. In cases where these relaxations are large, the PES is no more a single-valued function of the lateral position $(x, y)$, but in general a multi-valued function. In any case, detailed information about the PES of a specific system may be obtained from density-functional theory calculations. For a perfectly periodic surface of a crystal, the minima and saddle points of the PES can be mapped onto a periodic graph.

Modeling of epitaxial growth requires the bridging of time and length scales extending over several orders of magnitude. The smallest scales are associated

with atomic motion in the vicinity of a specific adsorption site (a minimum of the PES). The length scale of this process is Ångstrom, and the time scale is of the same order as for atomic vibrations in a crystal, i.e., $10^{-12}$ seconds. For an efficient description of diffusion, we need to go in most cases (when energy barriers are significantly larger than the thermal energy $k_BT$) to the much coarser description by discrete (possibly rare) events. These are hops between neighboring minima on the PES. The hopping rate can be calculated, at least approximately, within Transition State Theory. For studying growth on realistic samples (length scale micrometer or larger) and over time scales of seconds or longer, an even coarser description by a Fokker-Planck equation and the corresponding diffusion tensor is often appropriate. For perfectly ordered surfaces, i.e., for an infinite periodic network, the transition from discrete-event theory to a continuum description of diffusion is a mathematically well-defined procedure, which can be formalized e.g. by the concept of the continuous-time random walk.[3] We have followed these lines from density-functional theory via hopping rates to a diffusion tensor for a particular system, indium diffusion on a thin wetting layer of InAs on GaAs.[4] In cases where the surface is not perfectly ordered, e.g. because there are vacancies or additional adatoms present, it is still possible to calculate the energy barriers for all the occurring atomistic configurations. For calculating the diffusivity at a realistic, disordered surface close to thermal equilibrium, it is convenient to perform the thermal average by means of a kinetic Monte Carlo simulation. From its result, it is possible to extract the diffusivity, including its temperature dependence, as the long-time limit of the adatom's mean-square displacement.

As second topic of this contribution, I address the role of stress for hetero-epitaxy of lattice-mismatched systems. One materials system of particular interest is the growth of InAs on GaAs (lattice mismatch $\sim 7\%$), where spontaneous formation of three-dimensional islands of InAs is found to occur. After a second processing step, namely, overgrowth of these InAs islands by a capping layer of GaAs, these self-assembled nanostructures can be functionalized as quantum dots. Such nanostructures have already found technical applications in optoelectronic devices, and have a large technological potential for future information storage technologies and for quantum computing.

Density-functional theory calculations of thin epitaxial films of InAs on GaAs enable us to test the applicability of continuum elasticity theory to structures on the nanoscale. It turns out that continuum elasticity theory is useful for describing the elastic energy stored in thin films down to very small thickness of the film, typically $\sim 3$ monolayers. However, strained surfaces and interfaces display a linear term in the dependence of the elastic energy on strain which is lacking in bulk elasticity theory. This term, associated with surface or interface stress, is quantum-mechanical in origin and requires density-functional calculations for its proper quantification. It should be noted that bond-order potentials also allow to capture (at least in a qualitative way) the intrinsic surface or interface stress. For simulating growth kinetics, it is crucial to understand how energy barriers, e.g. diffusion barriers or the activation energy for desorption of molecules into the

gas phase, are affected by heteroepitaxial strain. Once again, density-functional calculations are able to provide us with this information: On metal surfaces, compressive strain usually leads to a smoothening of the potential energy surface, i.e. to a lowering of diffusion barriers.[5] On semiconductor surfaces, there is no unique trend (see, e.g. Ref. [6]); however, it has been proposed [7] that the response of diffusion barriers to strain is, at least to first order, governed by the intrinsic surfaces stress of the surface+adatom system, as compared to that of the bare surface.

We propose a promising route for the simulation of heteroepitaxial growth: The local stress at the surface of an epitaxial heterostructure is mostly determined by the mismatch strain, and can be calculated with reasonable precision by using continuum elasticity theory, e.g. in a finite-element implementation. Alternatively an atomistic model of the nanostructure together with a bond-order potential can be used to determine the relaxed positions of the atoms, and thus the remaining strain after relaxation. For the InAs/GaAs system, we have recently parameterized a bond-order potential of the Tersoff type that is capable of describing both the elastic properties of these materials and the surface energies of frequently found InAs and GaAs surfaces with good overall accuracy.[8] In a second step, it is necessary to determine the strain dependence of all kinetically relevant energy barriers by density-functional theory calculations. Third, kinetic Monte Carlo simulations are performed using rate constants derived from these energy barriers, including the effect of local strain at the surface of the nanostructure. The value of the strain is taken either from an atomistic model using the bond-order potential, or from a more coarse-grained continuum elasticity calculation, if applicable. As the local strain state of the surface changes while growth proceeds, it is required to relax the growing structures during the simulation in regular time intervals, and to update the local strain values (and thus the energy barriers).

The overall shape and the average size of the three-dimensional islands (or quantum dots) are mostly determined by thermodynamic considerations [9, 10], i.e., by an energy balance that takes both the elastic energy and the energy of the nanostructures' surfaces and edges into account. Recently, evidence has been given for the role of kinetics for some more subtle aspects of the island shape.[11] It has been found that the islands undergo an abrupt shape transition from a flat, pyramid- or hut-like shape to a steeper, dome-like shape as the islands grow larger. Identifying the atomistic mechanisms behind this kinetically driven shape transition will be one of the goals of future kinetic Monte Carlo simulations of heteroepitaxial growth.

## References

[1] P. Ruggerone, C. Ratsch, and M. Scheffler. *Density-functional theory of epitaxial growth of metals.* In: D. A. King and D. P. Woodruff (Eds.), *Growth and Properties of Ultrathin Epitaxial Layers.* Chemical Physics of Solid Surfaces, Vol. 8, Elsevier, Amsterdam (1997), 490–544.

[2] P. Kratzer and M. Scheffler. *Surface knowledge: Toward a predictive theory of materials.* Comp. Sci. Engineering **3** (2001), 16–25.

[3] J. W. Haus and K. W. Kehr. *Diffusion in regular and disordered lattices.* Phys. Rep. **150** (1987), 263–406.
[4] E. Penev, S. Stojković, P. Kratzer, and M. Scheffler. *Anisotropic diffusion of In adatoms on pseudomorphic $In_xGa_{1-x}As(001)$ films: First-principles total energy calculations.* Phys. Rev. B **69** (2004), 115335.
[5] C. Ratsch, A. P. Seitsonen, and M. Scheffler. *Strain dependence of surface diffusion: Ag on Ag(111) and Pt(111).* Phys. Rev. B **55** (1997), 6750–6753.
[6] E. Penev, P. Kratzer, and M. Scheffler. *Effect of strain on surface diffusion in semiconductor heteroepitaxy.* Phys. Rev. B **64** (2001), 085401.
[7] L. Huang, F. Liu, and X. G. Gong. *Strain effect on adatom binding and diffusion in homo- and heteroepitaxies of Si and Ge on ( 001 ) surfaces.* Phys. Rev. B **70** (2004), 155320.
[8] T. Hammerschmidt, P. Kratzer, and M. Scheffler. *Analytic many-body potential for the investigation of InAs/GaAs surfaces and nanostructures: Application to the formation energy of InAs quantum dots.* Phys. Rev. B **77** (2008), in print.
[9] L. G. Wang, P. Kratzer, M. Scheffler, and N. Moll. *Formation and stability of self-assembled coherent islands in highly mismatched heteroepitaxy.* Phys. Rev. Lett. **82** (1999), 4042–4045.
[10] L. G. Wang, P. Kratzer, N. Moll, and M. Scheffler. *Size, shape and stability of InAs quantum dots on the GaAs(001) substrate.* Phys. Rev. B **62** (2000), 1897–1904.
[11] P. Kratzer, Q. K. K. Liu, P. Acosta-Diaz, C. Manzano, G. Costantini, R. Songmuang, A. Rastelli, O. G. Schmidt, and K. Kern. *Shape transition during epitaxial growth of InAs quantum dots on GaAs(001): Theory and experiment.* Phys. Rev. B **73** (2006), 205347.

## Structure-preserving model reduction of partially observed differential equations: molecular dynamics and beyond

Carsten Hartmann
(joint work with V.-M. Vulcanov, Ch. Schütte)

Model reduction is a major issue for control, optimization and simulation of large-scale systems. We present a formal procedure for model reduction of perturbed linear second-order differential equations. Second-order equations appear in a variety of physical contexts, e.g., in molecular dynamics or structural mechanics to mention just a few. Common spatial decomposition methods such as Proper Orthogonal Decomposition, Principal Component Analysis or the Karhunen-Loève expansion aim at identifying a subspace of "high-energy" modes onto which the dynamics is projected (Galerkin projection). These modes, however, may not be relevant for the dynamics. Moreover these methods tacitly assume that all degrees of freedom can actually be observed or measured. An alternative procedure is known by the name of Balanced Truncation which is a method of model reduction for stable input-output systems. Unlike the aforementioned approaches Balanced Truncation accounts for incomplete observability. It consists in finding a coordinate transformation such that modes which are least sensitive to the external perturbation (controllability) also give the least output (observability) and therefore can be neglected. Accordingly, a dimension-reduced model is obtained by restricting the dynamics to the subspace of the best controllable and observable modes. A great advantage of the method is that it gives computable *a priori* error bounds; a drawback is that it typically fails to preserve the problem's physical structure and suffers from lack of stability [1, 2].

Here we adopt the framework of port-Hamiltonian systems which covers the class of relevant problems and that allows for a generalization of Balanced Truncation to second-order problems, while preserving stability and the underlying Hamiltonian structure. The restriction to the controllable/observable subspace is done by imposing a holonomic constraint using techniques from singular perturbation theory for deterministic or stochastic differential equations.

Given a quadratic Hamiltonian $H : \mathbb{R}^n \times \mathbb{R}^n \to \mathbb{R}$, we consider the system

$$\begin{aligned} \dot{x}(t) &= (J - D)\,\nabla H(x(t)) + Bu(t) \\ y(t) &= C\nabla H(x(t))\,, \end{aligned} \tag{1}$$

where $J = -J^T$ is the invertible skew-symmetric structure matrix, $D = D^T \succeq 0$, and $y \in \mathbb{R}^l$ denotes a linear observable. The function $u(\cdot) \in \mathbb{R}^m$ may be either deterministic or random. As can be readily checked, the second-order equation

$$\begin{aligned} M\ddot{x}_1(t) + R\dot{x}_1(t) + Lx_1(t) &= B_2 u(t) \\ y(t) &= C_1 x_1(t) + C_2 \dot{x}_1(t) \end{aligned}$$

is an instance of the port-Hamiltonian system (1).

## 1. Deterministic systems

We shall make make precise what it means that a state $x \in \mathbb{R}^n \times \mathbb{R}^n$ is controllable or observable. Let us assume that (1) is stable, i.e., all eigenvalues of $A = (J - D)\nabla^2 H$ are lying in the open left complex half-plane. Let us first confine ourselves to the case $u \in L^2(\mathbb{R})$ and consider the controllability function

$$L_c(x) = \min_{u \in L^2} \int_{-\infty}^{0} |u(t)|^2\, dt\,, \quad x(-\infty) = 0,\, x(0) = x$$

that measures the minimum energy that is needed to steer the system from $x(-\infty) = 0$ to $x(0) = x$. In turn, the observability function

$$L_0(x) = \int_{0}^{\infty} |y(t)|^2\, dt\,, \quad x(0) = x,\, u \equiv 0$$

measures the control-free energy of the output as the system evolves from $x(0) = x$ to $x(\infty) = 0$ (asymptotic stability). It is easy to see that

$$L_c(x) = x^T Q^{-1} x\,, \quad L_o(x) = x^T P x\,,$$

where the controllability Gramian $Q$ and the observability $P$ are the unique symmetric solutions of the Lyapunov equations

$$AQ + QA^T = -BB^T\,, \quad A^T P + PA = -W^T W$$

with the shorthands $A = (J - D)\nabla^2 H$ and $W = C\nabla^2 H$. Moore [3] has shown that if $Q, P \succ 0$ (complete controllability/observability) there exists a coordinate transformation $x \mapsto Tx$, such that the two Gramians become equal and diagonal,

$$T^{-1} Q T^{-T} = T^T P T = \operatorname{diag}(\sigma_1, \ldots, \sigma_{2n})\,.$$

The $\sigma_i$ are called the Hankel singular values of the system; they are positive and independent of the choice of coordinates. In the balanced representation all

states that are least controllable also give the lowest output (small Hankel singular values), and it seems reasonable to truncate these states. The usual approach of projecting the system onto, say, the first $d < 2n$ column of $T$ does not preserve the port-Hamiltonian structure as the balancing transformation mixes positions and generalized momenta. From a physical viewpoint it makes sense to consider the limit of vanishing small singular values, thereby forcing the system to the chosen subspace. To this end we scale the Hankel singular values according to

$$(\sigma_1, \ldots, \sigma_d, \sigma_{d+1}, \ldots, \sigma_{2n}) \mapsto (\sigma_1, \ldots, \sigma_d, \delta\sigma_{d+1}, \ldots, \delta\sigma_{2n}) \tag{2}$$

with $\delta > 0$ which implies that the balancing transformation $T = T_\delta$ becomes $\delta$-dependent as well. Upon introducing balanced coordinates $\xi = T_\delta^{-1} x$, the port-Hamiltonian system (1) becomes the singularly perturbed system of equations

$$\begin{aligned}
\dot\xi_1^\delta &= (\tilde J_{11} - \tilde D_{11})\frac{\partial \tilde H^\delta}{\partial \xi_1} + \frac{1}{\sqrt\delta}(\tilde J_{12} - \tilde D_{12})\frac{\partial \tilde H^\delta}{\partial \xi_2} + \tilde B_1 u \\
\dot\xi_2^\delta &= \frac{1}{\sqrt\delta}(\tilde J_{21} - \tilde D_{21})\frac{\partial \tilde H^\delta}{\partial \xi_1} + \frac{1}{\delta}(\tilde J_{22} - \tilde D_{22})\frac{\partial \tilde H^\delta}{\partial \xi_2} + \frac{1}{\sqrt\delta}\tilde B_2 u \\
y^\delta &= \tilde C_1 \frac{\partial \tilde H^\delta}{\partial \xi_1} + \frac{1}{\sqrt\delta}\tilde C_2 \frac{\partial \tilde H^\delta}{\partial \xi_2}\,,
\end{aligned} \tag{3}$$

where $\tilde J - \tilde D = T_1^{-1}(J - D)T_1^{-T}$, $\tilde B = T_1^{-1}B$, $\tilde C = CT_1^{-T}$, and the partition of $\xi = (\xi_1, \xi_2) \in \mathbb{R}^d \times \mathbb{R}^{2n-d}$ is according to the separation of singular values. The balanced Hamiltonian is given by $\tilde H^\delta(\xi) = H(T_\delta \xi)$. We have proved in [4] borrowing arguments from geometric singular perturbation theory that the system collapses to the controllable/observable subspace as $\delta \to 0$. The limit system

$$\begin{aligned}
\dot\xi_1(t) &= (\tilde J_{11} - \tilde D_{11})\nabla \bar H(\xi_1(t)) + \tilde B_1 u(t) \\
\bar y(t) &= \tilde C_1 \nabla \bar H(\xi_1(t))
\end{aligned} \tag{4}$$

turns out to be a stable port-Hamiltonian system with the effective energy

$$\bar H(\xi_1) = \frac{1}{2}\xi_1^T \tilde E_1 \xi_1\,, \quad \tilde E_1 = \tilde E_{11} - \tilde E_{12}\tilde E_{22}^{-1}\tilde E_{12}^T\,, \tag{5}$$

where $\tilde E = \nabla^2 \tilde H^{\delta=1}$ in the last equation. As following from standard singular perturbation results [5] for linear control systems (4) satisfies the error bound

$$\sup_\omega \|G(i\omega) - \bar G(i\omega)\| < 4(\sigma_{d+1}, \ldots, \sigma_{2n})\,.$$

Here $G$ and $\bar G$ are the matrix-valued transfer functions associated with (1) and (4) and $\|\cdot\|$ denotes spectral norm.

## 2. Partially observed Langevin equation

In equation (1), we replace the smooth control variable by Gaussian white noise, and consider the family of stable hypoelliptic Langevin equations

$$\begin{aligned}
\dot X_t^\varepsilon &= (J - D)\,\nabla H(X_t^\varepsilon) + \sqrt\varepsilon B \dot W_t \\
Y_t^\varepsilon &= C \nabla H(X_t^\varepsilon)\,,
\end{aligned} \tag{6}$$

where $W_t$ is standard Brownian motion in $\mathbb{R}^n$, and the parameter $\varepsilon > 0$ controls the temperature in the system. If $2D = BB^T$ the system admits the ergodic invariant measure $d\mu^\varepsilon \propto \exp(-H/\varepsilon)$.

There is no control variable any longer, but we may ask to what extend a state can be excited by the noise. To this end we define the rate function

$$L_r(x) = \inf_{W \in H^1} \int_0^T |\dot{W}(t)|^2 \, dt \,, \quad X_0^\varepsilon = 0, \, X_T^\varepsilon = x$$

and declare that $L_r(x) = \infty$ if no such realization $W \in H^1([0,T])$ exists. The typical white noise realizations are only Hölder continuous with exponent $\alpha = 1/2$, hence not absolutely continuous. At low temperature, however, Large Deviations Theory [6] asserts that the realizations of $W$ concentrate around (measure-zero) paths that are smooth. As we have shown in [7] the rate function is given by

$$L_r(x) = x^T \Sigma_T^{-1} x \,, \quad \Sigma_T = \mathbf{E}(X_T^\varepsilon \otimes X_T^\varepsilon) \,.$$

For $T \to \infty$, the rate Gramian (i.e., the covariance matrix) can again be computed as the unique positive definite solution of the Lyapunov equation

$$A\Sigma + \Sigma A^T = -\varepsilon BB \,.$$

Keeping the previous notion of observability (i.e., $L_o(x)$ for $\varepsilon = 0$), we can balance the system such that states that are most sensitive to the noise also give the highest output. Scaling the Hankel singular values according to (2) yields again a singularly perturbed system of the form (3). Unlike in the deterministic case, sending $\delta$ to zero does not result in contraction to the most excitable/observable subspace but rather in fast random oscillations around this subspace. In the limit $\delta \to 0$ the fast modes become Gaussian random variables with mean $-\tilde{E}_{22}^{-1}\tilde{E}_{12}^T\xi_1$ and covariance $\varepsilon\tilde{E}_{22}^{-1}$ and the Langevin process $Y_t^\varepsilon = C\nabla H(X_t^\varepsilon)$ converges in probability to the solutions of the low-dimensional Langevin equation (cf. [8])

$$\begin{aligned} \dot{Z}_t^\varepsilon &= (\tilde{J}_{11} - \tilde{D}_{11})\nabla\bar{H}(Z_t^\varepsilon) + \sqrt{\varepsilon}\tilde{B}_1\dot{W}_t \\ \bar{Y}_t^\varepsilon &= \tilde{C}_1\nabla\bar{H}(Z_t^\varepsilon) \end{aligned} \tag{7}$$

with $2\tilde{D}_{11} = \tilde{B}_1\tilde{B}_1^T$ and $\bar{H}$ as given in (5). The reduced system admits an ergodic invariant measure $d\rho^\varepsilon \propto \exp(-\bar{H}/\varepsilon)$. Moreover $\bar{H}$ is independent of $\varepsilon$ and has the meaning of the thermodynamical free energy

$$\bar{H}(z) = -\varepsilon \ln \mathbf{P}_\varepsilon(z) \,, \quad \mathbf{P}_\varepsilon(z) = \int \delta(\xi_1 - z) d\mu^\varepsilon \,.$$

## References


[1] Y. Chahlaoui, D. Lemonnier, A. Vandendorpe and P. Van Dooren. Second-order balanced truncation. *Linear Algebra and its Applications* **415** (2006), 373–384.

[2] T. Reis and T. Stykel.Balanced truncation model reduction of second-order systems. *Math. Comput. Model. Dyn. Syst.* (2008), to appear.

[3] B.C. Moore. Principal component analysis in linear systems: controllability, observability, and model reduction. *IEEE Trans. Auto. Contr.* **AC-26** (1981), 17–32.

[4] C. Hartmann, V.-M. Vulcanov, and Ch. Schütte.Balanced truncation of second-order systems: structure-preservation and stability, *J. Opt. Control* (2007), submitted.

[5] Y. Liu and B.D.O. Anderson. Singular perturbation approximation of balanced systems. *Int. J. Control* **50** (1989), 1379–1405.
[6] D.W. Stroock and S.R.S. Varadhan.On the support of diffusion processes with applications to the strong maximum principle. *Berkeley Symp. Math. Statist. Prob.* **3** (1972) 333–359.
[7] C. Hartmann and Ch. Schütte.Balancing of partially observed stochastic differential equations, *IEEE Conf. Decisions and Control* (2008), submitted.
[8] A. Yu Veretennikov.On rate of mixing and the averaging principle for hypoelliptic stochastic differential equations. *Math. USSR Izv.* **33** (1989), 221–231.

## Challenges in the Atomistic Modelling of Magnetic Materials

David Pettifor and Ralf Drautz

The development of analytic interatomic potentials for modelling the properties of magnetic materials presents a considerable challenge. Whereas noble gas solids and ionic systems are well described by simple pair potentials such as Lennard-Jones or Born-Mayer, magnetic alloys such as the iron-chromium ferritic-martensitic steels require interatomic potentials that are dependent not only on the nature of the local magnetic order (for example, ferromagnetic or anti-ferromagnetic) but also on the average number of valence electrons per atom $N$ (where across the Fe-Cr phase diagram $N$ ranges from 8 for pure iron to 6 for pure chromium).

We are addressing this problem of developing valence-dependent magnetic interatomic potentials by coarse graining the electronic structure in two well-defined stages. In the first stage density functional theory (DFT), which writes the energy as a functional of the electronic charges density $n(\boldsymbol{r})$ at each point $\boldsymbol{r}$ in space, is discretized within the tight-binding (TB) approximation by expressing the energy in terms of the two-centre bond integrals $\beta\left(\boldsymbol{R}_i - \boldsymbol{R}_j\right)$ between atoms centred at $\boldsymbol{R}_i$ and $\boldsymbol{R}_j$ [1]. In the second stage, the bond-order potential (BOP) theorem [2] is used to expand the on-site density matrix elements $\rho_{ii}$ and the intersite density matrix elements $\rho_{ij}$ in terms of the moments $\mu_i^p = \langle\phi_i|\,\hat{H}^p\,|\phi_i\rangle$ and interference paths $\zeta_{ij}^p = \langle\phi_i|\,\hat{H}^p\,|\phi_j\rangle$ respectively. This allows the energy to be expressed explicitly in the form of a many-body interatomic potential because $\mu_i^p$ and $\zeta_{ij}^p$ can be obtained by summing over all hopping or bonding paths of length $p$ that either start and end on atom $i$ or link the two ends of the bond $ij$ [3, 4].

The Stoner theory of band magnetism [5] is currently being included within the BOP formalism [6] so that magnetic alloys such as Fe-Cr can be modelled explicitly. It was already shown [7] nearly three decades ago that a simple second-moment rectangular band model led to a Ginzburg-Landau expansion for the magnetic energy of the form

$$\hat{U}_{\mathrm{mag}} = -A\,\hat{\Delta}^2 + B\,\hat{\Delta}^4,$$

where $\hat{U}_{\mathrm{mag}}$ and $\hat{\Delta}$ are the magnetic energy and local exchange field normalized by the band width $W$. Importantly the prefactors $A$ and $B$ depend not only on the relative orientation of the local magnetic moments $\theta$ but also on the number of valence 3d-electrons $N_d$ and normalized Stoner exchange integral $\hat{I} = I/W$

through

$$A = \left[ -\frac{1}{40\hat{I}^2} + \frac{3}{80} N_d \left(10 - N_d\right) \right] + \left[ \frac{1}{4\hat{I}} - \frac{1}{40\hat{I}^2} - \frac{3}{80} N_d \left(10 - N_d\right) \right] \cos\theta$$

$$B = \frac{3}{320\hat{I}^2} \left(1 - \cos 2\theta\right) + \frac{9}{1280} N_d \left(10 - N_d\right) \left(3 - 4\cos\theta + \cos 2\theta\right).$$

Although this simple model accounted for the observed valence-dependent trend of anti-ferromagnetism to ferromagnetism across the 3d transition metals from chromium through nickel [7], it cannot predict the relative stability of the different phases of iron, namely $\alpha$ (body-centred cubic), $\gamma$ (face-centred cubic) and $\epsilon$ (hexagonal close packed). This requires knowledge of the higher moments of the density of states [8] that are automatically included within the BOP formalism [6].

However, numerous challenges will have to be overcome before these BOPs achieve wide-spread use within the atomistic modelling community. Firstly, the potential is much more *complicated* than simple pair potentials or second-moment-based potentials, so that MD simulations are currently about two orders of magnitude slower than conventional schemes. Secondly, the analytic form of the potential is derived by coarse graining the DFT results within a TB framework, so that its *accuracy* would be questionable for systems such as the nickel superalloys which are poorly described by TB. Thirdly, the analytic form for the d-valent transition metals is based on a Chebyshev expansion of the *continuum* of states for a single band [6], whereas the analytic form for the sp-valent semiconductors and hydrocarbons is based on a *discrete* set of states [1, 9], so that simulating heterovalent sp-d systems such as the transition metal carbides remains an outstanding mathematical challenge.

## References


[1] Drautz, R., Zhou, X.W., Murdick, D.A., Gillespie, B., Wadley, H.N.G., and Pettifor, D.G.: *Analytic bond-order potentials for modelling the growth of semiconductor thin films.* Progress in Materials Science **52** (2007) 196–229.

[2] Aoki, M. and Pettifor, D.G.: *Angularly-dependent many-atom bond-order potentials within tight-binding Hückel theory.* In Physics of Transition Metals, Edds. Oppeneer, P.M. and Kübler, J. (World Scientific, Singapore) **1** (1993) 299–304.

[3] Pettifor, D.G.: *New many-body potential for the bond order.* Physical Review Letters **63** (1989) 2480.

[4] Pettifor, D.G. and Aoki, M.: *Bonding and structure of intermetallics: a new bond-order potential.* Philosophical Transactions of the Royal Society of London **A334** (1991) 439–449.

[5] Stoner, E.C.: *Collective electron ferromagnetism.* Philosophical Transactions of the Royal Society of London **A165** (1938) 372–414.

[6] Drautz, R. and Pettifor, D.G.: *Valence-dependent analytic bond-order potentials for transition metals.* Physical Review **B74** (2006) 174117.

[7] Pettifor, D.G.: *Electronic structure calculations and magnetic properties.* Journal of Magnetism and Magnetic Materials **15-18** (1980) 847–852; unpublished notes (1979).

[8] Hasegawa, H. and Pettifor, D.G.: *Microscopic theory of the temperature- pressure phase diagram of iron.* Physical Review Letters **50** (1983) 130–133.

[9] Pettifor, D.G. and Oleinik, I.I.: *Bounded analytic bond-order potentials for $\sigma$ and $\pi$ bonds.* Physical Review Letters **84** (2000) 4124–4127.

## Quantum Simulation of Materials at Micron Scales and Beyond

Gang Lu
(joint work with Qing Peng, Xu Zhang, Linda Hung, Emily A. Carter)

The ability to perform quantum simulations of materials properties over length scales that are relevant to experiments represents a grand challenge in computational materials science. If one could treat multi-millions or billions of electrons *effectively* at micron scales, such first-principle quantum simulations could revolutionize materials research and pave the way to the computational design of advanced materials. There are two principal reasons why quantum simulations at relevant experimental scales are important. First of all, it allows a direct comparison between theory and experiment. Secondly, quantum simulations at larger scales are essential even for extended bulk crystals where periodic boundary conditions may be used. This is due to the fact that a real bulk solid always contains lattice defects (or impurities) whose interactions are long range - dislocations being the prominent example. An insufficiently large periodic unit cell would lead to unrealistically high concentrations of defects and/or impurities, rendering the results of such simulations questionable.

We propose a multiscale approach that is based *entirely* on density functional theory (DFT) and allows quantum simulations at the micron scale and beyond. The method, termed QCDFT, combines the coarse graining idea of the quasicontinuum (QC) approach and the coupling strategy of the quantum mechanics/molecular mechanics (QM/MM) method, and represents a major advance in the quantum simulation of materials properties. It should be stated at the outset that QCDFT is *not* a brute-force electronic structure method, but rather a multiscale approach that can treat large systems - effectively up to billions of electrons. Therefore, some of the electronic degrees of freedom are reduced to continuum degrees of freedom in QCDFT. On the other hand, although QCDFT utilizes the idea of QM/MM coupling, it does not involve any classical/empirical potentials (or force fields) in the formulation - the energy calculation of QCDFT is entirely based on orbital-free DFT (OFDFT). This is an important feature and advantage of QCDFT, which qualifies it as a bona fide quantum simulation method.

QCDFT is formulated within the framework of the QC method, which models an atomistic system without explicitly treating every atom in the problem [1, 2]. This is achieved by replacing the full set of $N$ atoms with a small subset of $N_r$ "representative atoms" or *repatoms* ($N_r \ll N$) that approximate the total energy through appropriate weighting. Atoms experiencing large variations in the deformation gradient field on an atomic scale are computed in the same way as in a standard atomistic method and these atoms are called *nonlocal* atoms to reflect the fact that their energy depends on the positions of their neighbors in addition to their own position. In contrast, the energies of atoms experiencing a smooth deformation field on the atomic scale are computed based on the deformation gradient $\{\mathbf{G}\}$ in their vicinity as befitting a continuum model. These atoms are called *local* atoms because their energy is based only on the deformation gradient

at the point where it is computed. The basic assumption employed is the Cauchy-Born rule, which relates the continuum deformation at a point to the motion of the atoms in the underlying lattice represented by this point.

The calculations of energy and stress in the continuum regions is based on OFDFT, which is the same energy formulation used in the nonlocal atomistic region. This makes the passage from the atomistic to continuum regions seamless since the same underlying material description is used in both. OFDFT is an efficient implementation of density functional theory which approximates the kinetic energy of noninteracting electrons in terms of their density, instead of the KS orbitals [3]. In OFDFT, the total energy is expressed as an explicit functional of electron density $\rho(\mathbf{r})$:

$$E_{\mathrm{OF}}[\rho] = T_{\mathrm{s}}[\rho] + E_{\mathrm{H}}[\rho] + E_{\mathrm{e-i}}[\rho] + E_{\mathrm{xc}}[\rho] + E_{\mathrm{i-i}}. \tag{1}$$

The various terms in Eq. (1) represent the non-interacting electronic kinetic energy, the Hartree electron repulsion energy, the electron-ion attraction energy, the electron exchange-correlation energy, and the ion-ion repulsion energy, respectively.

The energy and force of each local repatom can be obtained from the strain energy density and the stress tensor of the finite elements that share the same repatom. More specifically, according to the Cauchy-Born rule, the deformation gradient $\mathbf{G}$ is uniform within a finite element, therefore the local energy density $\varepsilon$ and the stress tensor for each finite element can be calculated as a perfect infinite crystal undergoing a uniform deformation specified by $\mathbf{G}$. In other words, one could perform an OFDFT-based energy/stress calculation for an infinite crystal by using periodic boundary conditions with the primitive lattice vectors of the deformed crystal. Once the strain energy density $\varepsilon(\mathbf{G}_k)$ is determined, the energy contribution of the $j$th local repatom is given as

$$E_j^{\mathrm{loc}}(\{\mathbf{G}\}) = \sum_{k=1}^{M_j} w_k \varepsilon(\mathbf{G}_k)\Omega_0, \tag{2}$$

where $M_j$ is the total number of finite elements represented by the $j$th repatom, and $w_k$ is the weight assigned to the $k$th finite element. The force on the $j$th local repatom is defined as the gradient of the total energy with respect to its coordinate $\mathbf{R}_j^{\mathrm{loc}}$.

For the energy/force calculation in the nonlocal region, we resort to a novel QM/MM approach that was developed recently for metals [4]. The coupling between the QM and MM regions is achieved quantum mechanically within an OFDFT formulation. We wish to stress two important points here: (1) The original QC formulation assumes that the total energy can be written as a sum over individual atomic energies. This condition is not satisfied by quantum mechanical models. The total energy of QCDFT should be expressed as:

$$E_{\mathrm{tot}}^{\mathrm{QCDFT}} = E^{\mathrm{nl}}[\rho^{\mathrm{tot}}] + \sum_{j=1}^{N^{\mathrm{loc}}} n_j E_j^{\mathrm{loc}}(\{\mathbf{G}\}). \tag{3}$$

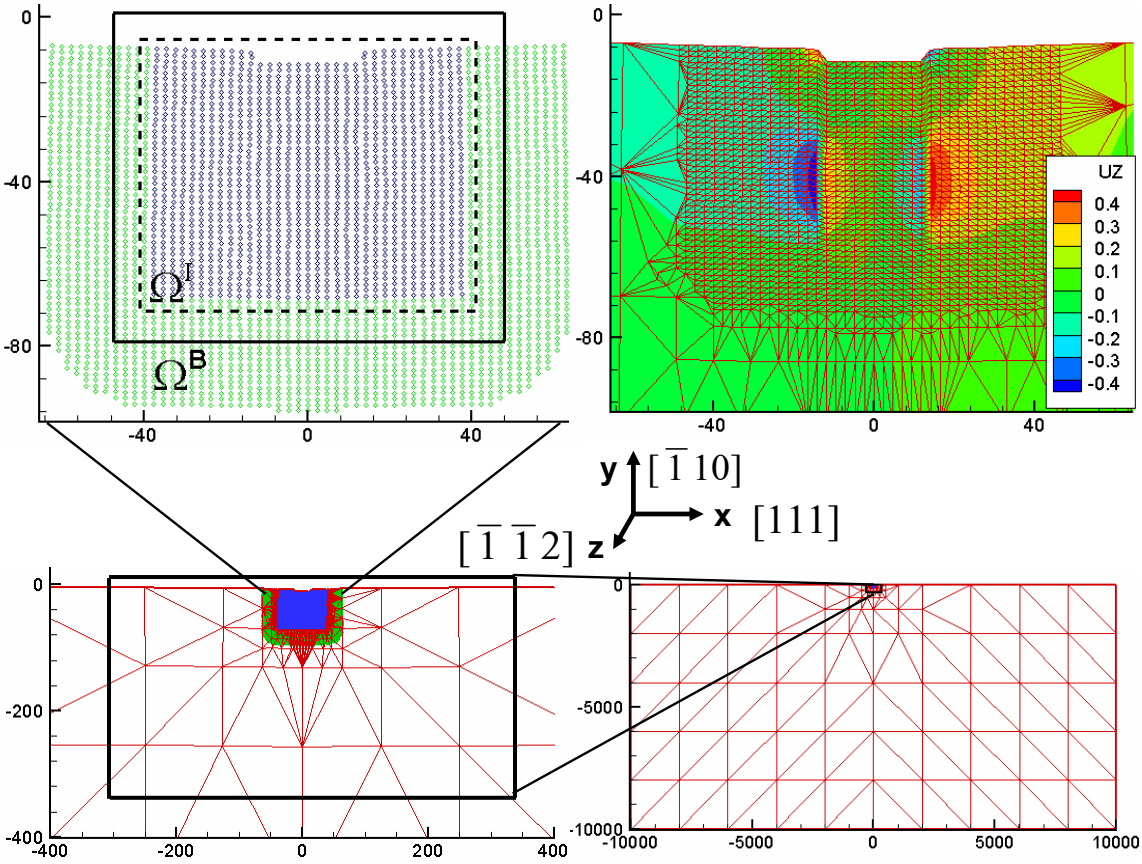


Figure 1: (Color online) The overview of the entire system and domain partition in QCDFT with nanoindentation as an example. The x, y and z axes are along [111],[$\bar{1}$10], and [$\bar{1}\bar{1}$2], respectively. $\Omega^{\mathrm{I}}$ and $\Omega^{\mathrm{B}}$ are 2.8 Å and 8 Å beyond the nonlocal region in $\pm x$ and $\pm y$ directions, respectively [4]. The colors indicate $u_z$, the out-of-plane displacement of atoms in the z-direction.

Here $\rho^{tot}$ is the total electron density in the nonlocal region as well as the coupling nonlocal/local region i.e., the buffer region in the following discussion. (2) The nonlocal energy, $E^{\mathrm{nl}}$ should be calculated with appropriate boundary conditions; that is to say, it should include the interaction energy between the nonlocal atoms and neighboring local atoms. In the original QC framework, this requirement is realized by including dummy atoms in the energy/force calculation of a given nonlocal repatom. These dummy atoms are in the local region and within the cut-off radius of the given nonlocal repatom. The dummy atoms are not independent degrees of freedom in the local region, but rather slaves to the local repatoms. In this way, the nonlocal calculation is carried out with the appropriate boundary conditions, and at the same time, the energy of the dummy atoms is still treated with the Cauchy-Born rule, consistent with their status. In the QCDFT approach, a buffer region including the dummy atoms and local repatoms that are adjacent to the nonlocal repatoms is selected as the "MM" region, and the nonlocal

atoms constitute the QM region. The nonlocal atoms are treated by OFDFT, and the coupling between the "MM" and QM region is also formulated within OFDFT. Therefore the entire system is formulated with one energy functional, OFDFT. Note that "MM" here is actually a misnomer: the local atoms are treated by OFDFT with the Cauchy-Born rule as mentioned earlier, and we retain the designation "MM" solely to indicate the similarity to the earlier coupling scheme [4].

The present QCDFT approach is applied to nanoindentation of an Al thin film resting on a rigid substrate with a rigid knife-like indenter. The crystallographic orientation of the system is displayed in Fig. (1). The size of the entire system is 2 $\mu$m $\times$ 1 $\mu$m $\times$ 4.9385 Å along the [111] (x direction), the $[\bar{1}10]$ (y direction), and the $[\bar{1}\bar{1}2]$ (z direction), respectively. The system is periodic in the z-dimension, has Dirichlet boundary conditions in the other two directions, and contains over 60 million Al atoms - a size that is well beyond the reach of any full-blown brute-force quantum calculation. The simulation is performed quasistatically with a displacement control where the indentation depth ($d$) is increased by 0.2 Å at each loading step. The final configurations were achieved by the relaxation of all repatoms using a conjugate gradient method until the maximum force on any repatom is less than 0.03 eV/Å.

The QCDFT results are validated by comparing against conventional QC with a OFDFT-refined EAM potential. The results suggest that QCDFT is an excellent method which represents a new direction for quantum simulation of materials properties at length scales relevant to experiments.

## References

[1] E.B. Tadmor, M. Ortiz, and R. Phillips, Philos. Mag. A **73**, 1529 (1996).
[2] V.B. Shenoy *et al.*, J. Mech. Phys. Solids **47**, 611 (1999).
[3] Y.A. Wang and E.A. Carter, in *Theoretical Methods in Condensed Phase Chemistry*, edited by S.D. Schwartz (Kluwer, Dordrecht, 2000) Chap. 5.
[4] X. Zhang and G. Lu, Phys. Rev. B **76**, 245111 (2007).

## Continuum approximation of the Peach-Koehler force on dislocations in a slip plane

Yang Xiang

We derive a continuum model for the Peach-Koehler force on dislocations in a slip plane. To represent the dislocations, we use the disregistry across the slip plane, whose gradient gives the density and direction of the dislocations. The continuum model is derived rigorously from the Peach-Koehler force on dislocations in a region that contains many dislocations. The resulting continuum model can be written as the variation of an elastic energy that consists of the contribution from the long-range elastic interaction of dislocations and a correction due to the line tension effect.

We consider dislocations $\gamma_j$, $j = ..., -2, -1, 0, 1, 2, ...$ in the $xy$ plane with the same Burgers vector $\mathbf{b}$. Without loss of generality, assume that the Burgers vector

is in the direction of the $x$ axis: $\mathbf{b} = (b, 0)$. We further assume that these dislocations are modulated from an array of straight parallel dislocations with same direction. We focus on a domain whose size $L$ is much larger than the length of the Burgers vector $b$ and which contains many dislocations, and assume periodic boundary conditions. The curvature of the dislocations is of $O(1/L)$. This kind of dislocation configurations can be found, e.g., when an array of dislocations moving in the slip plane and bypassing weak penetrable particles.

At a point $(x, y)$ on the dislocation $\gamma_n$, the Peach-Koehler force in the normal direction is

$$f = \sigma_{13}(x, y)b, \tag{1}$$

where

$$\begin{aligned} \sigma_{13}(x,y) &= \int_{-\infty}^{\infty} \delta(\omega)d\omega \int_{\gamma_n^\omega} \frac{\mu b}{4\pi}\left(\frac{\mathbf{r}\cdot\mathbf{n}}{r^3} + \frac{\nu}{1-\nu}\frac{(\mathbf{n}\cdot\mathbf{b})(\mathbf{r}\cdot\mathbf{b})}{b^2r^3}\right)ds \\ &\quad + \sum_{j\neq n}\int_{\gamma_j} \frac{\mu b}{4\pi}\left(\frac{\mathbf{r}\cdot\mathbf{n}}{r^3} + \frac{\nu}{1-\nu}\frac{(\mathbf{n}\cdot\mathbf{b})(\mathbf{r}\cdot\mathbf{b})}{b^2r^3}\right)ds. \end{aligned} \tag{2}$$

is a stress component at the point $(x, y)$. Here

$$\gamma_n^\omega = \{(x_1, y_1) + \omega\mathbf{n}(x_1, y_1) : (x_1, y_1) \in \gamma_n\}, \tag{3}$$

$\mathbf{n}(x_1, y_1)$ is the normal direction of dislocation $\gamma_n$ at the point $(x_1, y_1)$, $\delta(\omega)$ is a regularized delta function in the direction perpendicular to the dislocation representing the dislocation core, whose width is of the order of the Burgers vector $b$, $\mathbf{r} = (x - x_1, y - y_1)$, $r = \sqrt{(x - x_1)^2 + (y - y_1)^2}$, $\mu$ is the shear modulus, and $\nu$ is the Poisson ratio.

We use disregistry across the slip plane in the direction of the Burgers vector $\phi(x, y)$ to represent the continuous distribution of dislocations, as in the Peierls-Nabarro models. In the framework of dislocation based continuum plasticity theories, we are interested in a smooth profile of the density of dislocations without resolving the details of the core region. For this purpose, we define the function $\phi(x, y)$ to be a smooth approximation of the exact disregistry that connects the disregistry across dislocations smoothly. Using this representation, the density of the dislocation is given by $|\nabla\phi|$, the dislocation line direction is given by $\nabla\phi/|\nabla\phi| \times \mathbf{k} = (\phi_y, -\phi_x)/\sqrt{\phi_x^2 + \phi_y^2}$, where $\mathbf{k}$ is the unit vector in the $z$ direction, and the normal direction of the dislocation line is $\nabla\phi/|\nabla\phi|$.

The continuum approximation of the Peach-Koehler force, keeping the two leading order terms as $b \to 0$, is

$$
\begin{aligned}
f(x,y) &= \int_{\mathbf{R}^2} \frac{\mu b}{4\pi}\left(\frac{\mathbf{r}\cdot\nabla\phi}{r^3}+\frac{\nu}{1-\nu}\frac{(\nabla\phi\cdot\mathbf{b})(\mathbf{r}\cdot\mathbf{b})}{b^2r^3}\right)dx_1dy_1 \\
&\quad -\frac{\mu b^2}{4\pi}\left(\frac{1+\nu}{1-\nu}-\frac{3\nu}{1-\nu}\frac{(\mathbf{b}\cdot\nabla\phi)^2}{b^2|\nabla\phi|^2}\right)\nabla\cdot\left(\frac{\nabla\phi}{|\nabla\phi|}\right)\log\frac{b}{2\pi r_c|\nabla\phi|} \\
&\quad +\frac{\mu b^2}{4\pi}\left(1+\frac{\nu}{1-\nu}\frac{(\mathbf{b}\cdot\nabla\phi)^2}{b^2|\nabla\phi|^2}\right)\frac{\nabla\phi D^2\phi\nabla^T\phi}{|\nabla\phi|^3} \\
&\quad -\frac{\mu b^2\nu}{\pi(1-\nu)}\frac{(\mathbf{b}\cdot\nabla\phi)(\mathbf{b}\cdot(\nabla\phi\times\mathbf{k}))}{b^2|\nabla\phi|^2}\nabla\cdot\left(\frac{\nabla\phi\times\mathbf{k}}{|\nabla\phi|}\right).
\end{aligned} \tag{4}
$$

It can be written as the variation of the elastic energy $E$:

$$
f/b=\sigma_{13}=\frac{\delta E}{\delta\phi}, \tag{5}
$$

where

$$
\begin{aligned}
E &= \frac{1}{2}\int_{\mathbf{R}^2}\phi(x,y)dxdy\int_{\mathbf{R}^2}\left(\frac{\mathbf{r}\cdot\nabla\phi}{r^3}+\frac{\nu}{1-\nu}\frac{(\nabla\phi\cdot\mathbf{b})(\mathbf{r}\cdot\mathbf{b})}{b^2r^3}\right)dx_1dy_1 \\
&\quad +\int_{\mathbf{R}^2}\frac{\mu b}{4\pi}\left[\left(1+\frac{\nu}{1-\nu}\frac{(\mathbf{b}\cdot\nabla\phi)^2}{b^2|\nabla\phi|^2}\right)\log\frac{b}{2\pi r_c|\nabla\phi|}\right. \\
&\quad \left.+1+\frac{\nu}{3(1-\nu)}\left(2-\frac{(\mathbf{b}\cdot\nabla\phi)^2}{b^2|\nabla\phi|^2}\right)\right]|\nabla\phi|dxdy.
\end{aligned} \tag{6}
$$

The first integral in the above elastic energy corresponds to the well-known leading order, linear nonlocal term in the continuum approximation of the Peach-Koehler force. The second integral is a correction at the next order of $b$, whose physical meaning is the self energy of the dislocations, and which gives the last three local but nonlinear terms in the continuum approximation of the Peach-Koehler force given above.

The method we used in the derivation is to consider the Peach-Koehler force on the dislocation given by Eq. (2) as a numerical discretization of the well-known integral expression, with the length of Burgers vector $b$ as the numerical grid constant. An accurate continuum approximation of the Peach-Koehler force can be obtained by finding the error terms of the above numerical discretization. In the derivation, we have used the theorems on the error estimate of the trapezoidal rule for singular integrals (Sidi and Israeli, 1988; Xu and Xiang, 2008).

Although the formulas in Eqs. (4) and (6) are derived when the Burgers vector is in the direction of the $x$ axis, they hold when the Burgers vector is in any direction in the slip plane. Moreover, the derived approximation is expected to be a good approximation for any distribution of dislocations with the same Burgers vector as long as the curvature radius of the dislocations is comparable with the size of the domain, because the higher order approximation we obtained is a local term that mainly comes from the singularity near of the stress near dislocations. Future work may include the study of evolution of the continuous distribution of

dislocations using the obtained continuum approximation, and generalization to include elastic anisotropy and multiple slip planes.

More details can be found in (Y. Xiang, Continuum approximation of the Peach-Koehler force on dislocations in a slip plane, preprint, 2008). This work is partially supported by the Hong Kong Research Grants Council CERG 604604 and 603706.

## Electronic structure for elastically deformed solids

Jianfeng Lu
(joint work with Weinan E)

To develop multiscale method (e.g., sublinear scaling algorithm [2]) for solving electronic structure, it is important to have a systematic understanding of the electronic structure for elastically deformed solids. For perfect crystal without deformation, expoiting the translational symmetry of the system, the Bloch-Floquet theory provides a description of electronic structure through Bloch waves and band structure. However, the description based on Bloch waves is not stable under deformation of the solids. Since the symmetry is then lost, Bloch-Floquet theory no longer applies. For a stable characterization of the electronic structure for deformed solids, the Wannier function (generalized to the setting of deformed state) is more suitable. Moreover, these Wannier functions might be constructed locally using the local environment, the electronic structure for the entire system could be then constructed by putting the Wannier functions together. Hence, to obtain the occupied space for the whole system, it is sufficient to consider subsystems and put resulting Wannier functions together, this is the superposition principle for electronic structure. Refer [1] for details of the results presented in this talk.

We consider the one particle Schrödinger operator

$$H = -\Delta + V \tag{1}$$

with the effective potential given as the linear combinations of contributions from every nuclei site:

$$V(y) = \sum_i V_a(y - Y_i), \tag{2}$$

where $V_a$ is compact supported or fast decaying (due to screening).

The system is elastically deformed from perfect crystal with smooth displacement field $u$. Denote the nuclei positions for the perfect crystal as $X_i$, so after deformation, the nuclei are located at $Y_i = X_i + u(X_i)$. The Hamiltonian $H = H[u]$ depends on $u$ through the potential $V$. The characteristic length for the displacement is $1/\varepsilon$, where $\varepsilon$ is a small parameter we will use for taking the continuum limit:

$$u(x) = u^{(\varepsilon)}(x) = \varepsilon^{-1} u_0(\varepsilon x). \tag{3}$$

In the following, we will omit $\varepsilon$ when no confusion might occur.

We assume that the perfect crystal we considered is an insulator, which means that there is a gap in the spectrum between occupied and unoccupied spaces. The

projection operator to the occupied space (density matrix in physics terminology) is then defined as

$$P = \chi_{(-\infty,\varepsilon_F]}(H), \tag{4}$$

where $\varepsilon_F$ is the Fermi energy lies in the spectral gap. A fundamental theorem by Kohn [3] (with the extension to two and three dimension by [4]) states that an orthonormal basis of exponentially localized functions can be found for $\operatorname{Ran} P$. These functions are called Wannier functions, denoted as $W_{n,k}$. There exist exponent $\alpha > 0$ and bound $M$ such that

$$\int e^{2\alpha(|x-x_k|^2+1)^{1/2}} |W_{n,k}(x)|^2 \, \mathrm{d}x \leq M. \tag{5}$$

Here, $n$ is the band index (for notational ease, in the following, we will assume there is only band, the cases of multiple bands are simple extensions), $k$ is the position index, and $x_k$ is the center of the $k$-th Wannier function.

The Hamiltonian operator is defined in Eulerian coordinates, as we are considering elastically deformed systems, it is more convenient to use Lagrangian coordinates. For this, we define the Euler-Lagrange map for given displacement field $u$:

$$(U_u f)(x) = [\det(I + \nabla u(x))]^{1/2} f(x + u(x)). \tag{6}$$

$U_u$ maps a function of Eulerian coordinates to a function of Lagrangian coordinates. Using $u$, we get the Hamiltonian and density matrix in Lagrangian coordinates as

$$\widetilde{H}[u] = U_u H[u] U_u^{-1}, \quad \text{and} \quad \widetilde{P}[u] = U_u P[u] U_u^{-1}. \tag{7}$$

We can now define the *projected Wannier function*. For system under displacement $u$, the projected Wannier functions are given by

$$W_k[u] = U_u^{-1} \widetilde{P}[u] W_k. \tag{8}$$

In the situation that the deformation gradient is small and the parameter $\varepsilon$ is also small, we have the following result stating that the projected Wannier functions actually form a basis for occupied space and they are exponentially localized.

**Theorem 8** (Projected Wannier functions)**.** *There exist postive constants $\varepsilon_0$ and $K$, such that for all $\varepsilon \leq \varepsilon_0$ and $u^{(\varepsilon)}$ such that $\|\nabla u^{(\varepsilon)}\|_\infty \leq K$, the set $\{W_k[u^{(\varepsilon)}] = U_u^{-1} \widetilde{P}[u^{(\varepsilon)}] W_k\}$ forms a basis of $\operatorname{Ran} P[u^{(\varepsilon)}]$. Moreover, there exist exponent $\alpha > 0$ and bound $M$ such that*

$$\int e^{2\alpha(|y-y_k|^2+1)^{1/2}} |W_k[u^{(\varepsilon)}](y)|^2 \, \mathrm{d}y \leq M,$$

*where $y_k = x_k + u^{(\varepsilon)}(x_k)$ is the center of $W_k[u^{(\varepsilon)}]$.*

We then consider how to construct projected Wannier functions using only the local deformation gradient. For this, we have a Cauchy-Born-type rule for the Wannier functions. Consider the linearized displacement field at $x_k$:

$$\mathcal{L}_{x_k}(u^{(\varepsilon)})(x) = u^{(\varepsilon)}(x_k) + \nabla u^{(\varepsilon)}(x_k)(x - x_k). \tag{9}$$

For the linearized system, we have the Wannier function centered around $y_k = x_k + u^{(\varepsilon)}(x_k)$, denoted as $W_k[\mathcal{L}_{x_k}(u^{(\varepsilon)})$. This is a good approximation to the Wannier function of the original deformed system as shown by the following theorem.

**Theorem 9** (Cauchy-Born rule for electronic structure)**.** *There exist positive constants $\varepsilon_0$ and $K$, such that for all $\varepsilon \le \varepsilon_0$ and $u^{(\varepsilon)}$ such that $\|\nabla u^{(\varepsilon)}\|_\infty \le K$, we have*

$$\|W_k[u^{(\varepsilon)}] - W_k[\mathcal{L}_{x_k}(u^{(\varepsilon)})]\|_{H^1} \le C\varepsilon.$$

*The constant $C$ is independent with $\varepsilon$ and $k$.*

Notice that $W_k[\mathcal{L}_{x_k}(u^{(\varepsilon)})]$ is constructed using only the local gradient, as for the usual Cauchy-Born rule for nonlinear elasticity. This is actually a general philosophy of superposition principle for electronic structure, namely, the occupied space of the whole system could be constructed locally. This is in the same spirit with the near-sightedness of electronic matter in the physics literature [5].

The theorem shows that the Wannier function representation of the occupied space is helpful to describe the electronic structure for elastically deformed solids. Under deformation, the picture of localized basis still exists while we no longer have the band structure as for the perfect crystal. Therefore, in numerical computation of electronic structure, solving for the Wannier functions might be the right approach, especially for multiscale algorithms trying to exploit the structure of solution away from the defects, where the system is under elastic deformation. See [2] for a sublinear scaling algorithm in this direction.

## References


[1] W. E and J. Lu, in preparation.

[2] C. Garcia-Cervera, J. Lu, and W. E, *Asymptotics-based sub-linear scaling algorithms and application to the study of the electronic structure of materials*, Commun. Math. Sci. **5** (2007), 999–1024.

[3] W. Kohn, *Analytic Properties of Bloch Waves and Wannier Functions*, Phys. Rev. **115** (1959), 809–821.

[4] G. Panati, *Triviality of Bloch and Bloch-Dirac bundles*, Ann. Henri Poincare **8** (2007), 995–1011.

[5] E. Prodan and W. Kohn, *Nearsightedness of electronic matter*, Proc. Natl. Acad. Sci. USA **102** (2005), 11635–11638.

## The XY spin system and the Ginzburg-Landau energy

Marco Cicalese
(joint work with Roberto Alicandro)

We provide a variational approach to describe some of the features which are peculiar of those phase-transition phenomena which occur without breaking the symmetry of the system and that have been first studied in the seminal papers by Berezinskii [6], Kosterlitz [12] and Kosterlitz and Thouless [13] concerning the so-called two-dimensional $XY$ model. This model turns out to be the easiest model that contains all the interesting characteristics of this class of phase transitions. It is constructed on the two-dimensional square lattice $\mathbb{Z}^2$ whose points $i$ are occupied by a spin confined to a plane $u(i) \in S^1$. For a given configuration, the energy of the system is

$$F(u) = -\sum_{n.n.} u(i)u(j), \tag{1}$$

where $n.n.$ means that the summation is taken over all nearest neighbors. Following the Berezinskii-Kosterlitz-Thouless theory here the phase-transition phenomenon is mediated by the formation of topological defects or vortices. In particular under some critical temperature $T_c$ these vortices behave like 'topological charges' and bound together in pairs becoming the relevant degrees of freedom of the system. We are interested in this low-temperature regime where the cost of small fluctuations of the spin field around the uniform ground state is usually conveniently calculated by coarse-graining on a scale much larger than the lattice spacing thus obtaining a continuous model known as the Ginzburg-Landau model.

Here we present the results contained in [4] in which we prove a rigorous coarse-graining of the $XY$ model which leads to a Ginzburg-Landau (GL) energy in the regime in which the so called GL coherence length (here denoted by $\varepsilon$) is extremely small. In this case the GL energy can be conveniently written as

$$G_\varepsilon(u) = \frac{1}{2}\int \left( |\nabla u|^2 + \frac{1}{\varepsilon^2}(1-|u|^2)^2 \right) dx. \tag{2}$$

The analysis of the energy in (2), and in particular the appearance of vortex-like singularities associated to energy-concentration phenomena, has been successfully addressed by many authors both from the PDEs and the calculus of variations point of view (see e.g. [1], [7], [9], [10], [11], [14]). Since, to leading term, the cost of a vortex singularity is of order $|\log \varepsilon|$, the right energy scaling to be taken into account is $\frac{G_\varepsilon(u)}{|\log \varepsilon|}$. In this regime in [9] Jerrard has shown that the relevant tool to track energy concentration is the asymptotic analysis of the Jacobians of sequences $u_\varepsilon$ equibounded in energy. The variational analysis of the asymptotics of $\frac{G_\varepsilon(u)}{|\log \varepsilon|}$ has then been performed by Jerrard and Soner in [10] in the two-dimensional case and by Alberti, Baldo e Orlandi in [1] in the general $N$-dimensional case.

To set up the general $N$-dimensional problem for the $XY$ model in the framework of discrete-to-continuum variational limits (see for example [2], [3], [5], [8])

we scale the energy in (1) to a fixed domain $\Omega \subset \mathbf{R}^N$. Taking into account the interactions between nearest-neighbors on the lattice $\varepsilon\mathbb{Z}^N \cap \Omega$ (the lattice spacing $\varepsilon$ will go to zero in the continuum limit), the scaled energy reads:

$$F_\varepsilon(u) = -\sum_{n.n.} \varepsilon^N u(\varepsilon i) \cdot u(\varepsilon j).$$

Upon identifying the functions $u : \varepsilon\mathbb{Z}^N \cap \Omega \to S^1$ with proper piecewise-constant interpolations, the energies can be considered as being defined on $L^\infty(\Omega)$ and, in that framework, they can be described by a $\Gamma$-limit as $\varepsilon$ goes to 0. The bulk scaling we have chosen for $F_\varepsilon$ renders its $\Gamma$-limit trivially the constant value $-|\Omega|$, the only constraint being $|u| \leq 1$. Such a limit is the same even in the case of Ising-type models ($u$ is a scalar field such that $u \in \{-1, +1\}$) and summarizes the fact that it is possible to mix uniform states on a mesoscopic scale without changing the asymptotic energy. This description of the ground states can be improved by considering other scalings. In particular we can select sequences that realize the minimum value with a sharper precision; i.e.

$$F_\varepsilon(u_\varepsilon) = \min F_\varepsilon + O(k_\varepsilon)$$

where $k_\varepsilon \to 0$ as $\varepsilon \to 0$. In the Ising case it has been proven ([2]) that a relevant scaling is $k_\varepsilon = \varepsilon$. This scaling yields to a minimal-interface selection criterion, in the sense that, on such sequences $u_\varepsilon$, the limit is an interfacial-type energy reflecting the symmetries of the underlying lattice structure. In the present case we show that no interface-type selection can be obtained by a surface scaling and focus on a different scaling, namely $k_\varepsilon = \varepsilon^2|\log\varepsilon|$, which implies a selection criterion of topological nature. The sequence of scaled functionals we consider is

$$\begin{aligned} E_\varepsilon(u) = \frac{F_\varepsilon(u) - \min F_\varepsilon}{\varepsilon^2|\log\varepsilon|} &= \frac{1}{|\log\varepsilon|} \sum_{n.n.} (1 - u(\varepsilon i) \cdot u(\varepsilon j)) \\ &= \frac{1}{2|\log\varepsilon|} \sum_{n.n.} \varepsilon^2 \left| \frac{u(\varepsilon i) - u(\varepsilon j)}{\varepsilon} \right|^2. \end{aligned}$$

By associating to any given $u$ the function $v = A(u)$ defined as a continuous piecewise-affine interpolation of $u$ on the cells of the lattice, we have

$$E_\varepsilon(u) \sim \frac{1}{2|\log\varepsilon|} \int_\Omega |\nabla v|^2 \, dx. \tag{3}$$

Once we prove that the singular term in the Ginzburg-Landau energy is controlled by $E_\varepsilon(u)$, that is

$$\frac{1}{\varepsilon^2|\log\varepsilon|} \int_\Omega (|v|^2 - 1)^2 \, dx \leq C E_\varepsilon(u),$$

we recognize in the right hand side of (3) the leading term of $\frac{G_\varepsilon(v)}{|\log\varepsilon|}$. This fact suggests an analogy between the two models and leads us to track the formation of vortices associated to sequences $u_\varepsilon$ with bounded energy in the $XY$ model by studying the convergence, in a 'suitable sense', of the Jacobians $J(v_\varepsilon)$ of $v_\varepsilon = A(u_\varepsilon)$. We can describe the structure of the vortices as follows:

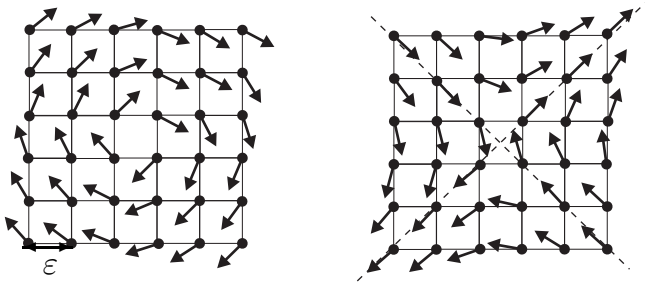


Figure 1: Discrete vortices: optimizing sequences for $M = \delta_{x_0}$ (+1 charged vortex) (left) and $M = -\delta_{x_0}$ (−1 charged vortex) (right).

**Compactness.** Let $(u_\varepsilon)$ be a sequence of functions such that $E_\varepsilon(u_\varepsilon) \leq C$ and let $v_\varepsilon = A(u_\varepsilon)$. Then we can extract a subsequence (not relabeled) such that $\mathbf{F}_\Omega(\star J(v_\varepsilon) - \pi M) \to 0$, where $M$ is an $(N-2)$-dimensional integral boundary in $\Omega$.

Here with $\star J(v_\varepsilon)$ we mean the $(N-2)$-current obtained from $J(v_\varepsilon)$ by the standard identification $\star$ of $k$-covectors with $(N-k)$-vectors. For any current $T$ $\mathbf{F}_\Omega(T)$ denotes its flat norm and the limit current $M$ is a $(N-2)$-dimensional boundary in the sense that, loosely speaking, it is supported on a $(N-2)$-dimensional rectifiable set which is also a boundary. This set represents the set of the vortex-type singularities of the spin field $u_\varepsilon$ as $\varepsilon$ goes to zero.

The coarse graining of the energies is given by the following Γ-convergence result:

**Lower-bound inequality** - Let $(u_\varepsilon)$ be a sequence of functions such that $\mathbf{F}_\Omega(\star J(v_\varepsilon) - \pi M) \to 0$, where $M$ is an $(N-2)$-dimensional integral boundary in $\Omega$. Then

$$\liminf_\varepsilon E_\varepsilon(u_\varepsilon) \geq \pi \|M\|;$$

**Upper-bound inequality** - Let $M$ be an $(N-2)$-dimensional integral boundary in $\Omega$. Then there exists a sequence $(u_\varepsilon)$ such that $\mathbf{F}_\Omega(\star J(v_\varepsilon) - \pi M) \to 0$ and

$$\lim_{\varepsilon \to 0} E_\varepsilon(u_\varepsilon) = \pi \|M\|. \tag{4}$$

To explain the previous results let us consider the case $N = 2$. In this case the limit current $M$ is a finite sum of Dirac masses, that is $M = \sum_{k=1}^n d_k \delta_{x_k}$, where $n \in \mathbf{N}$, $x_k \in \Omega$ represent the centers of the vortices and $d_k \in \mathbb{Z}$ are the winding numbers of the spin field around each $x_k$, also called *charges* of the topological singularity. In Figure 1 we have displayed two types of discrete vortices; that is, the microscopic configurations of the spin fields leading, in the continuum limit, to $M = +\delta_{x_0}$ and $M = -\delta_{x_0}$.

We point out that the limit energy in (4) does not reflect the underlying geometry of the lattice. In fact the parallel between the $XY$ and the $GL$ model carries

on to the characteristic length scale where energy concentrates that is much larger than the lattice spacing $\varepsilon$.

Starting from the previous analysis, we also address several other problems. The case of long range interactions, that is when the interactions between all the spins are taken into account, is the hardest. For this problem we prove a $\Gamma$-convergence result asserting that, in two dimensions, under a natural decay assumption on the weights of the interactions, the limit energy is still of the form (4). To prove this result a key ingredient is the idea, well known to people working in statistical mechanics, and here used in a variational setting, of decoupling the energy as a sum of 'weakly interacting' nearest-neighbors type energies to which the previous arguments apply. The $N$-dimensional problem is also addressed under some restrictive assumptions but remains open in its generality.

We finally present many challenging issues which are open in this framework such as the variational description of the $XY$ model in presence of an external magnetic field or the study of the energy accounting for the interaction between vortices.

## References


[1] G. Alberti, S. Baldo, G. Orlandi, Variational convergence for functionals of Ginzburg-Landau type, *Indiana Univ. Math. J.* **54** (2005), no. 5, 1411–1472.

[2] R. Alicandro, A. Braides, M. Cicalese, Phase and anti-phase boundaries in binary discrete systems: a variational viewpoint, *Netw. Heterog. Media* **1** (2006), no. 1, 85–107.

[3] R. Alicandro, M. Cicalese, A general integral representation result for the continuum limits of discrete energies with superlinear growth, *SIAM J. Math. Anal.* **36** (2004), no. 1, 1–37.

[4] R. Alicandro, M. Cicalese, Variational analysis of the asymptotics of the $XY$ model, to appear on *Arch. Rat. Mech. Anal.*, (download @ http://cvgmt.sns.it).

[5] R. Alicandro, M. Cicalese, A. Gloria, Integral representation and homogenization result for bounded and unbounded spin systems, to appear on *Nonlinearity*, (download @ http://cvgmt.sns.it).

[6] V.L. Berezinskii, Destruction of long range order in one-dimensional and two-dimensional systems having a continuous symmetry group. I. Classical systems *Sov. Phys. JETP*, **32** (1971), 493-500.

[7] F. Bethuel, H. Brezis, F. H?lein, Ginzburg-Landau vortices. *Progress in Nonlinear Differential Equations and their Applications*, 13. Birkh?user Boston MA, 1994.

[8] A. Braides, $\Gamma$-convergence for beginners. *Oxford Lecture Series in Mathematics and its Applications*, 22. Oxford University Press, Oxford, 2002.

[9] R.L. Jerrard, Lower bounds for generalized Ginzburg-Landau functionals, *SIAM J. Math. Anal.* **30** (1999), no. 4, 721–746.

[10] R.L. Jerrard, H.M. Soner, The Jacobian and the Ginzburg-Landau energy, *Calc. Var. Partial Differential Equations* **14** (2002), no. 2, 151–191.

[11] R.L. Jerrard & H.M. Soner, Limiting behavior of the Ginzburg-Landau functional, *J. Funct. Anal.* **192** (2002), no. 2, 524–561.

[12] J.M. Kosterlitz, The critical properties of the two-dimensional xy model, *J. Phys. C*, **6** (1973), 1046–1060.

[13] J.M. Kosterlitz, D.J. Thouless, Ordering, metastability and phase transitions in two-dimensional systems, *J. Phys. C*, **6** (1973), 1181–1203.

[14] E. Sandier and S. Serfaty, Vortices in the Magnetic Ginzburg-Landau Model, Progress in Nonlinear Differential Equations and their Applications, 70. Birkh?user Boston, Inc., Boston, MA, 2007.

## Equilibrium Methods for Non-Equilibrium Simulation

Ben Leimkuhler
(joint work with S. Bond, E. Noorizadeh and F. Theil)

The emphasis in molecular dynamics applications is shifting to problems involving transient dynamics, and the flow of energy from one part of a system (one set of variables) to another. There is now widespread agreement that, for many problems, the long timescales (relative to the shortest interatomic vibrational periods) and complexity of boundary interactions that must be incorporated to generate useful data in realistic computational time mean that the typical system must be modelled in a pre-equilibrium state. Computational methods are needed for this modern simulation setting. As examples, methods have been proposed recently for computing free energy along a reaction coordinate [4, 6] which rely on forcing the molecular system into infrequently visited domains to study slowly-unfolding transitions. A crucial part of these calculations is the computation of averages or time-correlation functions of a system subject to imposed constraints or initialization enforced as part of the modelling framework. The local equilibration/dynamics problem is nontrivial, so implementing these methods (which effectively require us to equilibrate the system in regions of rapid dynamical transition) is itself a major task.

Consider a finite dimensional Hamiltonian system in $\mathbf{R}^{2N}$ with Hamiltonian $H = H(z)$, $z = (q, p)$, with $q$ and $p$ position and momentum vectors, respectively. By *sampling*, we mean computing the average of a function $f = f(z)$,

$$\bar{f} = \frac{1}{\Omega} \int_D f(z)\rho(z)\mathrm{d}\omega, \qquad \Omega = \int_D \rho(z)\mathrm{d}\omega,$$

with respect to a suitable measure $\rho\mathrm{d}\omega$ ($\mathrm{d}\omega$ the standard volume form in $\mathbf{R}^{2N}$), and $D \subset \mathbf{R}^{2N}$. If we consider the natural (microcanonical) measure $\rho = \delta[H - E]$ associated to Hamiltonian dynamics with energy function $H = H(z)$, then, under an ergodicity assumption, we may replace spatial averaging by the time average,

$$\bar{f} = \lim_{T\to\infty} T^{-1} \int_0^T f(\zeta(t))\mathrm{d}t,$$

where $\zeta = \zeta(t)$ is the solution of the Hamiltonian dynamics for an arbitrary initial condition of energy $E$. Replacing Hamiltonian dynamics by a suitable Markov process (Langevin dynamics [8], or, in certain circumstances, an extended dynamics [9]), it is possible to use temporal averages to compute canonical averages, i.e. averages with respect to the Gibbs density $\rho^\theta_{\mathrm{can}}(z) = e^{-H/(k_B\theta)}$. This is often referred to as a "thermostat," although the term "thermostatted molecular dynamics" probably should be more restricted than this. In this report I will describe some recent and ongoing research to understand the foundations of molecular dynamics algorithms, specifically topics related to thermostatting molecular dynamics.

**1. Error estimates for averages from finite timestep numerics.** The pragmatic explanation for the usefulness of molecular dynamics comes from the geometric integration theory, and, in particular, the backward error analysis which tells us that we may(approximately) view the numerical solution as the exact solution of a perturbed dynamical system [3]. Analyzing the perturbation of averages due to use of a numerical method is easiest in the setting of canonical sampling by the Nosé-Poincaré thermostat (see, e.g., [1]), because of (i) the smoothness of the ensemble density function, and (ii) the ability to use symplectic integrator for which backward error analysis provides a perturbed Hamiltonian which can be averaged against. The Nosé-Poincaré formulation uses the extended Hamiltonian

$$H_{\mathrm{NP}} = s[H(q, p/s) + \frac{p_s^2}{2\mu} + Nk_B\theta \ln s - E_0],$$

where $H(q,p)$ is the energy of the system, $s$ and $p_s$ are thermostat variables, $N$ is the number of degrees of freedom, $k_B\theta$ is the temperature weighted by Boltzman's constant, and $E_0$ is a constant such that $H_{\mathrm{NP}}(q(0), p(0), s(0), p_s(0)) = 0$. The evolution is then on the surface $H_{\mathrm{NP}} \equiv 0$. It can be shown that this system has trajectories which are equivalent to those of Nosé-Hoover dynamics (which, however, does not have a Hamiltonian formulation).

In our recent work [1], we have derived the perturbed Hamiltonian expansion in powers of the stepsize $h$ of a symplectic integrator for the Nosé-Poincaré Hamiltonian. Next, we computed the marginal density including the expansion terms. From this we are able to compute an ensemble reweighting correction $\hat{\rho}_h$ such that (if ergodicity is assumed)

$$\lim_{t\to\infty} t^{-1} \int_0^t f(z(t))dt = \frac{1}{\Omega} \int_D f(z)\rho_{\mathrm{can}}(z)\hat{\rho}_h(z)\mathrm{d}\omega.$$

This allows, in principle, correction of any thermodynamic average, or even autocorrelation functions, for the effect of nonzero stepsize. One simply reweights statistics to recover the desired average, or else the correction factor $\hat{\rho}$ can be viewed as a localized error estimate.

**2. Adaptive Thermostats: Balancing Sampling and Dynamics**

Thermostats generate step sequences that can be, for some choices of parameters, modest perturbations of Hamiltonian dynamical trajectories. This latter fact is often ignored by mathematicians, but is crucial to explaining the role and value of thermostats. Strongly ergodic processes may control temperature well, but at the price of modifying diffusion rates. Such defects are easily seen for Langevin dynamics with damping (collision) coefficient $\gamma > 1\mathrm{ps}^{-1}$, when used in systems involving liquid water, in that the diffusion of energy from the OH bond stretch is corrupted. The figure below compares the effects of weak and strong thermostats on the velocity autocorrelation function of the vibration of a diatomic molecule in a detailed solvent bath.


Figure 1: velocity autocorrelation function computed using a weak (left) vs strong (right) Langevin thermostat; the example here is for an isolated bond stretch solvated in a bath of 100 atoms interacting in Lennard-Jones potential.

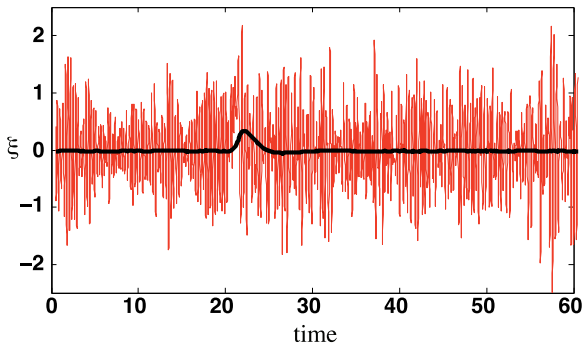


Figure 2: $\xi$ for NH (faint line) and weaker TRD thermostat (heavy line) for periodic box of liquid argon. At $t = 20$, a nonadiabatic pressure change was introduced.

Generating a distribution of energy to the degrees of freedom of a complex macromolecule that is consistent with equidistribution is an onerous task; a multi-stage process of "equilibration" must be used in which the system is allowed to evolve under the control of a thermostat, while specific sets of degrees of freedom are sequentially targeted [7]; after the initial equilibration process is completed, weak thermostatting is used [10], although this leads to difficulties when temperature fidelity is important (e.g., at phase transitions), or if the system is subject to external perturbations. When one dynamics or numerical procedure is switched off and another switched on, the effects are often dramatic. Not only does every Hamiltonian system have its own natural measure, but the numerical integrators themselves perturb this ensemble. Initial conditions which are "well equilibrated" for a certain ensemble may not be when an integrator is engaged with a large timestep, leading to unstable initial perturbation, re-equilibration, and a temperature shift. This is classically observed in the difficulty to locate microcanonical trajectories having specified average kinetic energy.

What is clearly needed are adaptive schemes that automatically control the "strength" of thermostatting used in simulation. Recently, the proposer has developed an adaptive *temperature regulated dynamics* (TRD)[2] for nonequilibrium applications which perturbs the conservative force by $\Delta = -\xi p$, where

$$\xi \propto \bar{K} - k_B\theta$$

where $\bar{K}$ is the kinetic energy averaged by particle number and time, with respect to a temporal weight function $\phi$. This leads to delay-differential equations, but for exponential weight ($\phi = e^{-t/\tau}$, $\tau$ a parameter) can be replaced by a simple closed dynamics. Like Nosé dynamics, the kinetic energy is controlled; unlike Nosé dynamics, this formulation has no obvious thermodynamic ensemble, but remains close to microcanonical dynamics for an ergodic system in equilibrium ($\xi$ is small in TRD compared to Nosé-Hoover (NH) dynamics, see Figure 2). TRD is not sufficiently ergodic in itself to thermostat biomolecules which trap energy in a network of stiff harmonic bonds.

**3. Ergodic Weak Thermostats** Although both dynamics-based and stochastic thermostats are found to be useful for MD simulation, robust ergodic sampling, especially for small systems or systems with strong harmonic components, appears to require a random perturbation. Langevin dynamics traditionally perturbs all components of a dynamical system. This leads to artificial effects which may damage autocorrelation functions. Currently, with F. Theil (Warwick) and E. Noorizadeh (U. of Edinburgh) we are exploring ergodic schemes which incorporate a modified weak stochastic perturbation of dynamics. These methods can be analyzed by studying the regularity properties of the associated Fokker-Planck operator.

We are currently developing adaptive thermostats which integrate the methods of Sections 2 and 3. In separate work, we are also studying nonequilibrium effects in small microcanonical molecular dynamical models.

## References


[1] S. Bond and B. Leimkuhler. Molecular dynamics and the accuracy of numerically computed averages. *Acta Numerica*, 16:1–65, 2007.

[2] B. Leimkuhler, F. Legoll, and E. Noorizadeh. A temperature control technique for nonequilibrium molecular simulation. *J. Chem. Phys.* **128**, 074105, 2008.

[3] B. Leimkuhler and S. Reich. *Simulating Hamiltonian Dynamics*. Cambridge University Press, 2005.

[4] E.A. Carter, G. Ciccotti, J.T. Hynes, and R. Kapral. Constrained reaction coordinate dynamics for the simulation of rare events. *Chem. Phys. Lett.*, 156:472–477, 1989.

[5] C. Dellago. Transition path sampling. In S. Yip, editor, *Handbook of Materials Modeling*. Springer, 2005.

[6] C. Dellago, P.G. Bolhuis, and P.L. Geissler. Transition path sampling. *Adv. Chem. Phys.*, 123:1–80, 2002.

[7] E. B. Walton and K. J. VanVliet. Equilibration of experimentally determined protein structures for molecular dynamics simulation. *Phys. Rev. E*, 74, 2006. 061901.

[8] Brunger, A.T., Brooks, C.L., and Karplus, M., *Chem. Phys. Lett.* **105**, 495–500, 1984.

[9] Nosé, S., A unified formulation of the constant temperature MD method, *J. Chem. Phys.* **81**, 511–519, 1984.

[10] Isgro,T., Phillips,J., Sotomayor, M., Villa, E., The NAMD Tutorial, Beckman Institute, University of Illinois, 2007. `http://www.ks.uiuc.edu/Training/Tutorials/`

## From quantum to classical molecular dynamics

Johannes Giannoulis
(joint work with Gero Friesecke)

Starting from the quantum mechanical description of the dynamics of nuclei of a molecule, which is governed by a time-dependent Schrödinger equation with singular potential, our aim is to derive and, more important, justify rigorously the reduced classical dynamics of the nuclei in the heavy nuclei limit, i.e. as the mass ratio $\varepsilon^2 := \frac{m_e}{m_n}$ of electronic to nucleonic mass tends to zero: $\varepsilon \to 0$. (The true ratio is $\sim 1/2000$ for hydrogen, and even smaller for the other atoms.) More precisely, we consider $M \in \mathbb{N}$ nuclei of equal mass with wavefunction $\Psi_\varepsilon(\cdot, t) \in L^2(\mathbb{R}^d)$, $d = 3M$, at time $t$. In atomic units ($m_e = |e| = \hbar = 1$) their (non-relativistic) quantum dynamics is determined by the Schrödinger equation

$$\text{(SE)} \qquad \begin{cases} \mathrm{i}\varepsilon\partial_t \Psi_\varepsilon(\cdot, t) = H^\varepsilon \Psi_\varepsilon(\cdot, t) & \text{for } t \in \mathbb{R}, \\ \Psi_\varepsilon(\cdot, 0) = \Psi^0_\varepsilon. \end{cases}$$

with the self-adfoint Schrödinger operator $H^\varepsilon := -\frac{\varepsilon^2}{2}\Delta + U \,:\, \mathcal{D}(H^\varepsilon) \to L^2(\mathbb{R}^d)$ of domain $\mathcal{D}(H^\varepsilon) = H^2(\mathbb{R}^d)$. By standard results on the unitary group generated by a self-adjoint operator, for any initial state $\Psi^0_\varepsilon \in \mathcal{D}(H^\varepsilon)$ this equation has a unique solution $\Psi_\varepsilon \in \mathrm{C}(\mathbb{R}; \mathbf{H}^2(\mathbb{R}^d)) \cap \mathrm{C}^1(\mathbb{R}; \mathrm{L}^2(\mathbb{R}^d))$ with $||\Psi_\varepsilon(t)|| \equiv ||\Psi^0_\varepsilon||$ for all $t \in \mathbb{R}$.

The crucial point of our analysis is that we want to consider the physically correct potential $U$, namely the Born-Oppenheimer ground state potential energy surface obtained by minimization over electronic states: For $x = (R_1, \ldots, R_M) \in \mathbb{R}^d$, with $R_\alpha \in \mathbb{R}^3$, $\alpha = 1, \ldots, M$, denoting the coordinates of the nuclei, $U : \mathbb{R}^d \to \mathbb{R}$ is given by

$$U = E_{e\ell} + V_{nn},$$

$$E_{e\ell}(R_1, .., R_M) = \inf_\psi \langle \psi, H_{R_1,..,R_M}\psi\rangle, \;\; V_{nn}(R_1, \ldots, R_M) = \sum_{1\le\alpha<\beta\le M} \frac{Z_\alpha Z_\beta}{|R_\alpha - R_\beta|},$$

$$H_{R_1,..,R_M} = \sum_{i=1}^N \Big(-\frac{1}{2}\Delta_{r_i} - \sum_{\alpha=1}^M \frac{Z_\alpha}{|r_i - R_\alpha|}\Big) + \sum_{1\le i<j\le N} \frac{1}{|r_i - r_j|}.$$

where $N \in \mathbb{N}$ and $r_i \in \mathbb{R}^3$ denote the number and the coordinates of the electrons of the system, $Z_\alpha \in \mathbb{N}$ are the charges of the nuclei (usually $N = \sum_{\alpha=1}^M Z_\alpha$), and where the infimum is taken over the usual subset of $\mathrm{L}^2((\mathbb{R}^3 \times \mathbb{Z}_2)^N; \mathbb{C})$ of normalized, antisymmetric electronic states belonging to the domain $\mathbf{H}^2((\mathbb{R}^3 \times \mathbb{Z}_2)^N; \mathbb{C})$ of $H_{R_1,..,R_M}$.

Hence, the physically correct potential $U$ contains Coulomb-type singular terms $V_{nn}$, reflecting the repulsion of nuclei, and moreover it can have kink type singularities if eigenvalue crossings are present, mirroring the electron-nuclei attraction and electron-electron repulsion terms of $H_{R_1,..,R_M}$. Thus, the gradient of the potential, i.e., the force field for exact ab-initio molecular dynamics, contains inverse

square "poles", and possibly also jump singularities across codimension one surfaces. This level of smoothness is far lower than that required in previous rigorous approaches, and – even worse – lower than the global Lipschitz continuity required for uniqueness for the limiting ODE system of classical molecular dynamics. In the present paper, we deal with potentials with Coulomb singularities but no crossings. (The absence of the latter is generally expected for dimers, and can be rigorously established for the hydrogen dimer $H_2$.)

We proceed by the following steps. First, we transform (SE) into the Wigner equation (WE) below for the Wigner function $W_\varepsilon$ of the wavefunction $\Psi_\varepsilon$ solving (SE). Then, we show that $W_\varepsilon$ converges to a *Wigner measure* $W$ which satisfies the Liouville equation (LE) below, that is the transport equation for classical molecular dynamics. Of course, at a formal level these results can be obtained by straightforward calculations. However, difficulties arise when one wants to justify these calculations rigorously, which is our main goal. We present here without proof the main steps of our justification result and refer for the details to [AFG08].

**Wigner transformation** Let $W_\varepsilon$ be the *Wigner function* (introduced by Wigner in [Wig32]) of lengthscale $\varepsilon$ of a solution $\Psi_\varepsilon$ of (SE), given by

$$W_\varepsilon(x,p,t) \quad = \quad \frac{1}{(2\pi\varepsilon)^d}\int_{\mathbb{R}^d} \Psi_\varepsilon(x+\frac{y}{2},t)\overline{\Psi_\varepsilon(x-\frac{y}{2},t)}\varepsilon^{-\mathrm{i}p\cdot y/\varepsilon}\,\mathrm{d}y.$$

$W_\varepsilon$ can be interpreted roughly as a joint position and momentum density for the quantum system: Altough it is *not* nonnegative (and hence not a density) it holds

$$\begin{aligned}\int_{\mathbb{R}^d} W_\varepsilon(x,p,t)\,\mathrm{d}p &= \left|\Psi_\varepsilon(x,t)\right|^2 \text{ (position density)},\\ \int_{\mathbb{R}^d} W_\varepsilon(x,p,t)\,\mathrm{d}x &= \left|\frac{1}{(2\pi\varepsilon)^{d/2}}\int_{\mathbb{R}^d}\varepsilon^{-\mathrm{i}p\cdot x/\varepsilon}\Psi_\varepsilon(x,t)\,\mathrm{d}x\right|^2 \text{ (momentum density)}.\end{aligned}$$

**Lemma 10.** *The Wigner function $W_\varepsilon$ of any solution $\Psi_\varepsilon \in \mathrm{C}(\mathbb{R};\mathbf{H}^2(\mathbb{R}^d)) \cap \mathrm{C}^1(\mathbb{R};\mathrm{L}^2(\mathbb{R}^d))$ to* (SE) *solves (WE) $\partial_t W_\varepsilon = -p\cdot\nabla_x W_\varepsilon - f_\varepsilon$ with*

$$\begin{aligned}f_\varepsilon := i\frac{1}{(2\pi)^d}&\\ \cdot\int_{\mathbb{R}^d}&\frac{U(x+\varepsilon y/2)-U(x-\varepsilon y/2)}{\varepsilon}\Psi_\varepsilon(x+\varepsilon y/2,t)\overline{\Psi_\varepsilon(x-\varepsilon y/2,t)}e^{-ip\cdot y}dy,\end{aligned}$$

*and it holds (for $i,j=1,\dots,d$)*

$$(1)\qquad W_\varepsilon \in \mathrm{C}^1(\mathbb{R};\mathrm{L}^\infty(\mathbb{R}^{2d})),\ \frac{\partial}{\partial x_i}W_\varepsilon,\ \frac{\partial^2}{\partial x_i\partial x_j}W_\varepsilon, f_\varepsilon \in \mathrm{C}(\mathbb{R};\mathrm{L}^\infty(\mathbb{R}^{2d})).$$

Equation (WE) is called the *Wigner equation* and is just a transformed and fully equivalent formulation of (SE).

**Passage to classical dynamics** In the limit $\varepsilon \to 0$, the difference quotient in the potential term (for the correct $U$, which can be shown to be locally lipschitz

away from the singular set $\mathcal{S} := \{(R_1, .., R_M) \in \mathbb{R}^{3M} \mid R_\alpha = R_\beta \text{ for some } \alpha \neq \beta\})$ satisfies

$$\frac{U(x + \varepsilon y/2) - U(x - \varepsilon y/2)}{\varepsilon} \to \nabla_x U(x) \cdot y \quad \text{a.e..}$$

Formally, substituting this convergence into (WE), yields as a limit the transport equation for classical molecular dynamics in $\mathbb{R}^d \times \mathbb{R}^d$, i.e. the *Liouville equation*

$$\partial_t W = -p \cdot \nabla_x W + (\nabla_x U(x)) \cdot \nabla_p W. \tag{LE}$$

We want to justify the Liouville equation (LE) rigorously. That is, we assume that we are given a sequence of initial data $\Psi_\varepsilon^0$ with $\varepsilon \to 0$ to (SE), consider the sequence of the corresponding solutions $\Psi_\varepsilon$ to (SE), or equivalently the Wigner functions $W_\varepsilon$ solving (WE), and ask the following question: Under which hypotheses on the initial data and the potential $U$ do the $W_\varepsilon$ converge to a limit $W$, in a sense and a space to be specified, and what equation does this limit solve?

For fixed $t$, say $t = 0$, the limit object of the sequence $W_\varepsilon(t, \cdot) = W_\varepsilon^0$ is well known: it is the *Wigner measure*, which was studied extensively by P.-L. Lions and T. Paul in [LP93]. (For an alternative construction to Wigner measures, cf. [Ger91].) However, here we are interested in the limit of *time-dependent* Wigner functions. Thus, relying on the time-independent results of Lions and Paul we prove an abstract time-dependent analogue, which concerns, instead of Wigner functions of elements of $L^2(\mathbb{R}^d)$, Wigner functions of paths in $L^2$, i.e. of elements of $\mathrm{C}(\mathbb{R}; L^2(\mathbb{R}^d)$.

**Lemma 11.** *(i) (compactness) Let $\{\Psi_\varepsilon\}$ be a sequence in $\mathrm{C}(\mathbb{R}; L^2(\mathbb{R}^d))$ such that*

$$\sup_{t \in \mathbb{R}} ||\Psi_\varepsilon(t)|| \leq C \tag{2}$$

*for some constant independent of $\epsilon$, and let $W_\varepsilon$ be the sequence of associated Wigner functions. Then for a subsequence, $W_\varepsilon \overset{*}{\rightharpoonup} W$ weak* in $L^\infty(\mathbb{R}; \mathcal{A}')$.*
*(ii) If in addition for any test function $\phi \in C_0^\infty(\mathbb{R}^{2d})$ the functions*

$$f_{\varepsilon,\phi}(t) := \int_{\mathbb{R}^{2d}} W_\varepsilon(x, p, t)\, \phi(x, p)\, dx\, dp$$

*are differentiable and satisfy*

$$\sup_{t \in \mathbb{R}} |\tfrac{d}{dt} f_{\varepsilon,\phi}(t)| \leq C_\phi \tag{3}$$

*for some constant $C_\phi$ independent of $\epsilon$, then $W \in \mathrm{C}_{weak*}(\mathbb{R}; \mathcal{M}(\mathbb{R}^{2d}))$, and $W(t) \geq 0$ for all $t$.*

Here, $\mathcal{A}$ denotes the Banach space

$$\mathcal{A} := \{\phi \in C_0(\mathbb{R}^{2d}) \mid ||\phi||_{\mathcal{A}} := \int_{\mathbb{R}^d} \sup_{x \in \mathbb{R}^d} |(\mathcal{F}_p \phi)(x, y)|\, \mathrm{d}y < \infty\},$$

where $C_0(\mathbb{R}^{2d})$ is the usual space of continous functions on $\mathbb{R}^{2d}$ tending to zero at infinity, and $\mathcal{F}_p \phi$ is the partial Fourier transform

$$(\mathcal{F}_p \phi)(x, y) = \int_{\mathbb{R}^d} \varepsilon^{-\mathrm{i}p \cdot y} \phi(x, p)\, \mathrm{d}p.$$

Since $\mathcal{A}$ is a dense subset of $C_0(\mathbb{R}^{2d})$, its dual $\mathcal{A}'$ contains $C_0'(\mathbb{R}^{2d}) = \mathcal{M}(\mathbb{R}^{2d})$, the space of not necessarily nonnegative Radon measures on $\mathbb{R}^{2d}$ of finite mass. In particular, the delta function $\delta_{x_0,p_0}$ centered at a single point $(x_0, p_0)$ in classical phase space belongs to $\mathcal{A}'$. A natural notion which allows convergence of smeared-out ("quantum") functions on phase space to delta functions (i.e., "classical" states) is weak* convergence in $\mathcal{A}'$.

Note, that while (i) is a straightforward adaptation of the time-independent theory of Lions and Paul, the key point here is the assertion in (ii) that the limit measure has slightly higher regularity in time than naively expected (continuous instead of $L^\infty$). This is crucial for the treatment of initial values for an evolution equation for $W$.

Having established the weak limit of time-dependent Wigner functions, we are then able to show under the additional assumption of the boundedness of $\{H^\varepsilon \Psi_\varepsilon^0\}_{\varepsilon>0}$ in $\mathrm{L}^2(\mathbb{R}^d)$ for the initial values $\{\Psi_\varepsilon^0\}_{\varepsilon>0}$ in $\mathrm{L}^2(\mathbb{R}^d)$ that the obtained limit $W$ of the corresponding Wigner functions satisfies the Liouville equation (LE) in the sense of distributions away from the set of Coulomb-singularities $\mathcal{S}$ of the potential $U = U_b + U_s$ with $U_b \in \mathrm{C}_b^1(\mathbb{R}^d)$, $U_s = V_{nn}$.

**Lemma 12.** *$W$ is a solution to the Liouville equation (LE) in $(\mathbb{R}^d \setminus \mathcal{S}) \times \mathbb{R}^{d+1}$ in the sense of distributions, i.e.,*

$$\int_{\mathbb{R}} \int_{\mathbb{R}^d} \int_{\mathbb{R}^d} (\partial_t \phi(x,p,t) + p \cdot \nabla_x \phi(x,p,t) - \nabla U(x) \cdot \nabla_p \phi(x,p,t)) W(\,\mathrm{d}x,\, \mathrm{d}p, t)\,\mathrm{d}t = 0$$

*for all $\phi \in \mathbb{C}_0^\infty((\mathbb{R}^d \setminus \mathcal{S}) \times \mathbb{R}^{d+1})$.*

As mentioned above, crucial for the proof of this result is the following estimate:

**Lemma 13.** *Let $\{\Psi_\varepsilon^0\}_{\varepsilon>0}$ satisfy $\|\Psi_\varepsilon^0\|_{\mathrm{L}^2(\mathbb{R}^d)} = 1$ and $\|H^\varepsilon \Psi_\varepsilon(\cdot,0)\|_{\mathrm{L}^2(\mathbb{R}^d)} \le c$ for some constant $c$ independent of $\varepsilon$. Then the solution $\Psi_\varepsilon(\cdot,t)$ to (SE) satisfies*

$$\sup_{t\in\mathbb{R}} \|U_s \Psi_\varepsilon(\cdot,t)\|_{\mathrm{L}^2(\mathbb{R}^d)} \le C, \tag{4}$$

*for some constant $C$ independent of $\varepsilon$.*

To see this, we use the conservation of the square of the Hamiltonian and a positive commutator argument. The latter exploits not just the repulsivity (i.e., positivity) of $U_s$, but relies essentially on its special Coulombic nature.

Finally, we conclude by mentioning that one can show that the obtained time-dependent Wigner measure is in fact supported outside the set of singularities, cf. [AFG08].

## References

[AFG08] L. Ambrosio, G. Friesecke, J. Giannoulis, *On the passage from quantum to classical molecular dynamics*, in preparation (2008).

[Ger91] P. Gérard, *Mesures semi-classiques et ondes de Bloch*, in: Séminaire EDP 1990–91, Ecole Polytechnique, Palaiseau, 1991.

[LP93] P.-L. Lions, T. Paul, *Sur les mesures de Wigner*, Topology **9** (1993), 553–618.
[Wig32] E. Wigner, *On the Quantum Correction for Thermodynamic Equilibrium*, Phys. Rev. **40** (1932), 749–759.

## A phase-field model for dislocations

Adriana Garroni

(Joint works with S. Cacace, S. Conti and S. Müller )

Dislocations are line defects in crystals that are responsible for plastic behavior. They usually arise on special planes (the slip planes) that are determined by the crystalline structure, and can bee seen as the discontinuities of a slip field defined on this plane. Depending on the crystalline structure on each slip plane several slip directions (Burgers vectors) are possible.

We study a multi-phase field model for dislocations on a given slip plane, ispired to the classical Peierls-Nabarro model (se e.g. [10]). For the latter, originally formulated for a one dimensional problem (i.e. straight dislocations), the free energy is given in terms of the slip $u$ as follows

$$E_{\text{free}}(u) = E_{\text{elastic}}(u) + E_{\text{interfacial}}(u)\,,$$

where the first term represents the long-range elastic distortion due to the slip and the second term is a nonlinear interfacial potential that remembers the crystal lattice and penalizes slips that are not integer multiples of the Burgers vectors. The main interest of this model is the coexistence of discrete features in a continuum setting. The reformulation of this model proposed by Koslowski-Cuitino-Ortiz [11] (see also [12]) for the case of dislocations on a given slip plane, using $N$ different slip systems (determined by the Burgers vectors $\mathbf{b}_1$, ..., $\mathbf{b}_N$) can be give in terms of a multi-phase $u : \Omega \subseteq \mathbb{R}^2 \to \mathbb{R}^N$ that represents the slip

$$u_1\mathbf{b}_1 + ... + u_N\mathbf{b}_N$$

on the given plane. The total energy, after a mesoscopic rescaling and a normalization takes the form

$$\sum_{i,j=1}^{3} \int_{\Omega\times\Omega} \Gamma_{ij}(x-y)\,[u_i(x)-u_i(y)]\,[u_j(x)-u_j(y)]\,dxdy + \frac{1}{\varepsilon}\int_{\Omega} \text{dist}^2(u,\mathbb{Z}^N)dx\,,$$

where $\Omega \subset \mathbb{R}^2$, $\Gamma$ is a matrix-valued kernel scaling as $|x-y|^{-3}$, i.e., the first term is bounded from above and below by a multiple of the $H^{1/2}$ norm, and $\varepsilon$ is a small parameter proportional to the lattice spacing.

Our scope is to study the asymptotic behavior in terms of $\Gamma$-convergence of this energy as $\varepsilon$ goes to zero. As $\varepsilon \to 0$ the multi-well potential forces the phase to take values in $\mathbb{Z}^N$ and in order to attribute a finite energy to non constant phases

we have to rescale the energy. Due to the critical singularity of the kernel the right rescaling is given by $|\log\varepsilon|$ and the functional becomes

$$(1)\, F_\varepsilon[u,\Omega] = \frac{1}{|\log\varepsilon|}\sum_{i,j=1}^{3}\int_{\Omega\times\Omega}\Gamma_{ij}(x-y)\,[u_i(x)-u_i(y)]\,[u_j(x)-u_j(y)]\,dxdy + \frac{1}{\varepsilon|\log\varepsilon|}\int_\Omega \mathrm{dist}^2(u,\mathbb{Z}^N)dx$$

The main feature of this functional is that it contains two competing terms: a nonconvex term which favors integer values of the multi-valued phase field $u$, and a regularizing term. This is an example of a large class of problems which share this structure, the classical example being the well-known Cahn-Hilliard model [5] from the gradient-theory of fluid-fluid phase transitions, which contains a two-well potential depending on a scalar phase field, and a local regularization given by the Dirichlet integral. The asymptotic behavior in terms of $\Gamma$-convergence for this functional goes back to Modica and Mortola [13], see also [14] and the references therein. For generalizations see e.g. [3, 7]. All these problems give rise in the limit to a sharp-interface model characterized by a line-tension energy density.

The scalar version of our functional (i.e. in the case of the activation of a single slip system) has been studied in [8] (see also [1] and [9]). In this case the $\Gamma$-limit is an anisotropic line-tension energy of the form

$$(2)\qquad \int_{J_u}\gamma(\nu)|[u]|\,d\mathcal{H}^1\,, \qquad u\in BV(\Omega;\mathbb{Z})\,,$$

where $J_u$ denotes the jump set of $u$, $\nu$ the corresponding norm, and $[u]$ the jump of $u$ across the jump set. Moreover, the line-tension energy density $\gamma$ can be completely characterized in terms of the kernel $\Gamma$, i.e.

$$\gamma(\nu) = 2\int_{x\cdot\nu=1}\Gamma(x)\,d\mathcal{H}^1(x)\,,$$

and can be obtain by mollifying the limiting configuration at scale $\varepsilon$. In this sense the optimal transition is "one-dimensional" and does not depend on the choice of the profile of the mollifier. In the present case the vector-valued nature of the phase-field do not permit to use the same technique used in the scalar case, however one can abstractly prove that a $\Gamma$-limit exists, and that it has the form

$$(3)\qquad \int_{J_u}\varphi(\nu,u^+-u^-)\,d\mathcal{H}^1\,, \qquad u\in BV(\Omega;\mathbb{Z}^2)\,,$$

as shown in [4], but the technique used does not give any further information on the line-tension energy density $\varphi$. One can naively try to use the natural generalization of the formula derived in the scalar case (2), namely,

$$(4)\qquad \gamma_0(\nu,s) = 2\int_{x\cdot\nu=1}s^T\Gamma(x)s\,d\mathcal{H}^1\,.$$

However, this does, in general, not produce a lower semicontinuous functional [4], whereas the $\Gamma$-limit must be lower semicontinuous. This in particular implies that

interfaces are more complicated and produce microstructure. In particular

$$F_{\text{flat}}(u) = \int_{J_u} \gamma_0(\nu, [u])\, d\mathcal{H}^1$$

is a non optimal upper bound for the limit energy, and hence also its lower semicontinuous envelope (i.e. its relaxation) is an upper bound. A natural question is whether it is the right limit.

In [6], under the condition that the kernel $\Gamma$ satisfies

$$\Gamma(z) = \frac{1}{|z|^3}\gamma\left(\frac{z}{|z|}\right), \tag{5}$$

where $\gamma \in L^\infty(S^1, \mathbb{R}^{N\times N}_+)$ obeys, for some $c > 0$,

$$\frac{1}{c}|\xi|^2 \le \xi \cdot \gamma(z)\xi \le c|\xi|^2 \qquad \text{for all } \xi \in \mathbb{R}^N,\ z \in S^1, \tag{6}$$

and $\mathbb{R}^{N\times N}_+$ denote the positive definite, symmetric, $N \times N$ matrices, we prove that the relaxation of the 1D energy is also a lower bound and hence it gives the $\Gamma$ limit of the energy (1). More precisely we prove the following theorem.

**Theorem.** *Let $\Omega \subset \mathbb{R}^2$ be a bounded Lipschitz domain, and suppose that $\Gamma$ satisfies (5) and (6). Then*

$$\Gamma\text{-}\lim_{\varepsilon\to 0} F_\varepsilon[u, \Omega] = F_0^{\text{rel}}[u, \Omega],$$

*where*

$$F_0^{\text{rel}}[u_0, \Omega] = \begin{cases} \displaystyle\int_{Ju_0\cap\Omega} \gamma_0^{\text{rel}}([u_0], \nu) d\mathcal{H}^1 & \text{if } u_0 \in BV(\Omega; \mathbb{Z}^N) \\ \infty & \text{else.} \end{cases}$$

*The surface energy $\gamma_0^{\text{rel}}$ is the BV-relaxation of $\gamma_0$, as defined in (4) (see* [2] *for the definition of the BV relaxation).*

## References


[1] G. Alberti, G. Bouchitté e P. Seppecher, *Un résultat de perturbations singulières avec la norme $H^{\frac{1}{2}}$*, C. R. Acad. Sci. Paris, **319-I** (1994), 333–338

[2] L. Ambrosio and A. Braides, *Functionals defined on partitions in sets of finite perimeter. II. Semicontinuity, relaxation and homogenization*. J. Math. Pures Appl. (9) **69** (1990), 307–333

[3] G. Bouchitté, *Singular perturbations of variational problems arising from a two-phase transition model*, Appl. Math. Opt. **21** (1990), 289–315.

[4] S. Cacace and A. Garroni, *A multi-phase transition model for dislocations with interfacial microstructure*, Preprint 2007.

[5] J.W. Cahn e J.E. Hilliard, *Free energy of a non-uniform system I - Interfacial free energy*, J. Chem. Phys. **28** (1958), 258–267

[6] S. Conti, A. Garroni and S. Müller, *Singular kernels, multiscale decomposition of microstructure, and dislocation models*, in preparation.

[7] I. Fonseca and L. Tartar, *The gradient theory of phase transitions for systems with two potential wells*, Proc. Roy. Soc. Edin. Sect. A **111** (1989), 89–102

[8] A. Garroni e S. Müller, *$\Gamma$-limit of a phase field model of dislocations,* SIAM J. Math. Anal., **36** (2005), no. 6, 1943–1964

[9] A. Garroni e S. Müller, *A variational model for dislocations in the line tension limit*, Arch. Ration. Mech. Anal. **181** (2006), 535-578
[10] J.P. Hirth and J. Lothe, *Theory of Dislocations*, John Wiley and Sons, Inc., 1982.
[11] Koslowski M. and Cuitiño A. M. and Ortiz M., *A phase-field theory of dislocation dynamics, strain hardening and hysteresis in ductile single crystal,* J. Mech. Phys. Solids **50** (2002), 2597–2635
[12] M. Koslowski e M. Ortiz, *A Multi-Phase Field Model of Planar Dislocation Networks*, Model Simul. Mater. Sci. Eng. **12** (2004), 1087–1097.
[13] L. Modica e S. Mortola, *Un esempio di* Γ*-convergenza*, Boll. Un. Mat. Ital. **14** (1977), 285–299.
[14] L. Modica, *The gradient theory of phase transition and the minimal interface criterion*, Arch. Rational Mech. Anal. **98** (1987), 123–142

## Mathematical Foundations and Algorithms for the Quasicontinuum Method

Mitchell Luskin
(joint work with Marcel Arndt, Matthew Dobson)

We gave an overview of the current state of numerical analysis and algorithms for the quasicontinuum method. We presented atomistic-to-continuum coupling methods and corresponding error, rates of convergence for iterative solution methods, and *a posteriori* error estimatation and corresponding adaptive modeling and coarsening algorithms.

### References

[1] Matthew Dobson and Mitchell Luskin. Analysis of a force-based quasicontinuum approximation. *Mathematical Modelling and Numerical Analysis*, pages 113–139, 2008.
[2] Marcel Arndt and Mitchell Luskin. Goal-oriented atomistic-continuum adaptivity for the quasicontinuum approximation. *International Journal for Multiscale Computational Engineering*, 5:407–415, 2007.
[3] Marcel Arndt and Mitchell Luskin. Error estimation and atomistic-continuum adaptivity for the quasicontinuum approximation of a frenkel-kontorova model. *SIAM J. Multiscale Modeling & Simulation*, 7:147–170, 2008.
[4] Marcel Arndt and Mitchell Luskin. Goal-oriented adaptive mesh refinement for the quasicontinuum approximation of a Frenkel-Kontorova model. *Computer Methods in Applied Mechanics and Engineering*, to appear.
[5] Matthew Dobson and Mitchell Luskin. Iterative solution of the quasicontinuum equilibrium equations with continuation. *Journal of Scientific Computing*, to appear.

## Mesoscale Hamiltonians in elasticity and plasticity

Luca Mugnai
(joint work with Stephan Luckhaus)

I presented some first results concerning the possible use of an Hamiltonian of "Kac-type", acting on finite systems of particles, in order to define elastic (and plastic) deformations without postulating a reference configuration. Our main result says that for those systems of particles on which the Hamiltonian assumes a

small enough value, we can define (locally) an elastic deformation describing with "good approximation" our system.

### Objective Molecular Dynamics

Richard D. James
(joint work with Kaushik Dayal, Traian Dumitrica and Stefan Müller)

We describe a method of constructing exact solutions of the equations of molecular dynamics. These solutions rely on a time-dependent invariant manifold of the equations of molecular dynamics, with forces determined by the Hellmann-Feynman theorem based on Born-Oppenheimer quantum mechanics. Solutions of the equations of molecular dynamics that correspond to viscometric flows of fluid dynamics and to the bending and twisting of beams are constructed: from this viewpoint the bending and twisting of beams and the viscometric flows of fluids are the same. A key question is whether such solutions are representative in some sense. This is explored in the context of the Maxwell-Boltzmann equation. One can infer from the structure of the solutions their "statistics" and this suggests a natural ansatz for the molecular density function. It is shown that this ansatz reduces the M-B equation. This apparently describes the molecular density function corresponding to all known solutions of the equations of the moments for special molecules. The presence of this invariant manifold suggests an addition to the Principle of Material Frame Indifference, a cornerstone of nonlinear continuum mechanics. Many interesting solutions on this invariant manifold remain to be explored, which are perhaps best described as "flowing nanostructures".

### Dislocation driven problems in material science

Duc Nguyen-Manh

In this talk, I pick up those problems of the past and current investigation of dislocation behavior from atomistic modeling. The first problem is related to construction of interatomistic potentials for materials with negative Cauchy relation w.r.t. the tight-binding bond approach. We showed that the environmental dependence of pairwise approximations is necessary for reproducing correctly elastic constant properties of brittle metallic systems such as fcc. bromine or intermetallics like TiAl. The second problem is related to discontinuity of bonding in different environments due to the lack of the transferability in two-centre TB integrals. The analytic solutions for screened bricks allows to improve the modeling of screw dislocations in free transition metals. The last problem is related to the analytic solution for migration potentials in crowdion defects for irradiated bcc. transition metals.

## Coupling Molecular Dynamics to Continuum Models through Perfectly Matched Discrete Layers

Murthy N. Guddati
(joint work with Senganal Thirunavukkarasu)

Many important physical phenomena such as dynamic fracture and friction involve activity at various scales, necessitating simultaneous use of fine-scale and coarse-scale computational models. For example, in the context of dynamic fracture, coarse-scale continuum models are sufficient away from the tip, while fine-scale molecular dynamics (MD) simulation is needed to model the near-tip processes. When MD and continuum regions are coupled, proper interface conditions are critical to avoid spurious heat up of the MD region caused by artificial trapping of energy in the MD region. This is primarily because the high-frequency lattice vibrations (phonons) in the MD region are not resolved in the continuum scale and get reflected back into the MD region. Ideal interface conditions should transmit the low-frequency vibrations to the continuum, while absorbing the high-frequency phonons. A critical step towards the development of these interface conditions are absorbing boundary conditions for molecular dynamics (MD-ABCs) that should absorb the phonons. Several MD-ABCs are developed to date, but many of them are either accurate or efficient, but not both.

Based on our recent research in ABCs for wave propagation [1], we have started the development of a new class of MD-ABCs that are more efficient and accurate than the existing counterparts. Named perfectly matched discrete layers (MD-PMDL), these ABCs require just few layers of atoms to absorb almost the entire high-frequency energy from phonons. The basic idea behind MD-PMDL is to replace the discrete system with continuous system of equivalent impedance, then use PMDL concepts in [1] to effectively absorb high-frequency phonons. A publication containing all the details of MD-PMDL is currently in preparation, while the details of PMDL for wave propagation problems can be found in [1]. The development is complete for square lattice systems, and extension to triangular and complex lattice systems is underway based on more general concepts derived in [2].

### References

[1] M.N. Guddati, K.W. Lim, *Continued Fraction Absorbing Boundary Conditions for Convex Polygonal Domains*, International Journal for Numerical Methods in Engineering **66** (2006), 949-977.

[2] M.N. Guddati, *Arbitrarily Wide Angle Wave Equations for Complex Media*, Computer Methods in Applied Mechanics and Engineering, **195** (2006), 65-93.

# A Linear Scaling Algorithm for Density-Functional Theory with Optimally Localized Non-Orthogonal Wave Functions

Carlos J. García-Cervera
(joint work with Jianfeng Lu, Yulin Xuan, Weinan E)

We present a new linear scaling method for electronic structure computations of insulators, in the context of Kohn-Sham Density Functional Theory (DFT) [1]. The method takes advantage of the non-orthogonal formulation of the Kohn-Sham functional, and the improved localization properties of non-orthogonal wave functions. We use a real-space formulation and finite differences, avoiding the use of basis functions, orthogonalization, plane waves, and a supercell (for the computation of non-periodic problems).

## 1. Kohn-Sham Density Functional Theory

1.1. **Introduction.** In the Born-Openheimer approximation, the spinless Kohn-Sham energy functional is [1, 2]

$$E_{KS}[\{\psi_j\}] = 2\sum_{j,k}(\mathbf{S}^{-1})_{jk}\int_{\mathbb{R}^3}\psi_j\left(-\frac{1}{2}\Delta\psi_k\right)d\boldsymbol{x} + F_{\mathrm{XC}}[\rho] + \frac{1}{2}\int_{\mathbb{R}^3}\int_{\mathbb{R}^3}\frac{(\rho-m)(\boldsymbol{x})(\rho-m)(\boldsymbol{y})}{|\boldsymbol{x}-\boldsymbol{y}|}\,d\boldsymbol{x}\,d\boldsymbol{y} + E_{\mathrm{ion}}[\{\psi_i\}], \tag{1}$$

where the electron density is defined as

$$\rho(\boldsymbol{x}) = 2\sum_{jk}\psi_j(\boldsymbol{x})(\mathbf{S}^{-1})_{jk}\psi_k(\boldsymbol{x}), \tag{2}$$

and $\mathbf{S}$ is the overlap matrix:

$$\mathbf{S}_{jk} = \int\psi_j\psi_k, \quad j,k = 1,\dots,N.$$

Note that when orthogonal wave functions are used, the overlap matrix becomes the identity matrix. In (1), the exchange and correlation energy $F_{\mathrm{XC}}[\rho]$ is unknown, and needs to be approximated. We adopt here the local density approximation (LDA) [3]. Finally, $E_{\mathrm{ion}}$ is the ionic or pseudopotential energy. This term, together with the ionic function $m$, defines the molecular environment. We use the Troullier-Martins pseudopotential [4], in the Kleinman-Bylander form [5].

When the Kohn-Sham functional (1) is minimized under the orthogonality constraint ($\mathbf{S} = \mathbf{I}$),the Euler-Lagrange equations lead to the following nonlinear eigenvalue problem:

$$\mathbf{H}\psi_i = \varepsilon_i\psi_i; \quad i = 1,\dots,N. \tag{3}$$

The Hamiltonian in (3) is defined as

$$\mathbf{H} = -\frac{1}{2}\Delta + V_{\mathrm{eff}}[\rho], \tag{4}$$

where

$$V_{\text{eff}}[\rho](x) = \int \frac{\rho(y)}{|x-y|}\, dy + V_{\text{ion}}(x) + \frac{\delta F_{\text{XC}}[\rho]}{\delta \rho}.$$

The traditional approach for solving this nonlinear eigenvalue problem consists of two iterations: an inner iteration in which the Hamiltonian is diagonalized for a given electron density, and an outer iteration in which the electron density is updated. The numerical complexity of diagonalization and/or orthogonalization is $O(N^3)$, which is prohibitively expensive for relatively small problems. A number of methodologies have been presented in the last twenty years that reduce the complexity, or even achieve linear scaling. For a review, see [6].

## 2. Localized Subspace Iteration Algorithm for Kohn-Sham Density Functional Theory

In addition to avoiding the orthogonalization step, one of the main advantages of the non-orthogonal formulation comes from the fact that the Kohn-Sham functional (1) is invariant under nonsingular linear transformations of the $N$-dimensional subspace generated by the wave functions:

$$\text{span}\{\psi_{\text{i}}\} = \text{span}\{\phi_{\text{i}}\} \Longrightarrow \text{F}_{\text{KS}}[\{\psi_{\text{i}}\}] = \text{F}_{\text{KS}}[\{\phi_{\text{i}}\}]. \tag{5}$$

As a consequence, the Kohn-Sham functional can be thought of as a functional acting on subspaces, and the goal is to find the *minimizing subspace*. This is the subspace generated by the eigenfunctions corresponding to the smallest eigenvalues of the self-consistent Hamiltonian. The advantage of this viewpoint is that the specific representation of the subspace is not relevant, and therefore we can choose a representation that is convenient for our purposes. Linear scaling can be achieved by choosing a representation in terms of optimally localized non-orthogonal wave functions, as described in [7].

To find the minimizing subspace, we start with a subspace of dimension $N$, and successively improve it by filtering out the components corresponding to the unoccupied states, i.e., eigenvalues above the Fermi energy. After the filtering step, the locality of the representation needs to be reestablished, and this is achieved with the algorithm presented in [7] and described below in section 2.2.

### 2.1. Chebyshev-Filtered Subspace Iteration.

One of the simplest filtering strategies is the Shifted Power Method, by which a certain portion of the spectrum of the Hamiltonian is amplified, effectively eliminating the remainder portions. A more efficient filter can be constructed with the use of Chebyshev polynomials, $T_n$. They have the property that $|T_n(x)| \leq 1$ for $x \in [-1, 1]$ and $|T_n(x)| \gg 1$ for $|x| > 1$. They satisfy a three-term recursion, which can be used to evaluate $T_n(\mathbf{H})$ efficiently without explicitly computing the operator.

2.2. **Localization.** Given a set of wave functions, $\{\psi_j\}_{j=1}^N$, centered at the locations $\{\boldsymbol{b}_j\}_{j=1}^N$, respectively, we obtain a localized representation of $V = \text{span}\{\psi_j\}_{j=1}^N$ by minimizing, for each $j \in \{1, \ldots, N\}$,

$$F[\phi] = \frac{\int_{\mathbb{R}^3} |\boldsymbol{x} - \boldsymbol{b}_j|^{2p} |\phi(\boldsymbol{x})|^2 \, d\boldsymbol{x}}{\int_{\mathbb{R}^3} |\phi(\boldsymbol{x})|^2 \, d\boldsymbol{x}}, \tag{6}$$

among functions $\phi$ of the form

$$\phi(\boldsymbol{x}) = \sum_{k=1}^{r} \alpha_k \psi_k(\boldsymbol{x}) \in V. \tag{7}$$

The minimization (6) leads to $\mathbf{W}a = \lambda \mathbf{S}a$ where

$$W_{kl} = \int_{\mathbb{R}^3} |\boldsymbol{x} - \boldsymbol{b}_j|^{2p} \psi_k(\boldsymbol{x}) \psi_l(\boldsymbol{x}) \, d\boldsymbol{x}, \quad k, l = 1, \cdots, r,$$

and $\lambda$ is the smallest generalized eigenvalue.

Given that the wave functions $\{\psi_i\}$ are compactly supported, only a fixed number of wave functions appear in (7), i.e., $r$ is bounded independently of $N$. Therefore the localized basis can be obtained with $O(N)$ scaling. The improved decay properties of these wave functions can be found in [7, 8].

2.3. **Electron density.** Under the assumption that both $\mathbf{S}$ and $\mathbf{S}^{-1}$ decay exponentially fast away from the diagonal, $\mathbf{S}^{-1}$ can computed with $O(N)$ complexity in a similar way to [9].

2.4. **Algorithm for Kohn-Sham DFT.** We combined all these steps to define a linear scaling algorithm for Kohn-Sham density functional, based on Chebyshev-filtered subspace iteration with optimally localized wave functions [10]:

Given (localized) wave functions $\Psi_0$.
**repeat** {(*Self-Consistency Loop (SCF)*)}
  Compute electronic density: $\rho$
  Compute effective potential: $V_{\text{eff}}[\rho]$.
  **repeat** {(*Localized Subspace Iteration*)}
    Filtering Step: $\Phi = T_n(H)\Psi$.
    Localization Step: Localize $\psi_r$ for $r = 1, \cdots, k$.
    Truncation beyond cut-off radius.
  **until** Convergence of linear iteration
  Update electronic density (mixing).
**until** Convergence of self-consistent iteration

The algorithm is similar to the subspace iteration method of Zhou, Saad, Tiago, and Chelikowsky [11], but by avoiding diagonalization and orthogonalization linear scaling is achieved. In figure 1 we show the electron density obtained with our algorithm for an alkane chain with 38 atoms.

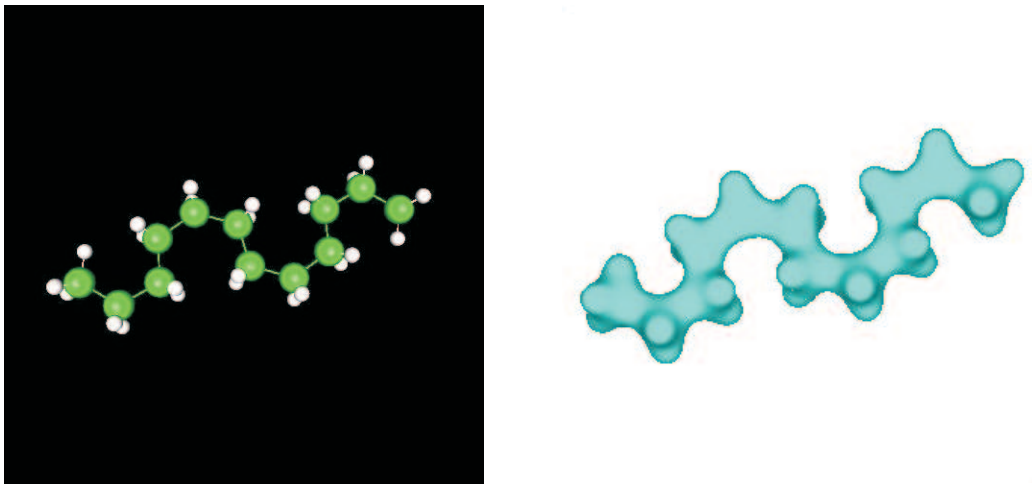

(a) Alkane Chain $CH_3(CH_2)_{10}CH_3$. (b) Electron Density.

Figure 1: Electronic density of an Alkane chain obtained with the LSI algorithm. (a) Atomic configuration. (b) Electron density.

## 3. Acknowledgments

CJGC and JL would like to thank Weinan E, Gero Friesecke, and David Pettifor for organizing this meeting at Oberwolfach. We would also like to thank the staff at Oberwolfach for providing such a pleasant environment. The work of CJGC was supported by and NSF CAREER award (DMS-0645766). The work of E and Lu is supported in part by ONR grant N00014-01-1-0674, DOE grant DOE DE-FG02-03ER25587, NSF grants DMS-0407866 and DMR-0611562.

## References

[1] W. Kohn and L.J. Sham. Self-Consistent Equations Including Exchange and Correlation Effects. *Phys. Rev.*, 140(4A):1133–1138, 1965.

[2] F. Mauri, G. Galli, and R. Car. Orbital formulation for electronic-structure calculations with linear system-size scaling. *Phys. Rev. B*, 47(15):9973–9976, Apr 1993.

[3] J.P. Perdew and A. Zunger. Self interaction correction to density functional approximations for many electron systems. *Phys. Rev. B*, 23(10):5048–5079, 1981.

[4] N. Troullier and J.L. Martins. Efficient pseudopotentials for plane-wave calculations. *Phys. Rev. B*, 43(3):1993–2006, 1991.

[5] L. Kleinman and D. M. Bylander. Efficacious form for model pseudopotentials. *Phys. Rev. Lett.*, 48(20):1425–1428, 1982.

[6] S. Goedecker. Linear scaling electronic structure methods. *Rev. Mod. Phys.*, 71(4):1085–1123, 1999.

[7] Weinan E, Tiejun Li, and Jianfeng Lu. Localized basis of eigen-subspaces and operator compression. *submitted*, 2007.

[8] Jianfeng Lu. PhD thesis, Princeton University.

[9] W. Yang. Absolute-energy-minimum principles for linear-scaling electronic-structure calculations. *Phys. Rev. B*, 56(15):9294–9297, 1997.

[10] C.J. García-Cervera, J. Lu, and W. E. Asymptotics-based sublinear scaling algorithms and application to the study of the elctronic structure of materials. *Comm. Math. Sci.*, 5(4):999–1026, 2007.

[11] Y. Zhou, Y. Saad, M.L. Tiago, and J.R. Chelikowsky. Self-consistent-field calculations using chebyshev-filtered subspace iteration. *J. Comput. Phys.*, 219(1):172–184, 2006.

## Coarse-graining Molecular Dynamics

Xiantao Li

(joint work with Weinan E)

Models at the molecular scale usually involve a huge number of particles. In many practical situations, the behavior of interest occurs in a very localized region, while the rest of the particles merely act as the surrounding environment. The direct approach of treating these excessive particles explicitly would either introduce finite size effect, or lead to a rather large system, which makes the computation prohibitably expensive. Therefore it is of considerable practical interest to develop an alternative approach in which the effect of these particles is incorporated implicitly. This talk presents a coarse-graining strategy for molecular dynamics in which the excess degrees of freedom are removed and effective equations are derived for the representative variables. A variational approach to obtain the effective equations will be discussed.

To begin with, we consider a molecular dynamics system with interatomic potential $V(\mathbf{u}_1, \mathbf{u}_2, \cdots, \mathbf{u}_N)$. The Newton's equations of motion read,

$$m\ddot{\mathbf{u}}_i = -\nabla_{\mathbf{u}_i} V. \tag{1}$$

Here $m$ is the mass of an atom and $\mathbf{u}_i$ is the position. We will assume that the system has an underlying lattice structure with the equilibrium position of an atom denoted by $R_i$. The displacement is the deviation of the current position, $\mathbf{r}_i$, from the reference position, i.e. $\mathbf{u}_i = \mathbf{r}_i - R_i$.

We will partition the system into two groups: the atoms that will be included in the computation, called retained atoms, and the atoms in the surrounding area, called bath atoms. We will partition the displacement,

$$\mathbf{u} = (\mathbf{u}_I, \mathbf{u}_J), \tag{2}$$

where $\mathbf{u}_I$ and $\mathbf{u}_J$ represent the displacement of the retained atoms and bath atoms respectively. We decompose the velocity accordingly,

$$\mathbf{v} = (\mathbf{v}_I, \mathbf{v}_J), \tag{3}$$

Our next step is to derive the equations only involving the retained variables. This has been done in [2]. The resulting equation, referred to as generalized Langevin equation (GLE), can be expressed as,

$$m\ddot{\mathbf{u}}_I = -\nabla\Phi(\mathbf{u}_I) + \Theta(0)\mathbf{u}_I - \int_0^t \Theta(\tau)\dot{\mathbf{u}}_I(t-\tau)d\tau + F(t). \tag{4}$$

It has been shown that $F(t)$ is a stationary Gaussian process, and satisfies the fluctuation dissipation theorem,

$$\left\langle F(t+s)F(s)^T \right\rangle = k_B T \Theta(t). \tag{5}$$

Therefore, once the function $\Theta(t)$ is available, the equations are closed, and the dimension reduction is thus accomplished. In this take, we discuss how to find efficient approximation of such memory function.

## References

[1] X. Li and W. E, *Boundary conditions for molecular dynamics simulations of solids at low temperature*, Comm. Com. Phys. **1** (2006), 136–176.

[2] X. Li and W. E, *Boundary conditions for molecular dynamics simulations of solids I: Treatment of the heat bath*, Physical Review B **76** (2007), 104107.

## Analysis of the nonlocal quasicontinuum method

Pingbing Ming

(joint work with W. E and Jerry Z. Yang)

The quasicontinuum (QC) [13] method is among the most successful multiscale methods for modeling the mechanical deformation of solids. So far its main success is in modeling the static properties of crystalline solids at zero temperature, even though various attempts have been made to extend QC to modeling dynamics at finite temperature. At the same time, QC has attracted a great deal of attention from the numerical analysis community, since it provides the simplest example for understanding the algorithmic issues in coupled atomistic-continuum methods. Indeed one main challenge in multiscale, multi-physics modeling is to understand the stability and accuracy of multi-physics algorithms. This is of particular interest for coupled atomistic-continuum algorithms, since the nature of the continuum models and atomistic models are quite different. Specifically, we would like to understand:

(1) whether new numerical instabilities can arise as a result of atomistic-continuum coupling;
(2) whether the matching between the continuum and atomistic models causes large error.

The second issue is particularly important: It is inevitable to introduce some error at the interface where the atomistic and continuum models are coupled together. The question is how large this error is and whether this error also affects the accuracy of the numerical solution away from the interface. We also note that Weiqing Ren [9] has demonstrated, using examples from fluid mechanics, that new numerical instabilities can arise as a result of coupling atomistic and continuum models.

QC provides the simplest example for analyzing the issues outlined above for the following reason: At zero temperature, the atomistic model can be regarded as a consistent discretization of the Cauchy-Born continuum model. We note that the

Cauchy-Born continuum model is the right continuum limit of the atomistic model whenever the system is in the elastic regime [2, 3]. Since QC uses the Cauchy-Born rule in the continuum region (or the local region, in the QC terminology), the models used in the continuum and atomistic regions (or local and nonlocal regions) are consistent. The only remaining issue is what happens at the interface when the two models couple.

Indeed errors are introduced by QC at the interface. The simplest and most well-known example is the "ghost force", i.e., forces that act on th atoms when they are in equilibrium positions. When atoms are in equilibrium positions, the forces acting on them should vanish. So whatever forces present is numerical error.

We view the interface as as an internal numerical boundary where two different numerical schemes meet, both are consistent with the underlying PDE, in this case the Cauchy-Born elasticity model. We will show in this note and a follow-up paper [8] that the accuracy and stability issues in QC can be understood following standard practices in classical numerical analysis: We consider the case when the interface is planar. After Fourier transform in the direction of the interface, the problem reduces to a one-dimensional problem, which can be analyzed in detail. One thing we learn from classical numerical analysis is that the essence of most issues can be understood from one-dimensional examples. This is what we will focus on in this note. Since our problem is generally nonlinear, we will not be able to use Fourier transform. But as is shown in a follow-up paper, the conclusions of the present note are still valid for high dimensional problems when the interface is planar. This leaves out the situations when the interface has corners. At this point, very little is known in that case.

The accuracy of the quasicontinuum method is analyzed using a series of models with increasing complexity [5]. It is demonstrated that the existence of the ghost-force may lead to large errors, not just near the local-nonlocal interface, but over a rather extended region. We calculate the local truncation error (LTE) of the different variants of QC. We will see that even though the LTEs for the ghost-force removal procedures are all $\mathcal{O}(1)$, they are of divergence form and are actually $\mathcal{O}(\varepsilon)$ in a weak norm, which is actually the so-called *Spijker norm* appeared in the homogeneous difference schemes [14, 12, 6]. We also study the stability issues and give an example of a geometrically consistent scheme that is unstable. We then show, following the strategies presented in [2], that the stability condition and the LTE analysis implies that ghost-force removal procedures recover uniform first order accuracy. The ghost-force removal strategy includes the force-based QC [10, 7], the quasinonlocal QC [11] and the geometrically consistent scheme proposed by E, Lu and Yang [1]. The details may be found in [5, 4].

## References

[1] W. E, J. Lu and Jerry Z. Yang, *Uniform accuracy of the quasicontinuum method*, Phys. Rev. B **74** (2006), 214115.

[2] W. E and P.B. Ming, *Cauchy-Born rule and the stability of the crystalline solids: static problems*, Arch. Rational Mech. Anal. **183**(2007), 241–297.

[3] W. E and P.B. Ming, *Cauchy-Born rule and the stability of the crystalline solids: dynamic problems*, Acta Math. Appl. Sin. Engl. Ser. **23**(2007), 529–550.
[4] W. E and P.B. Ming, *Analysis of the nonlocal quasicontinuum method*, preprint, 2008.
[5] W. E, P.B. Ming and Jerry Z. Yang, *Analysis of the quasicontinuum method*, preprint, 2008.
[6] H.-O. Kreiss, T.A. Manteuffel, B. Swarts, B. Wendroff and A.B. White, Jr., *Supra-convergent schemes on irregular grids*, Math. Comp. **47**(1986), 537–554.
[7] R. Miller and E.B. Tadmor, *The quasicontinuum method: overview, applications and current directions*, J. Comput. Aided Mater. Des. **9**(2002), 203–239.
[8] P.B. Ming, *Analysis of quasicontinuum method in higher dimension*, in preparation.
[9] W.Q. Ren, preprint.
[10] V.B. Shenoy, R. Miller, E.B. Tadmor, R. Phillips and M. Ortiz, *An adaptive finite element approach to atomic scale mechanics-the quasicontinuum method*, J. Mech. Phys. Solids **47**(1999), 611–642.
[11] T. Shimokawa, J.J. Mortensen, J. Schiøz and K.W. Jacobsen, *Mathching conditions in the quasicontinuum method: removal of the error introduced in the interface between the cosrse-grained and fully atomistic region*, Phys. Rev. **B 69** (2004), 214104.
[12] M.N. Spijker, *Stability and convergence of finite difference schemes*, Thesis, University of Leiden, 1968.
[13] E.B. Tadmor, M. Ortiz and R. Phillips, *Quasicontinuum analysis of defects in solids*, Phil. Mag. **A73**(1996), 1529–1563.
[14] A.N. Tikhonov and A.A. Samarskiĭ, *Homogeneous difference schemes on nonuniform nets*, Zh. Vychisl. Mat. i Mat. Fiz., **2**(1962), 812–832; English tranl. in U.S.S.R. Comput. Math. and Math. Phys. **2**(1962), 927–953.

*Reporter: Christian Mendl*

# Participants

**Yuen Au Yeung**
Zentrum für Mathematik
TU München
Boltzmannstr. 3
85748 Garching bei München

**Prof. Andrea Braides**
Dipartimento di Matematica
Universita di Roma "Tor Vergata"
Via della Ricerca Scientif. 1
I-00133 Roma

**Dr. Marco Cicalese**
Dipartimento di Matematica e Appl.
Universita di Napoli
Complesso Monte S. Angelo
Via Cintia
I-80126 Napoli

**Prof. Dr. Luciano Colombo**
Dipartimento di Fisica
Universita di Cagliari
Cittadella Universitaria
I-09042 Monserrato (CA)

**Prof. Dr. Sergio Conti**
FB Mathematik
Universität Duisburg-Essen
Lotharstr. 65
47057 Duisburg

**Dr. Luigi Delle Site**
Max-Planck Institut für
Polymerforschung
Ackermannweg 10
55128 Mainz

**Prof. Dr. Ralf Drautz**
ICAMS
Ruhr-Universität Bochum
Stiepeler Str. 129
44801 Bochum

**Prof. Dr. Weinan E**
Department of Mathematics
Princeton University
Fine Hall
Washington Road
Princeton, NJ 08544-1000
USA

**Prof. Dr. Christian Elsässer**
Fraunhofer-Institut für
Werkstoffmechanik
Wöhlerstr. 11
79108 Freiburg

**Prof. Dr. Björn Engquist**
Department of Mathematics
The University of Texas at Austin
1 University Station C1200
Austin, TX 78712-1082
USA

**Prof. Dr. Gero Friesecke**
Zentrum Mathematik
Technische Universität München
Boltzmannstr. 3
85747 Garching bei München

**Prof. Dr. Carlos J. Garcia**
Department of Mathematics
University of California at
Santa Barbara
Santa Barbara, CA 93106
USA

**Prof. Dr. Adriana Garroni**
Dipartimento di Matematica
"Guido Castelnuovo"
Universita di Roma "La Sapienza"
Piazzale Aldo Moro, 2
I-00185 Roma

**Dr. Johannes Giannoulis**
Zentrum Mathematik
Technische Universität München
Boltzmannstr. 3
85747 Garching bei München

**Prof. Dr. Murthy Guddati**
Department of Civil Engineering
North Carolina State University
Stinson Drive
Raleigh, NC 27695-7908
USA

**Carsten Hartmann**
Fachbereich Mathematik & Informatik
Freie Universität Berlin
Arnimallee 6
14195 Berlin

**Dr. Peter D. Haynes**
Department of Materials
Imperial College London
Exhibition Road
GB-London, SW7 2AZ

**Prof. Dr. Richard D. James**
Department of Aerospace Engineering
and Mechanics
University of Minnesota
110 Union Street S. E.
Minneapolis, MN 55455
USA

**Stefan Kahler**
Zentrum Mathematik
Technische Universität München
Boltzmannstr. 3
85747 Garching bei München

**Peter Koltai**
Zentrum Mathematik
Technische Universität München
Boltzmannstr. 3
85747 Garching bei München

**Prof. Dr. Peter Kratzer**
Institut für Physik der
Universität Duisburg-Essen
Lotharstr. 1
47048 Duisburg

**Dr. Carl-Friedrich Kreiner**
Lehrstuhl C für Mathematik
RWTH Aachen
Templergraben 55
52062 Aachen

**Prof. Dr. Ben Leimkuhler**
School of Mathematics
University of Edinburgh
James Clerk Maxwell Bldg.
King's Buildings,Mayfield Road
GB-Edinburgh EH9 3JZ

**Prof. Dr. Xiantao Li**
Department of Mathematics
Pennsylvania State University
University Park, PA 16802
USA

**Prof. Dr. Gang Lu**
Physics and Astronomy Department
California State University Northridge
18111 Nordhoff Street
Northridge, CA 91330-8268
USA

**Jianfeng Lu**
Program in Applied & Computational
Mathematics
Princeton University
Fine Hall, Washington Road
Princeton, NJ 08544-1000
USA

**Prof. Dr. Stephan Luckhaus**
Mathematisches Institut
Universität Leipzig
Johannisgasse 26
04103 Leipzig

**Prof. Dr. Mitchell B. Luskin**
School of Mathematics
University of Minnesota
127 Vincent Hall
206 Church Street S. E.
Minneapolis MN 55455-0436
USA

**Christian Mendl**
Zentrum für Mathematik
TU München
Boltzmannstr. 3
85748 Garching bei München

**Prof. Dr. Pingbing Ming**
Institute of Computational Mathematics
Academy of Math. and Systems Sc.
Chinese Academy of Sciences
No. 55, Zhong-Guan-Cun East Road
100 190 Beijing
P.R. CHINA

**Prof. Dr. Stefan Müller**
Max-Planck-Institut für Mathematik
in den Naturwissenschaften
Inselstr. 22 - 26
04103 Leipzig

**Dr. Luca Mugnai**
Max-Planck-Institut für Mathematik
in den Naturwissenschaften
Inselstr. 22 - 26
04103 Leipzig

**Prof. Dr. Duc Nguyen-Manh**
Theory and Modelling Department
Culham Science Centre
Ukaea
GB-Abingdon, OX14 3DB

**Christoph Ortner**
Computing Laboratory
Oxford University
Wolfson Building
Parks Road
GB-Oxford OX1 3QD

**Dr. Mariapia Palombaro**
Max-Planck-Institut für Mathematik
in den Naturwissenschaften
Inselstr. 22 - 26
04103 Leipzig

**Prof. Dr. David Pettifor**
Department of Materials
University of Oxford
Parks Road
GB-Oxford OX1 3PH

**Dr. Anja Schlömerkemper**
Max-Planck-Institut für Mathematik
in den Naturwissenschaften
Inselstr. 22 - 26
04103 Leipzig

**Dr. Bernd Schmidt**
Division of Engineering and
Applied Sciences; MS 104-44
California Institute of Technology
Pasadena, CA 91125
USA

**Bernhard Seiser**
Department of Materials
University of Oxford
Parks Road
GB-Oxford OX1 3PH

**Dr. Gabriel Stoltz**
CERMICS - ENPC
Cite Descartes, Champs-sur-Marne
6 et 8 avenue Blaise Pascal
F-77455 Marne La Vallee Cedex 2

**Dr. Florian Theil**
Mathematics Institute
University of Warwick
GB-Coventry CV4 7AL

**Dr. Johannes Zimmer**
Department of Mathematical Sciences
University of Bath
GB-Bath BA2 7AY

**Prof. Dr. Yang Xiang**
Department of Mathematics
Hong Kong University of
Science & Technology
Clear Water Bay
Kowloon
Hong Kong
P.R. China